Flat-Plate Solar
Array Project
5101-210

DOE-JPL-1012-72
Distribution Category UC-63b

Photothermal Characterization of Encapsulant Materials for Photovoltaic Modules

Ranty H. Liang
Amitava Gupta
Salvador Di Stefano

June 1, 1982

Prepared for
U.S. Department of Energy
Through an Agreement with
National Aeronautics and Space Administration
by
Jet Propulsion Laboratory
California Institute of Technology
Pasadena, California

(JPL PUBLICATION 82-42)

Flat-Plate Solar
Array Project
5101-210

DOE-JPL-1012-72
Distribution Category UC-63b

Photothermal Characterization of Encapsulant Materials for Photovoltaic Modules

Ranty H. Liang
Amitava Gupta
Salvador Di Stefano

June 1, 1982

Prepared for
U.S. Department of Energy
Through an Agreement with
National Aeronautics and Space Administration
by
Jet Propulsion Laboratory
California Institute of Technology
Pasadena, California

(JPL PUBLICATION 82-42)

Prepared by the Jet Propulsion Laboratory, California Institute of Technology, for the U.S. Department of Energy through an agreement with the National Aeronautics and Space Administration.

The JPL Flat-Plate Solar Array Project is sponsored by the U.S. Department of Energy and is part of the Photovoltaic Energy Systems Program to initiate a major effort toward the development of cost-competitive solar arrays.

This publication reports on work done under NASA Task RD-152, Amendment 66, DOE/NASA IAA No. DE-AI01-76ET20356.

ABSTRACT

A photothermal test matrix and a low-cost testing apparatus for encapsulant materials of photovoltaic modules have been defined and illustrated. Photothermal studies were conducted in order to screen and rank existing as well as future encapsulant candidate materials and/or material formulations in terms of their long-term physiochemical stability under accelerated photothermal aging conditions. Photothermal characterization of six candidate pottant materials and six candidate outer cover materials have been carried out. Principal products of photothermal degradation were identified. Certain critical properties were also monitored as a function of photothermal aging.

GLOSSARY

BP	4,4'Dimethoxy, 2-Hydroxy 2-Allyl Benzophenone/Acrylic Copolymer
BT	5-Vinyl 2-Hydroxyphenyl Benzotriazole/Acrylic Copolymer
CER	Controlled Environmental Reactor
EMA	Ethylene/Methylacrylate Copolymer
EVA	Ethylene/Vinylacetate Copolymer (Springborn A9918)
FSA	Flat-Plate Solar Array Project
FT-IR	Fourier Transform Infrared Spectroscopy
Hg	Mercury
HPLC	High Pressure Liquid Chromatography
PC	Polycarbonate
PE	Polyethylene
PnBA	Poly-n-Butylacrylate
PU	Aliphatic Polyurethane (Quinn)
PVB	Polyvinyl Butyral (Monsanto Saflex)
PVC	Polyvinyl Chloride
RTV	Poly Dimethylsiloxane (GE RTV 615)
SEA	Surface Energy Analysis
UV	Ultraviolet
W/V	Weight-to-Volume Ratio

CONTENTS

SECTION I

DESIGN APPROACH

A. INTRODUCTION

An objective of the FSA Project Environmental Isolation Task is to demonstrate that an encapsulation system with a service life potential of 20 years or more can be constructed using low-cost materials that are not themselves intrinsically weatherable. Weatherability of the overall design is achieved by: (1) modification of the low-cost materials in order to achieve greater outdoor stability and (2) adopting a multilayer design concept in which each layer provides protection from a specific environmental stress to all layers below.

Assessment and demonstration of life potential of low-cost encapsulation designs involves the following activities:

(1) Photothermal characterization of encapsulation materials, which involves measurements of chemical/physical properties and performance parameters (e.g., electrical, optical, mechanical, thermal properties) as a function of aging in an accelerated stress environment.

(2) Testing of candidate encapsulation designs in an accelerated stress environment; submodules and minimodules are tested in controlled environment test chambers. Designs of the test chambers have been described in References 1 and 2.

(3) Outdoor deployment and testing of PV modules, minimodules and submodules in selected outdoor sites. Performance data have been obtained as a function of exposure period. This activity will be described in a future report.

(4) Identification and quantitative assessment of degradation mechanisms/rates and their correlation with failure mechanisms, and construction of failure envelopes. Estimations and predictions of module survival probability have been attempted for certain specific failure modes; e.g., cracking of glass superstrate (Ref. 3), fatigue failure of interconnects (Ref. 4) and cell cracking caused by hail impact (Ref. 3 and Ref. 5).

This report describes photothermal characterization of selected encapsulation materials. So far, emphasis has been placed on photothermal ranking of these materials (see Section I.D). Continued effort will be carried out to predict and correlate the thermal response of these materials based on their long-term chemical stability.

B. PHOTOTHERMAL DEGRADATION PHENOMENA

Degradation of a polymeric material formulated with UV stabilizers and antioxidants is expected to have a complex time dependence. The principal processes leading to degradation are as follows:

(1) Loss of Stabilizers: The process of losing UV stabilizers by diffusion and evaporation or leaching has a low activation energy if the stabilizers are merely blended or compounded in the material (for relationship between activation energy and reaction rate, see Section II.C). The gradual loss of this protection controls the overall rate of degradation of the polymer, and may also cause inhomogeneous degradation, as a concentration gradient of stabilizers may be set up. Inhomogeneous degradation may lead to new types of material failures; e.g., cracking, development of cloudiness, chalking, etc.

(2) Photothermal Bond Cleavage: Photothermal bond cleavage involves cleavage of chemical bonds in the material due to simultaneous absorption of photons and heat. Certain materials; e.g., saturated carbonyl-containing compounds are inherently unstable to photolytic bond cleavage ($\lambda < 350$ nm). Hence, if these carbonyl-containing polymers are used for encapsulation they must be protected from active solar radiation (295 to 400 nm); e.g., radiation that is absorbed and that induces bond cleavage processes in these materials. An example is polyvinyl butyral (PVB), which always contains some aldehyde groups. If PVB is placed behind a glass plate, glass (Pyrex, low-iron and iron-rich) will absorb solar radiation in the wavelength range of 295 to 320 nm and provide adequate shielding for the aldehyde groups in PVB. Aliphatic acrylics also undergo photolytic bond cleavage at wavelengths less than 290 nm, but no protection is needed by acrylics from this type of degradation process (e.g., bond cleavage) for terrestrial applications because radiation of wavelength shorter than 290 nm is not transmitted through the atmosphere.

Thermal bond cleavage is a process that can be inhibited by lowering service temperatures. All organic polymers are ultimately susceptible to thermal bond cleavage, hence service temperature for systems containing organic polymeric components must be limited for long-term applications. Acrylics undergo thermal bond cleavage at a measurable rate at 130°C and above. Other polymers such as EVA, PVC, and PVB have lower temperature thresholds, ranging from 100°C.

(3) Hydrolytic Bond Cleavage: Hydrolysis is a process by which water adds to a chemical bond, inducing bond cleavage in a temperature-activated process. It can be eliminated by preventing access of water vapor or liquid water to materials at temperatures higher than the threshold temperature for hydrolysis. Certain chemical linkages such as esters (present in EVA, EMA, and acrylics) and acetals (PVB) are particularly susceptible to hydrolysis.

Simultaneous occurrence of high temperature (>90°C) and appreciable concentrations of water vapor must be avoided in these materials. Typical products of hydrolysis reactions are small organic molecules, including organic carboxylic acids and alcohols.

(4) Thermal and Photothermal Oxidation: Oxidative degradation may be initiated by solar radiation and also may take place in the absence of radiation. Oxidation initiated by solar radiation, known as photo-oxidation, has lower activation energy (temperature coefficient of the degradation rate determined assuming an exponential temperature dependence, see Section II.C) than thermal oxidation. Oxidative degradation mechanisms of encapsulant materials in PV modules deployed outdoors include photochemical-activating and thermally-driven chain radical processes. This mechanism may be termed photothermal oxidation. Both types of oxidative processes render the material more sensitive to subsequent thermal oxidation. Thus, unprotected polyethylenes (PE) or EVA, which are thermally stable (resistant to pure thermal oxidation up to 85°C), readily undergo photo-oxidation at 30°C and become sensitive to thermal oxidation at temperature ranges of 50 to 85°C when exposed to light. Photothermal oxidation therefore includes enhanced thermal oxidation and thermally activated photo-oxidation. Common oxidation products are carbonyl groups, which are, as noted earlier, susceptible to photochemical cleavage processes, thus generating radicals (molecular fragments) that are highly reactive in the presence of oxygen. Hence, a synergistic mode of degradation can be expected, solar radiation performing the role of a catalyst species.

C. INHIBITION OF PHOTOTHERMAL DEGRADATION

In addition to the protective design concept of screening out harmful UV wavelengths as discussed above, low-cost materials may be formulated by adding UV stabilizers and antioxidants in order to minimize the net extent of degradation caused by photothermal stresses. A UV absorber added to the bulk pottant will absorb most of the UV radiation that is not removed by the outer cover. By itself, addition of UV absorber in the bulk of an unstable polymer is not sufficient protection against photodegradation; in fact, it can initiate unique degradation modes arising from heterogeneous degradation processes. Used in conjunction with a UV screening outer cover, a UV absorber additive provides a useful additional safeguard against photodegradation.

A UV stabilizer quenches and deactivates excited states in the polymer to be protected. UV stabilizers may also act as chemical traps of reactive species, which are then inhibited from causing chemical degradation in the polymer via chain processes. UV stabilizers are especially useful in quenching photodegradation in rubbers and also in certain plastics such as polycarbonate of bisphenol A.

Antioxidants are additives that react with and deactivate primary products of polymer oxidation; e.g., chain radicals. In the absence of antioxidants that are radical traps, chain radicals may undergo chain radical

scission, causing many units of chain breakage for every single site of initial attack. Antioxidants and certain UV stabilizers are consumed as they fulfill their protective function.

UV stabilizers and antioxidants are used in certain combinations, because very effective or powerful synergistic stabilization may be obtained for specific UV stabilizer/antioxidant combinations. Certain UV stabilizer-antioxidant combinations are antagonistic; i.e., they nullify each other's effect. Recent literature contains several examples of such synergistic and antagonistic combinations. This synergistic action may sometimes be interpreted in terms of molecular processes, but often the mechanism is obscure. Most of the rules of formulation are derived from empirical experimental data and experience.

D. PHOTOTHERMAL RANKING TESTS FOR MATERIALS

Preliminary degradation models that have been developed to date have been used to define a certain test protocol that may be used to rank encapsulant candidate materials and material formulations in terms of their long-term physiochemical stability and ability to fulfill performance requirements under accelerated stresses. In these tests, materials were exposed to accelerated solar ultraviolet fluxes, elevated temperatures, and variable oxygen levels. Separate tests also involved soaking materials in water and testing under high humidity levels. It is expected that most of these test conditions preserved the basic mechanisms of photo/thermal oxidative or hydrolytic degradation commonly observed in encapsulants deployed outdoors, although the "mix" of the degradation processes controlling degradation product ratios will be a function of stress magnitudes. Hence, photothermal test data can be utilized for prediction of long-term chemical changes only if a comprehensive degradation model is available that correlates rates of changes in chemical properties with environmental stresses for complex multistress environments. Such a comprehensive model is being developed for EVA (Springborn formulation A9918) by the University of Toronto (Ref. 6). Modeling of uncompounded EVA (Elvax 150) has been completed for a constant temperature test. Predictions from this model are discussed in Section III.C of this report.

Photothermal test data have another, more immediate application: ranking candidate materials for a specific encapsulation function. One approach to establishing ranking criteria might involve measurement of relevant performance parameters (chemical, optical, mechanical, thermal and electrical) as a function of aging time in a photothermal environment. This approach has potential pitfalls in that it assumes that changes in performance parameters measured in an accelerated test correlate with changes in the same parameters during outdoor deployment. The approach adopted in this report is somewhat different. Certain key chemical and physical properties have been identified that are expected to control long-term performance of the encapsulation design. Changes in these properties have been monitored in photothermal tests on candidate pottants and outer cover materials. A small test matrix has been developed for this.

E. MATERIAL PROPERTIES

The material properties described below were monitored during accelerated tests of candidate pottants and these properties were placed in order of priority with the limits defined as follows:

(1) Instrumental limit is the accuracy or reproducibility of the measuring instrument. Comparison of values below this limit is meaningless.

(2) Experimental limit is a statistical value related to specimen variations that must be exceeded to signify that the material property has changed due to photothermal aging, and not due to sampling variations.

Material properties described in this section can be used not only to rank existing candidate materials, but more importantly to screen new materials that will be developed in the future. A realistic ranking study should involve, at the minimum, application of the first three modes (E.1, E.2, and E.3) of detection and monitoring of material properties.

1. Absorbance/Transmission

Absorbance/transmission is measured on a UV-visible spectrophotometer in the wavelength range of 250 to 800 nm. Both direct and hemispherical absorbance measurements are desirable. Absorbance measurements should be made as a function of wavelength. In case equipment to perform this measurement is not available, measurement may be made at the following wavelengths: 320 nm, 360 nm, 380 nm, 400 nm, and 500 nm. Measurements in the ultraviolet region will indicate whether additives are being lost, or whether chemical degradation is taking place in the material. Absorbance increase at 400 nm correlates with yellowing. Although loss of transmission at 400 nm has little effect on the efficiency of the silicon solar cell, yellowing at 400 nm is the first indicator of degradation. Experimentally, it is easier to set limits in terms of percent transmission, with a typical instrumental limit being $\pm$1% transmission and experimental limit being $\pm$3% transmission at a particular wavelength. Integrated transmission (transmission of the total solar spectrum) instrumental limit is $\pm$0.2% transmission, with the experimental limit being $\pm$1% transmission. It is important to note that although gain in transmission may indicate polymer degradation due to loss of absorbers, it is only the loss in transmission that leads directly to loss of module performance.

2. Weight Loss

Weight loss instrumental limit is $\pm$0.1 mg, experimental limit is $\pm$0.3 mg. Weight loss measurements monitor loss of additives, loss of volatiles (e.g., acetic acid from EVA), and oxidation products; e.g., CO, CO_2, etc. In general, weight loss will correlate with shrinkage, which may cause cell cracking, delamination and other failure processes. It is important to follow the weight loss as a function of aging time in order to establish a behavior trend for ranking.

3. Mechanical Properties

Although modulus obtained by stress-strain measurement is essential engineering data, it may not render itself as a good ranking parameter because modulus, in most cases, is dependent on both physical entanglement of the polymer network and chemical crosslinking. The entanglement is insensitive to early stages of photothermal aging, whereas degree of chemical crosslinking can change quite extensively when samples are subjected to a photothermal aging process. On the other hand, swelling ratio measurement is very sensitive to detection of changes in chemical crosslinking. This technique may be preferred over measurement of tensile modulus for purposes of establishing the rate and trend of photothermal degradation at an early state. It is recommended that both types of measurement be carried out.

a. Stress-Strain Measurements. Instrumental limit: ±10% of the tensile modulus; experimental limit: ±20% of the tensile modulus. Measurement of mechanical properties is needed in order to predict deformation, creep, and yield stresses as a function of exposure period. In general, pottants are crosslinked to obtain a desirable modulus E ($200 < E < 2500$ psi). The lower limit of 200 psi has not been clearly defined. Photothermal aging will either increase the modulus as a result of crosslinking, or decrease the modulus by way of scission. During the initial period of photothermal aging, modulus tends to increase due to decomposition of the residual crosslinking agent regardless of the mode of subsequent photothermal degradation (crosslinking or scission) in the pottant. It is therefore important to establish the mechanism (mode) of degradation before ranking can be applied. Also, initial modulus of the ranked material and the rate of degradation are equally important in the ranking.

b. Swelling. Experimental limit: ±10% extraction of the sol content may be carried out by using a hot solvent such as toluene, MEK or tetrahydrofuran. Several hours (>3) of extraction are needed, preferably in a continuous extraction mode. The crosslinked materials should be exhaustively extracted. The sol/gel ratio may be used to predict the rate of creep at a given temperature. Molecular weight information can be obtained by running HPLC (High Pressure Liquid Chromatography) of the sol fraction. Swelling of the gel will yield swelling ratio and from this the degree of effective crosslinking can be obtained.

4. Density

Density instrument limit is ±0.1%; experimental limit: ±0.5%. Density measurements are specially useful for glassy polymers, which are candidate top and back cover films. Changes in density due to physical aging have been shown to correlate with changes in modulus and Poisson's ratio in glassy polymers.

5. Infrared Analysis

Infrared analysis is a well known analytical technique that can be used to measure changes in chemical structure.

6. Surface Energy Analysis

Surface energy analysis (SEA) may be carried out by measuring contact angles for a series of reference liquids and calculating the polar and dispersive components of the surface energy. Contact angle measurements using water have been employed as a useful measure of surface polarity and hydrophilicity.

SECTION II

ACCELERATED PHOTOTHERMAL TESTING: METHOD AND SETUP

A. INTRODUCTION

Accelerated testing is usually performed with one or more of the following objectives:

(1) Duplicate the overall outdoor degradation profile in a shorter time. [However, the magnitudes of the stress components (UV flux, temperature, humidity) may not scale linearly, and the scaling function and parameters for each stress may be different.]

(2) Duplicate a particular degradation process observed outdoors and determine the contribution of all of the environmental stresses in causing the specific degradation mode. These tests usually involve systematic variation of one stress, keeping everything else constant. This is a shorter term and more easily attainable objective and, when successful, contributes significantly to the overall understanding of the degradation mechanism.

In multi-stress accelerated tests, particularly those involving acceleration of more than one type of stress, particular care has to be taken in interpreting degradation data. In these tests, synergistic effects involving interaction of one type of stress with the initial (or primary) degradation products formed by another type of stress may dominate the effects of individual stresses. For example, accelerated photothermal aging under a pure oxygen environment may involve UV-induced reaction of chain radicals formed by photocleavage of carbonyl groups, an oxidation product. This reaction would not occur outdoors, and hence would constitute an artifact of the test conditions. For this reason, accelerated tests involving acceleration of more than two stresses are scarcely useful in a quantitative sense. Even in a "qualitative, worst-case scenario sense" they are not very useful, as one stress may actually inhibit, bleach out, or otherwise destroy degradation products formed by other stresses and hence not allow them to accumulate and contaminate the system. In such a case, multi-stress accelerated tests often tend to produce a higher estimate of life potential than is actually obtained in real-time outdoor testing.

In photothermal characterization, the initial emphasis has always been to evaluate the effects of accelerating a single stress factor (UV, temperature, O_2 level), keeping everything else constant. Once the ensuing degradation process is identified, it has been possible to accelerate two stresses simultaneously, and determine the effects of synergism between two stresses. As expected, synergism often dominates test results, but because the nature and magnitude of this synergistic effect can then be estimated, it is possible to test and validate the degradation model obtained from single-stress experiments under more extreme conditions.

B. PHOTOTHERMAL TEST DESIGN

The source of UV radiation used in these photothermal degradation tests was a filtered medium-pressure Hg arc lamp, approximatly 200 W/in. in power. The lamp was placed inside a water-cooled Pyrex jacket. An annular transparent Pyrex or quartz oil bath was then fitted around the jacket. The samples were mounted in the space between the Pyrex jacket and the quartz bath, and were in contact with the hot oil bath. The radiation facility is shown in Figure 2-1. Samples (3 in. x 1/2 in.) were mounted directly on the inner surface of the jacket in order to allow free access of oxygen (UV/ambient air). A sample may also be placed between sheets of Pyrex; the sandwich is then mounted on the bath. This arrangement (UV/sandwich) allows limited access of air and exaggerates edge effects, as illustrated in Figure 2-2. An edge seal may also be placed around the sandwiches in order to achieve virtual exclusion of air. Control experiments were also performed by aging materials in a dark oven, which was closed but full of air (dark/oven).

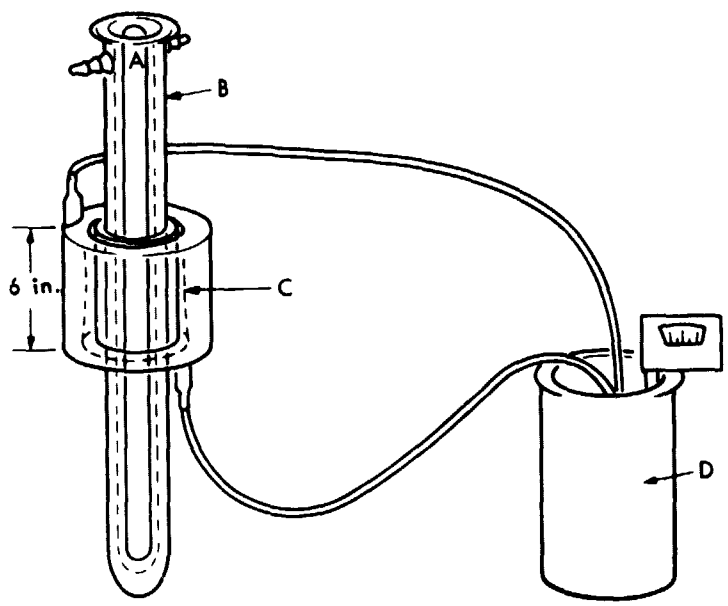

A = 450-WATT MEDIUM PRESSURE HG LAMP

B = PYREX H_2O COOLING JACKET

C = OIL JACKET

D = THERMOSTATICALLY CONTROLLED HOT OIL BATH (SAMPLE SPECIMEN PLACED BETWEEN C AND D)

Figure 2-1. Photothermal Radiation Apparatus

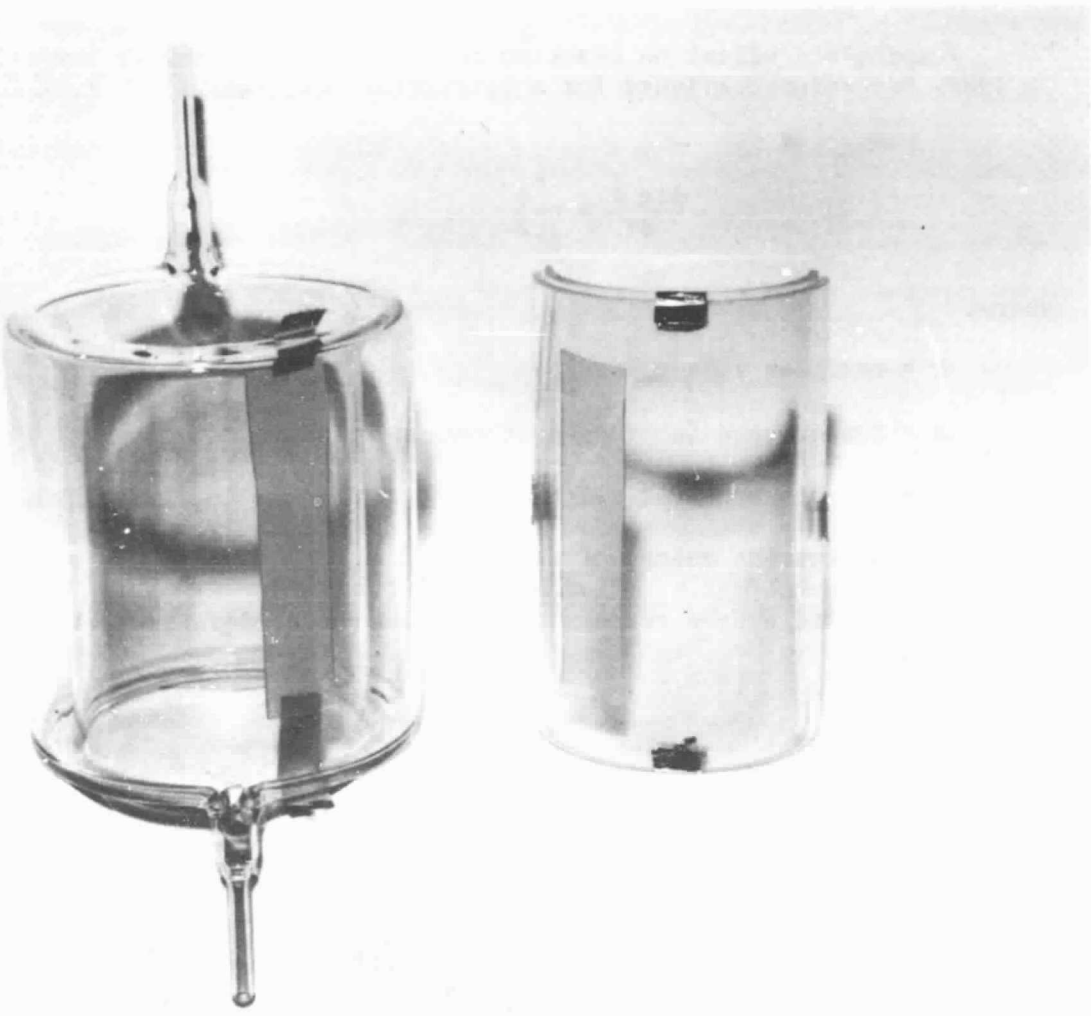

Figure 2-2. Photothermal Aging Sample Placement

Temperature and UV levels were monitored either continuously or at discrete intervals. By using a filtered selenium radiometer, UV levels may be continuously monitored. Such a radiometer is being developed and evaluated at JPL. A considerably different version of this radiometer is commercially available (Ref. 7). Test exposure period was 800 hours, and data were taken at 0, 50, 100, 200, 400, and 800 hours, if possible, in order to establish the trends of degradation. Eight-hundred hours of aging at 6 suns of equivalant UV is equivalent to approximately 3 years of outdoor exposure. This is by no means an adequate testing time to assess material lifetime potential of 20 years. The test period of 800 hours is set for ranking purposes only. In determining an appropriate ranking test period, considerations were given to establishing one that is long enough to establish the trend of degradation, yet short enough to be practical. Photothermal aging periods of longer than 800 hours are being carried out in order to determine and assess material lifetime potential.

C. ACTIVATION ENERGY

Temperature effect on reaction rate has been thoroughly investigated. In 1889, Arrhenius concluded for a particular reaction:

$$\frac{d\ln k}{dT} = \frac{E_a}{RT^2} \tag{1}$$

where,

k = reaction rate constant

T = temperature (expressed in degree Kelvin)

R = gas constant - 2 cal/mole

E_a = activation energy of this reaction

If E_a is constant over a certain temperature range, Eq. (1) yields on integration,

$$\ln k = \frac{-E_a}{RT} + \ln C \tag{2}$$

when $\ln C$ is the constant of integration, hence,

$$B = \frac{k_1}{k_2} = \exp - \frac{E_a}{R} \left(\frac{1}{T_1} - \frac{1}{T_2} \right) \tag{3}$$

where B is the relative rate of this reaction at temperature T_1 and T_2. Activation energy (E_a) can now be calculated according to Eq. (3) by measuring B, T_1 and T_2 experimentally. In general, physical processes have activation energy less than 10 kcal/mole, whereas chemical processes require much higher activation energy, ranging from 10 to 100 kcal/mole.

Throughout this report, activation energy (E_a) of various degradative processes have been listed. By inserting a specific value of E_a into Eq. (3), the rate of this particular degradative process at different temperatures can be calculated and can then be used to predict the extent of this type of degradation, at these temperatures, for various aging times. As a word of caution, activation energy is reaction-specific, and different reactions can get turned on or off as the temperature is varied. Therefore, activation energy can only be defined in a certain temperature range in which the reaction mechanism is conserved. Activation energies listed in this report were found to be constant in a certain temperature range. Extrapolation of any reaction rate beyond this temperature range must be substantiated by evidence that the degradation mechanism is conserved and/or that E_a is remaining independent of temperature for this mechanism.

SECTION III

PHOTOTHERMAL CHARACTERIZATION OF POTTANT MATERIALS

A. SCOPE OF TESTS

Photothermal testing of six pottant materials was initiated. These six pottant materials are listed in Table 3-1. Four of these six materials were tested in detail: ethylene/vinylacetate (EVA, Rawland), silicone rubber (RTV615, GE) polyvinylbutyral (PVB Saflex, Monsanto), and aliphatic polyurethane (PU, Quinn). Principal products of degradation have been identified and used in developing preliminary degradation models. Certain critical properties were also monitored in order to rank candidate materials in terms of their long-term stability under accelerated stresses. Table 3-2 illustrates a segment of the test matrix employed.

Samples were tested under two design configurations: (1) free suspended film with full oxygen access (UV/ambient air) and (2) samples sandwiched between two Pyrex plates with no edge seal; limited oxygen access (UV/sandwich).

PVB and PU readily degraded at 70°C during photothermal aging under the nonhermetic design, as might have been expected. Therefore, these two materials were not tested at temperatures higher than 70°C.

Table 3-1. Pottant Materials

MATERIAL	SOURCE AND IDENTIFICATION	ENCAPSULATION PROCESS
(1) ETHYLENE/VINYL ACETATE CLEAR 20-mil FILM	SPRINGBORN LABORATORIES ENFIELD, CT A9918	VACUUM-BAG LAMINATION
(2) SILICONE ELASTOMER	GE SILICONE PROD. DEPT. WATERFORD, NY RTV 615	LIQUID CAST (REQUIRES CATALYST)
(3) ALIPHATIC POLYURETHANE TWO-PART SYSTEM: (a) RESIN (3.86 PARTS) (b) CATALYST (1 PART)	H. J. QUINN Q626 Q621	LIQUID CAST
(4) POLYVINYLBUTYRAL SAFLEX	MONSANTO	VACUUM-BAG LAMINATION
(5) POLY-n-BUTYL ACRYLATE	JPL SPRINGBORN LABORATORIES (UNDER DEVELOPMENT)	LIQUID CAST
(6) ETHYLENE/METHACRYLATE	GULF OIL COMPANY TD 938 SPRINGBORN LABORATORIES	VACUUM-BAG LAMINATION

Table 3-2. Photothermal Test Matrix for Pottant Materials

TEMP, °C	AGING TIME, h / CONDITION	EVA	RTV	PVB	PU
30	DARK/OVEN	600	—	—	—
	UV/AMBIENT AIR	600	—	—	—
	UV/SANDWICH	600	—	—	—
55	DARK/OVEN	—	—	400	400
	UV/AMBIENT AIR	—	—	400	400
	UV/SANDWICH	—	—	400	400
70	DARK/OVEN	400	400	400	400
	UV/AMBIENT AIR	400	400	400	400
	UV/SANDWICH	400	400	400	400
85	DARK/OVEN	800	800	—	—
	UV/AMBIENT AIR	800	800	—	—
	UV/SANDWICH	800	800	—	—
105	DARK/OVEN	800	800	—	—
	UV/AMBIENT AIR	800	800	—	—
	UV/SANDWICH	800	800	—	—

B. PHOTOTHERMAL RANKING OF POTTANTS

In all of the formulated polymers, loss of additives is a potentially critical degradation mode that will limit weatherability of these materials. The rate of loss of additives is mostly controlled by the degree of access of the outside environment to the pottant material and is therefore controlled by design configurations. Hermetic design that can eliminate physical loss of additives as well as the access of oxygen to pottant material may not, however, be cost effective. In ranking the four materials or material formulations that were more extensively tested, considerations were given to their physio-chemical stability in a nonhermetic design. Figure 3-1 illustrates the change in transmission at 400 nm of pottant materials as a function of photothermal aging. Although there was no change (<0.5%) in transmission at 400 nm for RTV and EVA, a 5% and 15% loss of transmission at 400 nm was observed for PVB and PU respectively as a result of photothermal aging in air at 6 suns and 70°C for 400 hours. Figure 3-2 shows the weight loss profile of the same four pottant materials with respect to photothermal aging. Again, RTV and EVA were found to be stable (≤0.1% weight change) at 6 suns and 70°C in air for 400 hours. A weight loss of up to 0.5% was detected for PVB and 0.3% for PU during the same period. These two figures clearly demonstrate the superiority of RTV and EVA as formulated when compared to PVB and PU in their respective formulations. Other analyses such as stress-strain measurement, molecular

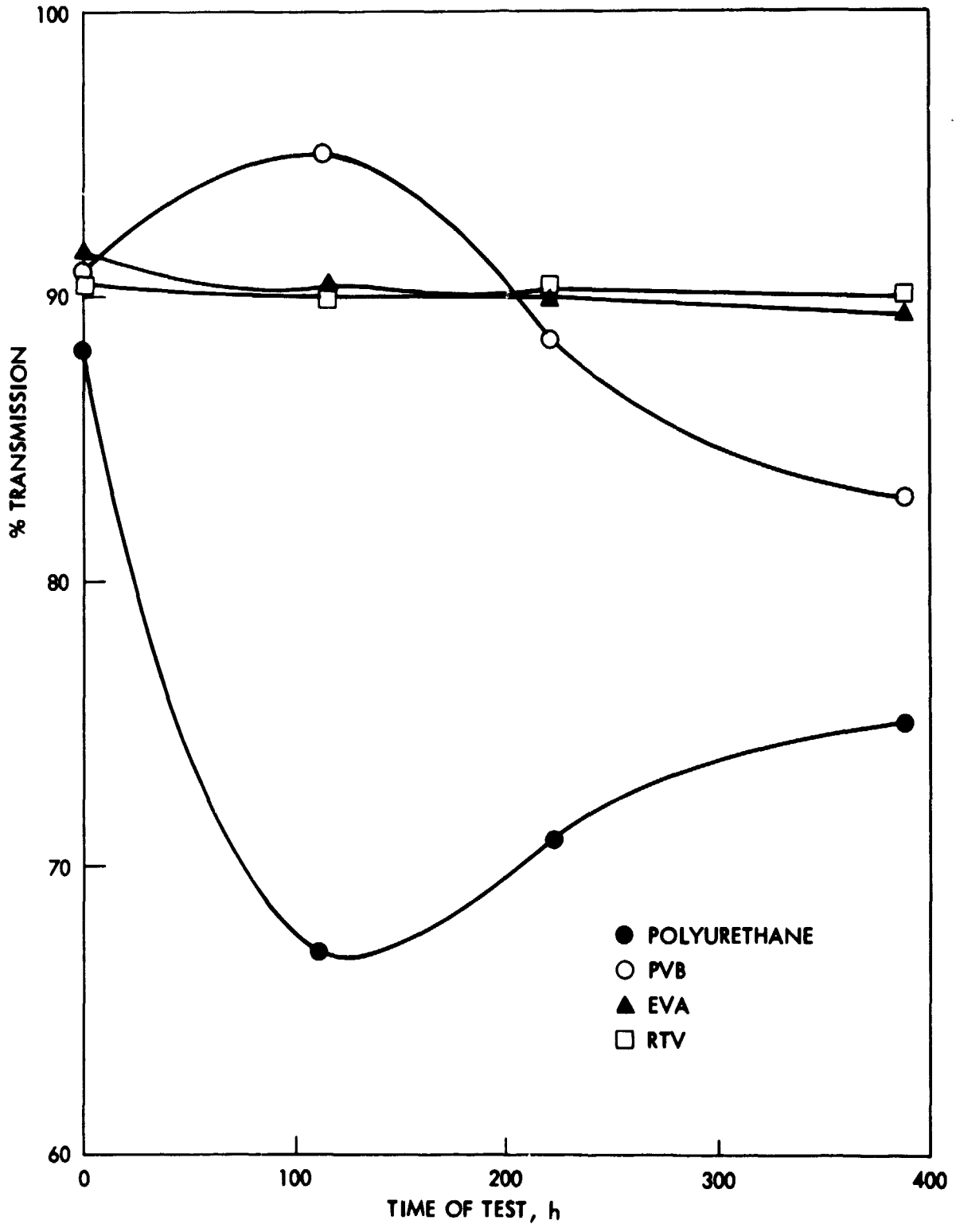

Figure 3-1. Change of Transmission at 400 nm of Pottant Materials as a Function of Photothermal Aging in Air at 6 suns and 70°C

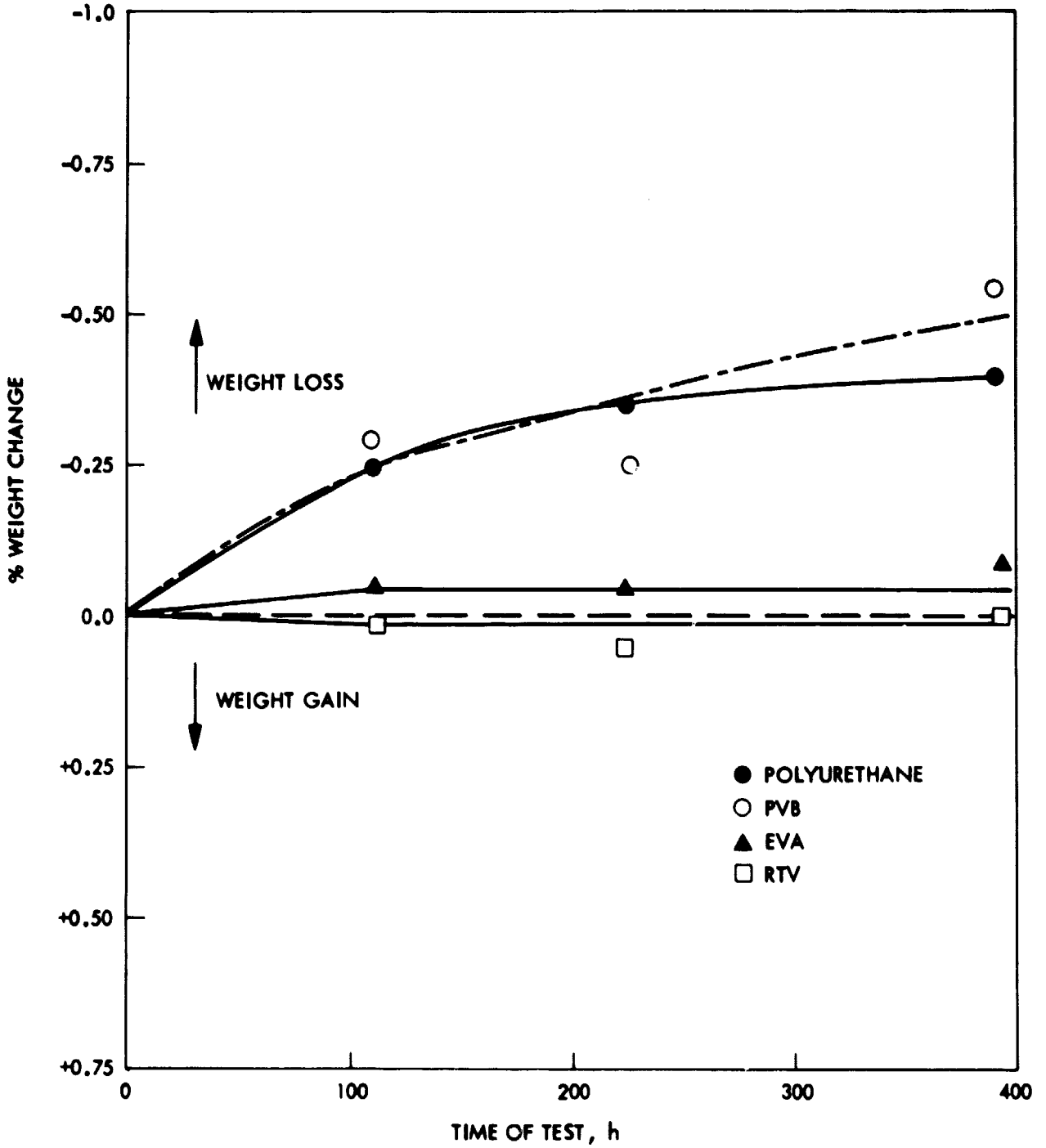

Figure 3-2. Percentage of Weight Change of Pottant Materials as a Function of Photothermal Aging in Air at 6 suns and 70°C

weight analysis, and FT-IR also show more extensive photothermal degradation of PVB and PU.

C. PHOTOTHERMAL TESTING OF EVA

EVA specimens were made by Springborn Laboratories (Enfield, Connecticut) and the formulation is shown in Table 3-3. This same formulation is being marketed by Roland, Inc. Photodegradation of EVA films was studied at room temperature (30°C). This mechanistic study later served as baseline for accelerated tests conducted at high temperatures (70 to 105°C). Samples were tested under 6 suns with nonhermetic designs as described in Section II.B.

Previous studies indicated that during exposure to UV and oxygen, ethylene vinyl acetate (Elvax 150, Du Pont Co.) undergoes: (1) chain scission, (2) crosslinking, and (3) formation of hydroxyl and carbonyl group as well as unsaturation (Refs. 8 and 9). These lead to changes in mechanical modulus and loss of optical transmission. During the photothermal testing of EVA A9918, it was found that EVA A9918 is physically stable at temperatures up to 80°C between two sheets of Pyrex. In the presence of air, photothermal oxidation becomes important at temperatures above 80°C, as evidenced by the detection of hydroxyl formation. Loss of additives also takes place under these conditions. Because EVA without additives undergoes degradation on outdoor exposure to UV and oxygen leading to yellowing, cracking and onset of creep within 1 to 2 years, loss of additives will be one of the rate-determining processes controlling its physical and chemical stability. The activation energy of the rate of loss of additives is approximately 5 $\pm$2 kcal/mole. Gradual weight loss of 1.5% had been detected when EVA A9918 was exposed to photothermal aging at 6 suns and 105°C in air for 800 hours. Chemical crosslinking was found to take place and crosslinking density increased from 10^{-6} mole/cm^3 to 10^{-5} mole/cm^3 during this period. The modulus also decreased as a result of photothermal aging in this period.

Table 3-3. Formulation of EVA A9918

COMPOUND	TRADE NAME	FUNCTION
ETHYLENE/VINYL ACETATE	ELVAX 150	ELASTOMER
2-HYDROXY-4-n-OCTYL BENZOPHENONE	CYASORB UV 531	UV ABSORBER
PHENYLPHOSPHITE ESTERS	NAUGARD-P	ANTIOXIDANT
BIS (2,2,6,6-TETRAMETHYL-PIPERIDINYL-4) SEBACATE	TINUVIN 770	UV STABILIZER
2,5-DIMETHYL-2,5-BIS-(t-BUTYL PEROXY HEXANE)	LUPERSOL	CROSSLINKING AGENT

Work by the University of Toronto shows that chemical and physical property changes in EVA show a substantial inhibition period, followed by an autocatalytic loss of chemical and physical integrity (Ref. 6). Figures 3-3 and 3-4 show calculated plots of concentration of alcohol (ROH) and alkene vs. aging time. One method to ensure physical stability of EVA would be to extend the inhibition period to 20 years. It was also shown by this work that during this inhibition period potentially harmful chemical products (e.g., alcohols, acids) gradually build up in the pottant even in the presence of additives. These chemicals could cause corrosion of the interconnects, metallization, and delamination. These slow chemical processes during the inhibition period may be further slowed down by using either a hermetic design (no oxygen) or advanced stabilization techniques currently under development by the project. Photothermal characterization of these advanced EVA materials requires simultaneous monitoring of stabilizers and degradation products. This may be accomplished by simultaneous monitoring of change in absorbance at 320 and 420 nm, as well as of weight loss and changes in FT-IR.

1. Photodegradation of EVA at 30°C

a. Loss of Additives. In EVA and all other formulated polymers, loss of additives is a critical degradation mode that will limit weatherability of these materials.

Ethylene/vinyl acetate copolymer (EVA A9918) was obtained in the stabilized and cured formulation from Springborn Laboratories, Inc., Enfield, Connecticut. The formulation is outlined in Table 3-3. Figure 3-5 illustrates the UV-VIS absorption spectra of various components present in this formulation. Their absorption coefficients at 275 to 360 nm have been measured in order to calibrate concentrations of individual components in the formulated EVA. Samples of EVA were cut into 1 x 5-cm strips and were irradiated with light from a Pyrex-filtered medium pressure Hg (Hanovia) lamp. Actinometric and spectroradiometric measurements on the lamp have been previously described (Ref. 10). Figure 3-6 shows the absorption spectra of two extracts of a 20-mg sample sonicated for 20 minutes in 20 ml of CH_2Cl_2. It clearly demonstrates that 20 minutes of sonication is adequate to extract >95% of the extractables. Only Cyasorb® has appreciable absorption in the 280 to 360-nm region, and its concentration in formulated EVA can be calculated from its absorption coefficient and the absorption spectra of the extract. The concentration of Cyasorb was found to be 0.1% in these EVA samples furnished by Springborn. This is equivalent to only one third of the Cyasorb added in the original formulation (Table 3-3), implying that two thirds of this UV stabilizer must have been lost during processing (i.e., extrusion, curing, etc.).

When EVA was exposed to Pyrex-filtered irradiation (290 to 400 nm) for varying periods of time, the UV-VIS absorption spectra of the extracted Cyasorb remained unchanged. The extract was evaporated to dryness under nitrogen and the residues were dissolved in enough chloroform to make a 0.1% W/V solution. Part of the chloroform solution was used for HPLC analysis. The low molecular weight components (e.g., the residual curing agent and stabilizers) were analyzed using two capillary columns packed with μ-styragel (2 x 100 Å). Figure 3-7 illustrates a typical HPLC chromatogram and Figures 3-8 and 3-9 show the changes in additive concentration as a function

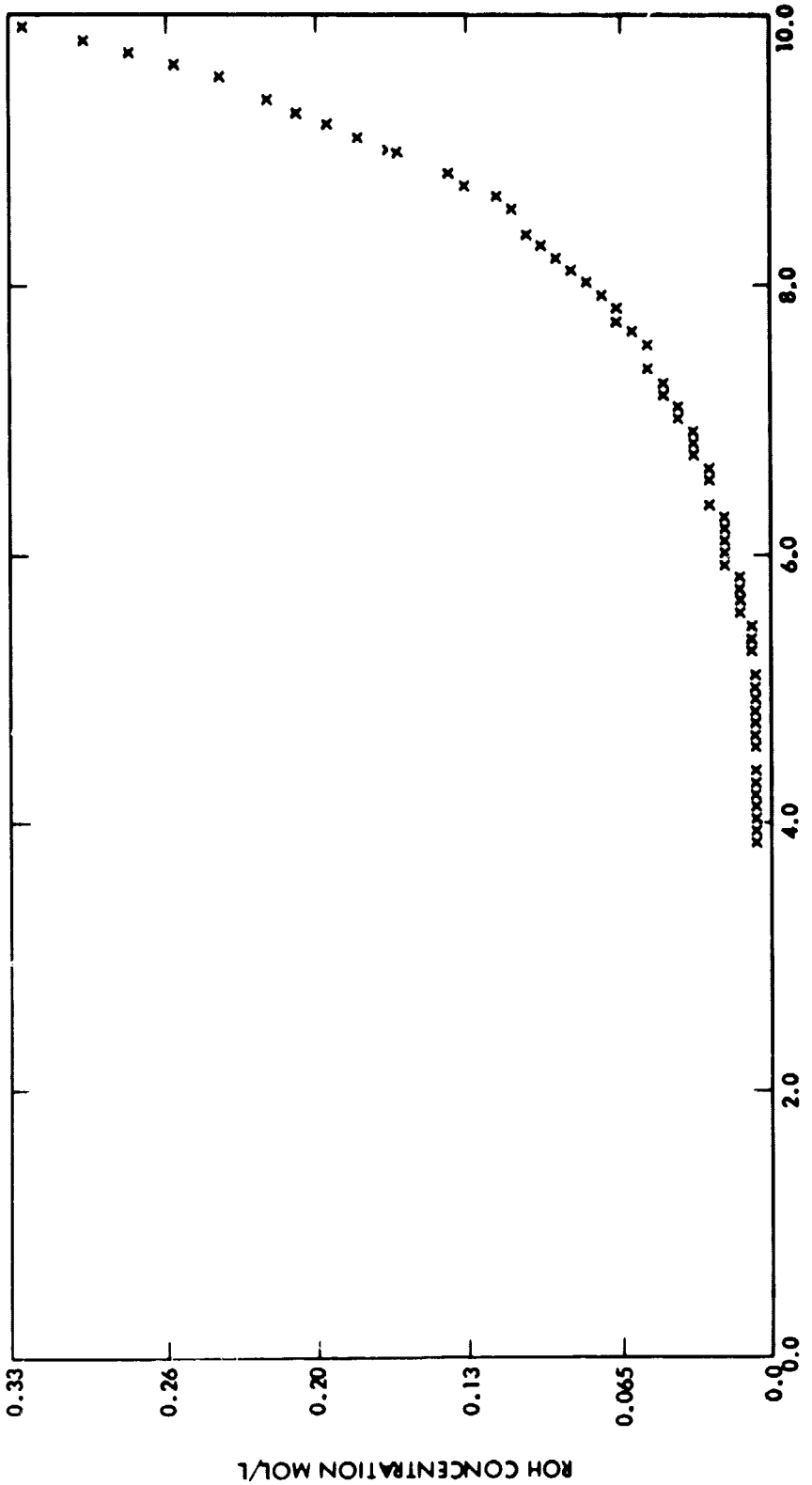

Figure 3-3. Calculated Alcohol (ROH) Concentration as a Function of EVA Outdoor Exposure (from the Annual Report, University of Toronto)

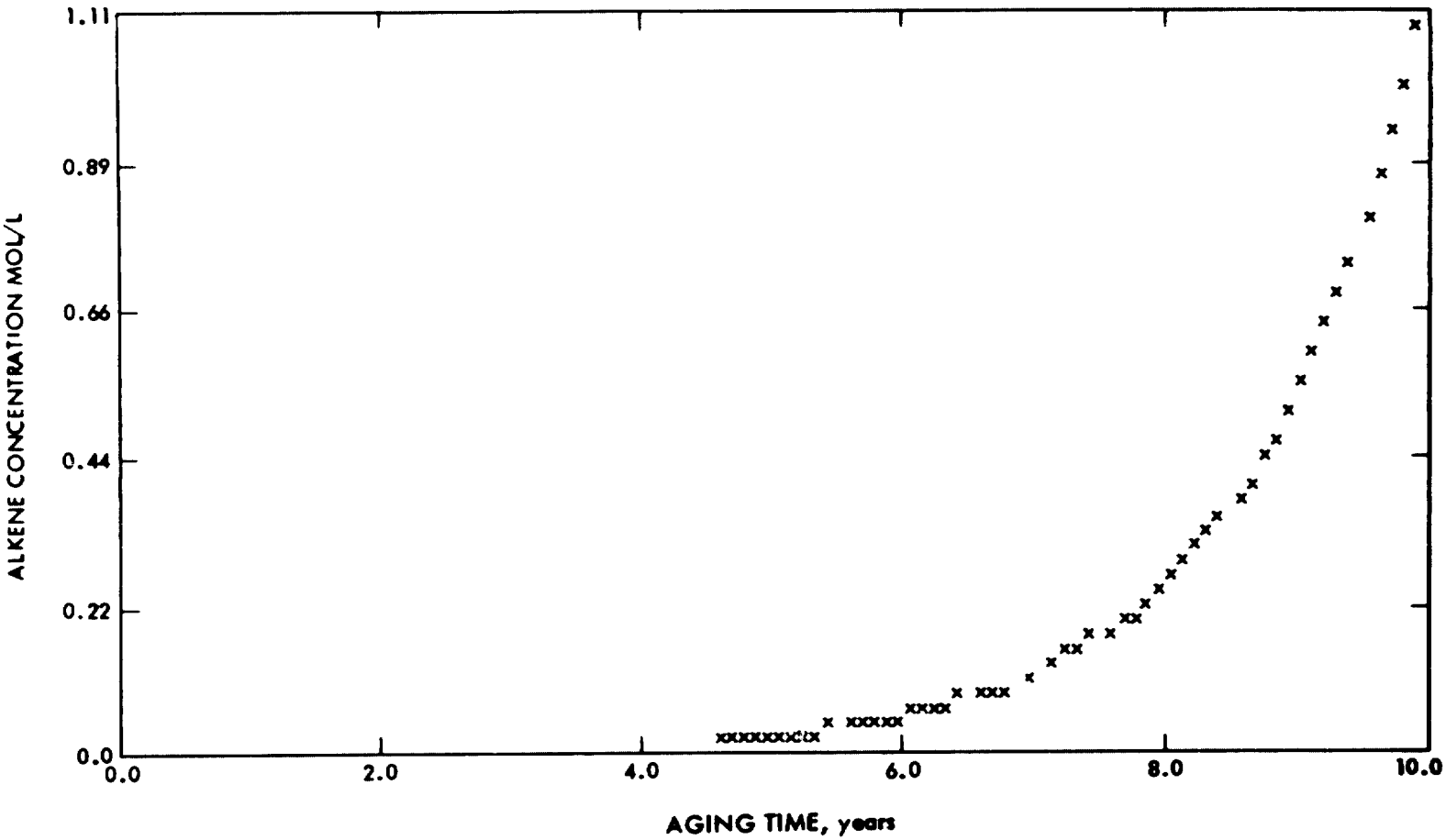

Figure 3-4. Calculated Alkene Concentration as a Function of EVA Outdoor Exposure (from the Annual Report, University of Toronto)

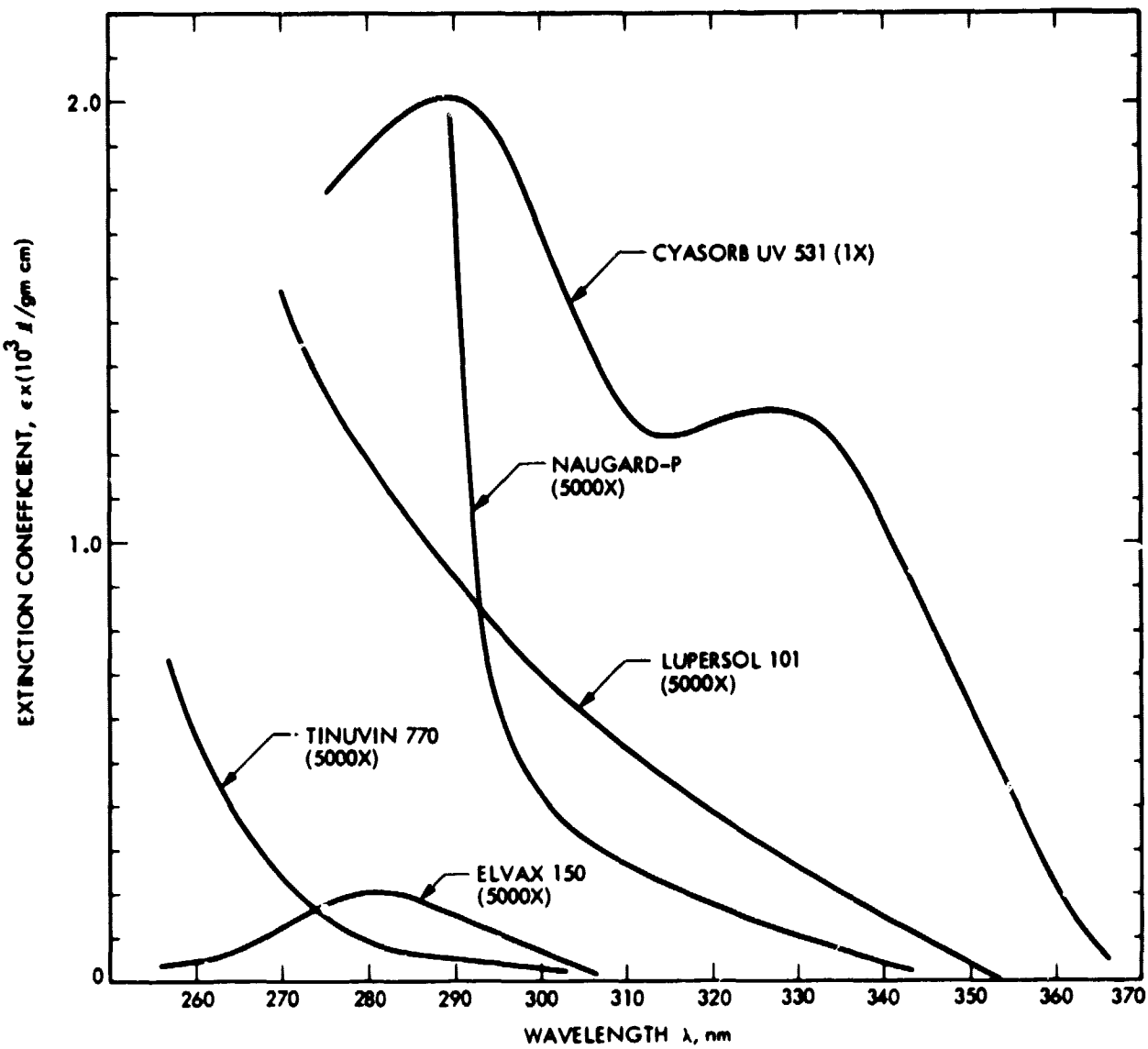

Figure 3-5. UV-VIS Absorption Spectra of Each Component in Formulated EVA A9918

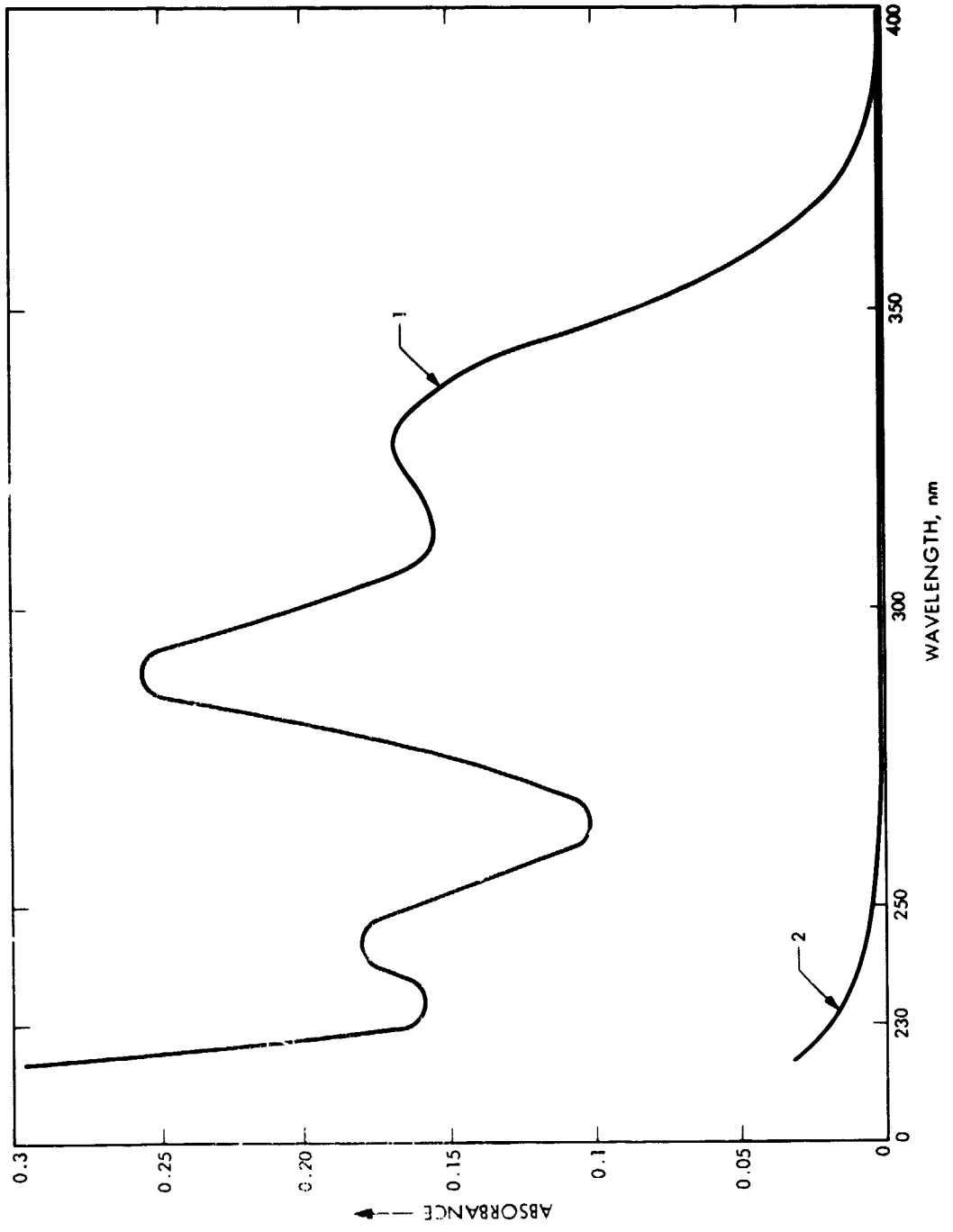

NOTE: (1) first extraction, (2) second extraction. Each extraction consisted of 20 mg of EVA in 20 ml of CH_2Cl_2, sonicated for 20 minutes.

Figure 3-6. UV-VIS Absorption Spectra of CH_2Cl_2 Solution Extracts of EVA A9918

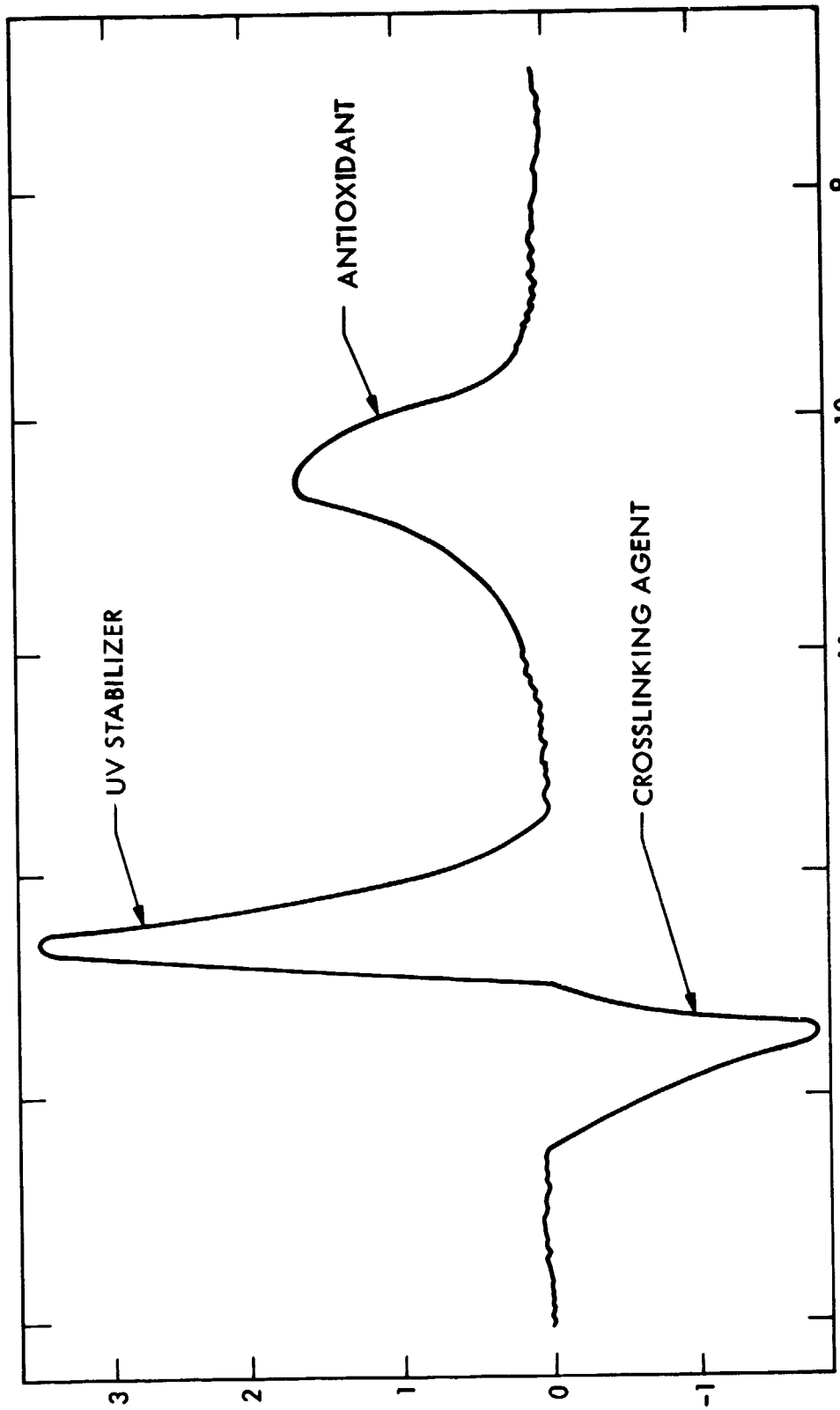

Figure 3-7. HPLC Chromatogram of CH_2Cl_2 Solution Extracts of EVA A9918

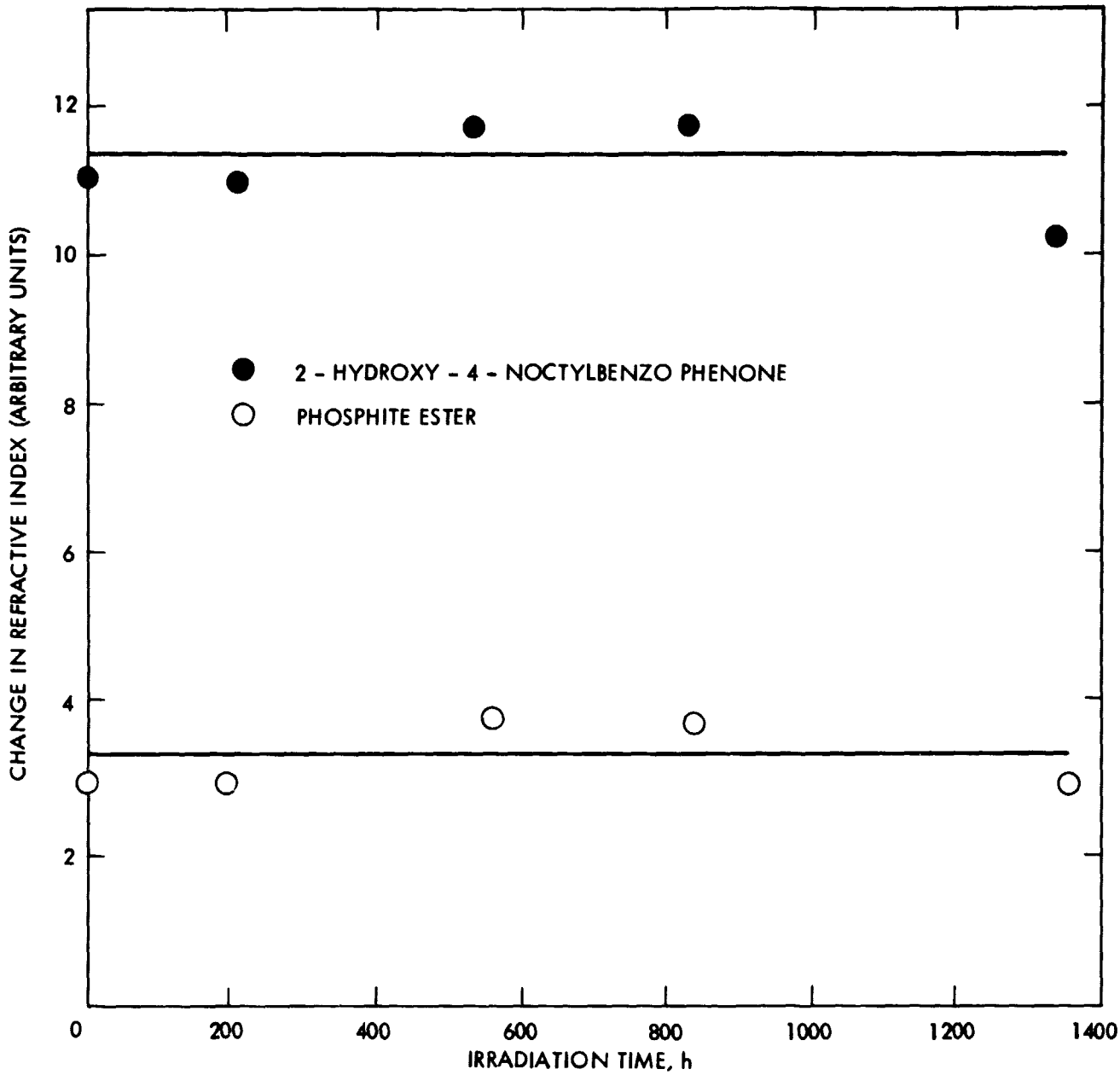

Figure 3-8. Concentration of UV Absorber and Antioxidant of EVA A9918 as a Function of Photo-Aging at 6 suns, 30°C, in Air as Detected by HPLC

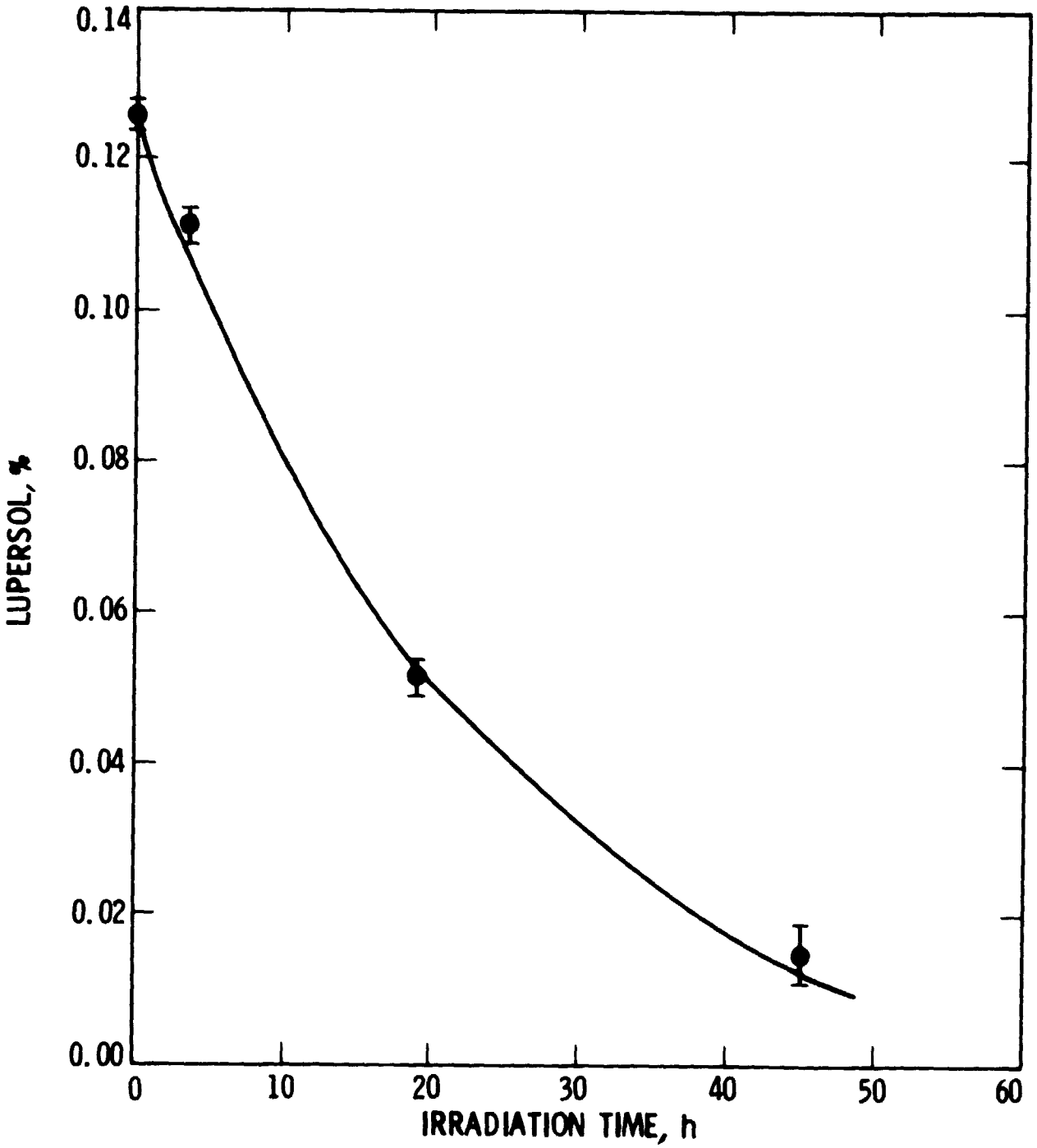

Figure 3-9. Concentration of Residual Curing Agent of EVA A9918 as a Function of Photo-Aging at 6 suns, 30°C, in Air as Detected by HPLC

of exposure period. Although there was no change in the UV absorber and anti-oxidant concentration (Figure 3-8), there was an efficient removal of residual curing agent (Figure 3-9) through photolytic cleavage induced by energy transfer from Cyasorb (Ref. 11).

b. Oxidation. FT-IR was used to detect oxidation in EVA. Samples of EVA were irradiated and extracted as previously described. FT-IR spectra of the extracted residues were generated by evaporating a known amount of the 0.1% W/V chloroform solution on KBr plates. Figure 3-10 shows the normalized difference in IR intensities. There is a slow increase in the intensity of the hydroxyl absorption at 3360 cm^{-1}. The slow hydroxyl formation of the extracted uncrosslinked polymer as a function of exposure could be generated by insertion of O_2 to form hydroperoxide and subsequent decomposition of the hydroperoxide. The fact that unexposed specimens remained unchanged leads to the proposed thesis that the observed photo-oxidation was caused by an energy transfer from the excited state of Cyasorb.

c. Chain Scission and Mechanical Properties. To assess the occurrance of chain scission, EVA samples were irradiated and extracted as before. The extracted solution was evaporated to dryness under nitrogen and 0.1% W/V of the residue in chloroform was made. This solution was used for HPLC analysis of the molecular weight (e.g., uncrosslinked polymer) using 4 μ-styragel columns (10^5, 10^4, 10^3, 500). Table 3-4 shows the weight loss and the molecular weight distribution of the uncrosslinked polymers. No significant change in molecular weight distribution or percent weight of extractable were found.

Table 3-4. Percent of Weight Loss Due to Ch_2Cl_2 Extraction and Molecular Weight Distribution of the Extract of EVA Irradiated at 6 suns, 30°C, in Air

UV IRRADIATION TIME, h	% OF EXTRACTABLE	$\overline{M}_n$	$\overline{M}_w$	$\overline{M}_w/\overline{M}_n$
0	21	35,000	101,000	2.91
168	23	38,000	114,000	3.01
524	23	34,000	112,000	3.26
836	22	41,000	116,000	2.84
1078	22	35,000	106,000	3.00
1388	20	38,000	108,000	2.88

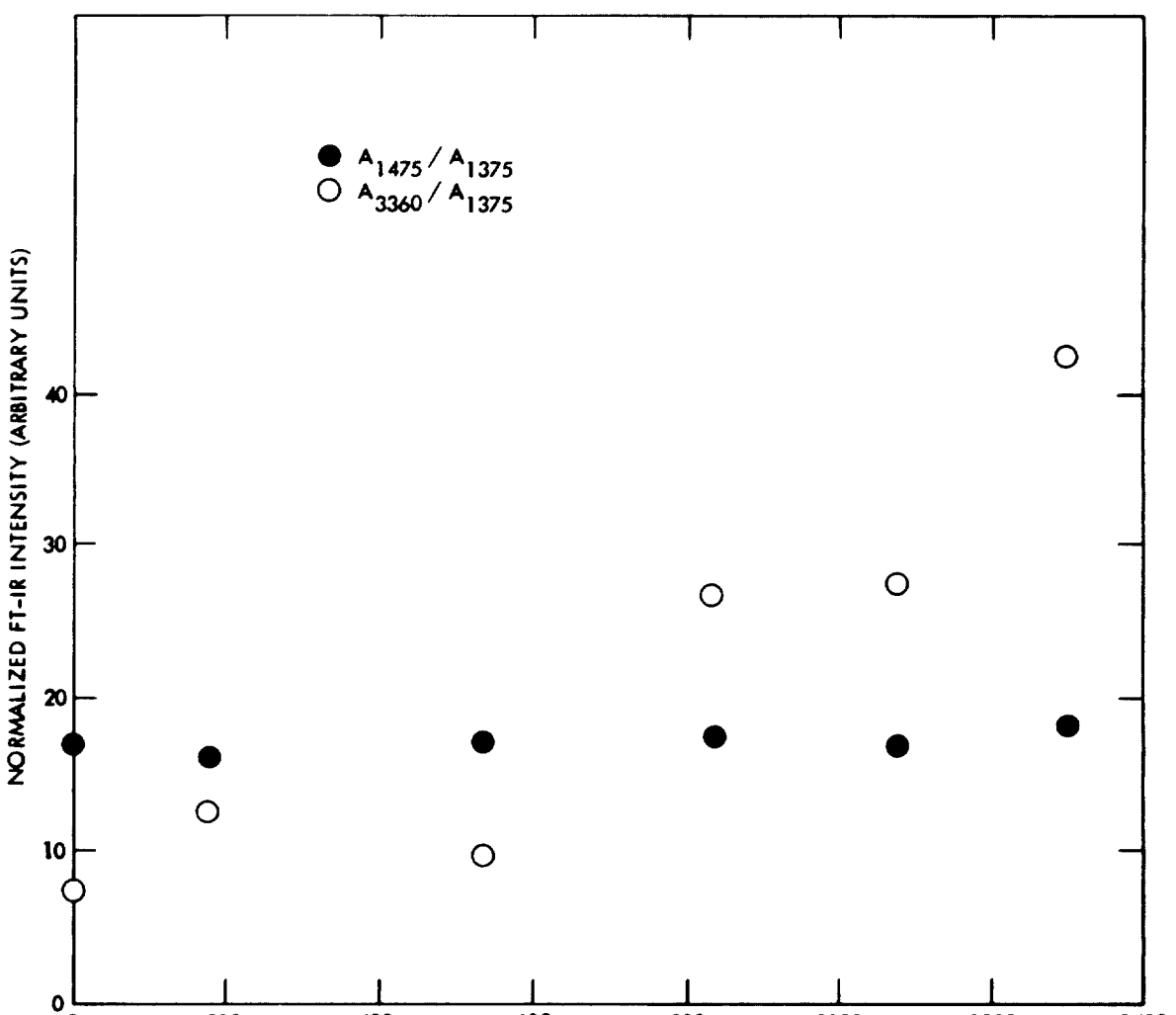

NOTE: A_{1475}, A_{1375} are absorbance of $-CH_2$ vibration, A_{3360} is absorbance of -OH vibration.

Figure 3-10. Normalized FT-IR Intensities of EVA A9918 as a Function of Photo-Aging at 6 suns, 30°C, in Air

d. Optical Properties. Samples were irradiated and extracted. The swollen films were then immersed in CH_2Cl_2 and their UV-VIS spectra obtained. Figure 3-11 shows a normalized absorption spectra of the cross-linked EVA film as a function of irradiation. Spectra indicate initial formation of conjugated carbonyl chromophores absorbing at the near-UV (400-nm) region, which subsequently reached a photostationary equilibrium.

2. Photothermal Degradation of EVA (70 to 105°C)

Degradation studies of EVA were performed at elevated temperatures using three different oxygen environments (see Section II.B, Test Design): full access of air (UV/ambient air), oxygen access through edges only (UV/sandwich), and a closed stagnant oven (dark/oven). Ultraviolet levels of 6 suns (295 to 370 nm) were used to expose these samples, except those in the oven, which were not exposed to UV. Actinometric and radiometric measurements were carried out as previously described (Ref. 10).

a. Optical Properties. Transmission data show no change in transparency at wavelengths longer than 450 nm. Figures 3-12 (A) and 3-13 (A) illustrate absorbance change as a function of thermal aging (dark/oven) at 400 nm and 360 nm, respectively. There is a definite increase in absorption at wavelengths longer than 400 nm for the thermally aged samples, which causes the sample to appear yellow. This yellowing, observed only in oven-aged samples, has also been reported by Solar Power Corp. Transmission at 360 nm and shorter wavelengths shows a definite increase, which is caused by gradual loss of the UV absorber. The data at 360 nm and 500 nm taken together demonstrated that the yellowing effect shows up best at 450 nm, as there is no compensating increase of transmission due to the loss of the UV absorber at this wavelength. At 360 nm, however, the increase in absorption due to yellowing is more than compensated for by the gain in transmission due to the loss of UV absorber, and hence there is a net gain in transmission at 360 nm.

Transmission changes of photothermally aged samples, as can be seen from Figures 3-12 (B,C) and 3-13 (B,C), indicated contribution by three processes: (1) loss of additives, (2) buildup of polymer photo-products, and (3) bleaching of these photo-oxidation products. Loss of additives such as the UV absorber causes a gain in transmission at 360 nm without causing any change in transmission at 400 nm. Buildup of photo-oxidative products initially causes yellowing; i.e., increase in absorption at 400 nm and a greater rate of increase at 360 nm. This increase in absorption then causes accelerated photolysis, which in turn leads to bleaching of these absorbing species. The result is attainment of a photostationary equilibrium in transmission at 400 nm, as shown in Figure 3-12 (B,C). Absorption at 360 nm is clearly dominated by the contribution from the UV absorbers and the loss of UV absorber therefore results in gradual increase in transmission at 360 nm. Using the absorption data, it can be estimated that the photoproducts formed via photothermal degradation actually absorb eight times more light at 360 nm than they do at 400 nm (i.e., $\epsilon_{360} = 8\ \epsilon_{400}$), but this increase in absorption is more than compensated for by the decrease in absorption of UV absorber. Thus, the transmission also attains a photostationary equilibrium at 360 nm, as can be seen from Figure 3-13 (B,C). Quantitatively, loss of UV

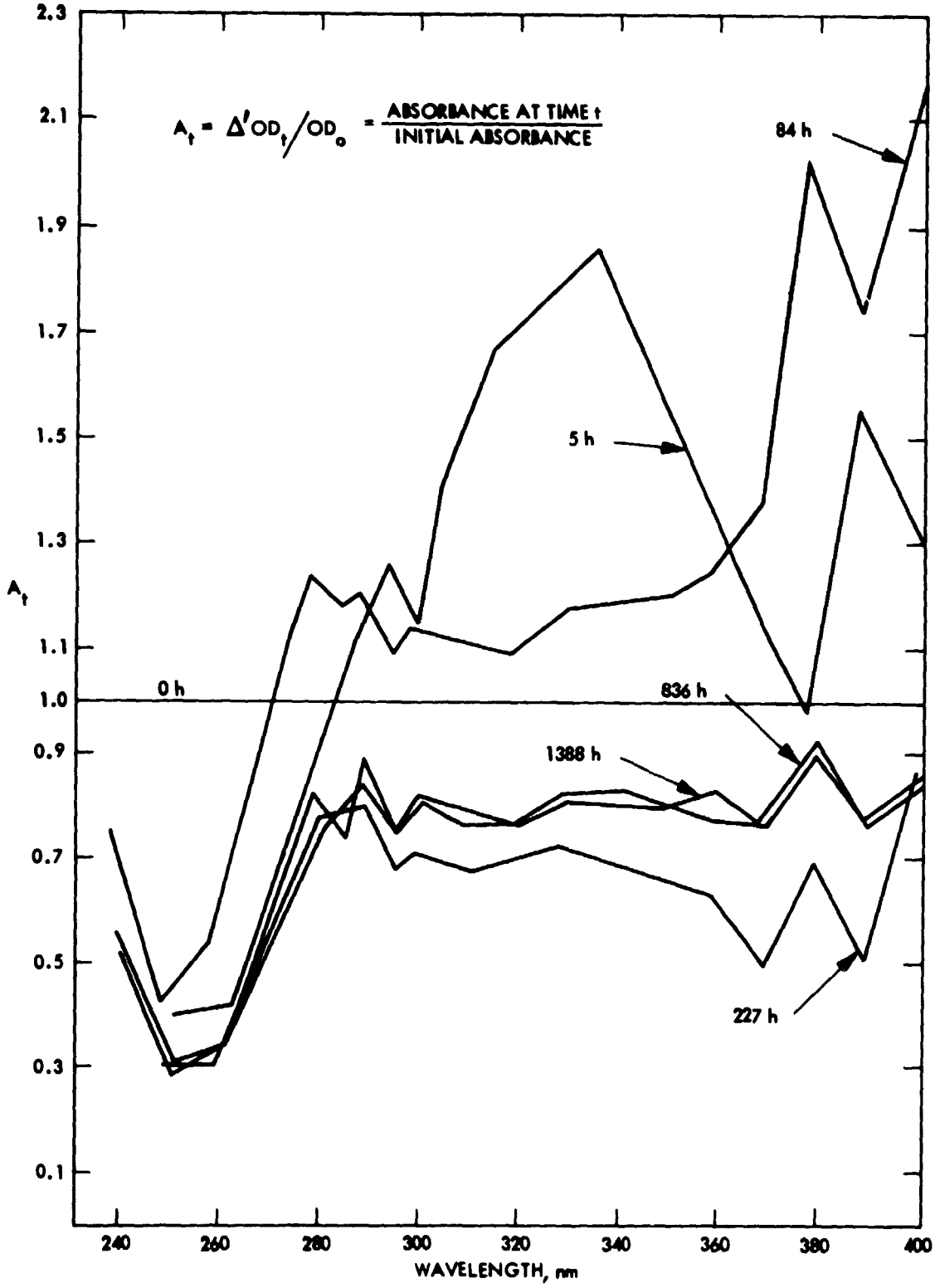

Figure 3-11. Normalized UV-VIS Absorption Spectra of EVA Film A9918 as a Function of Photo-Aging at 6 suns, 30°C, in Air

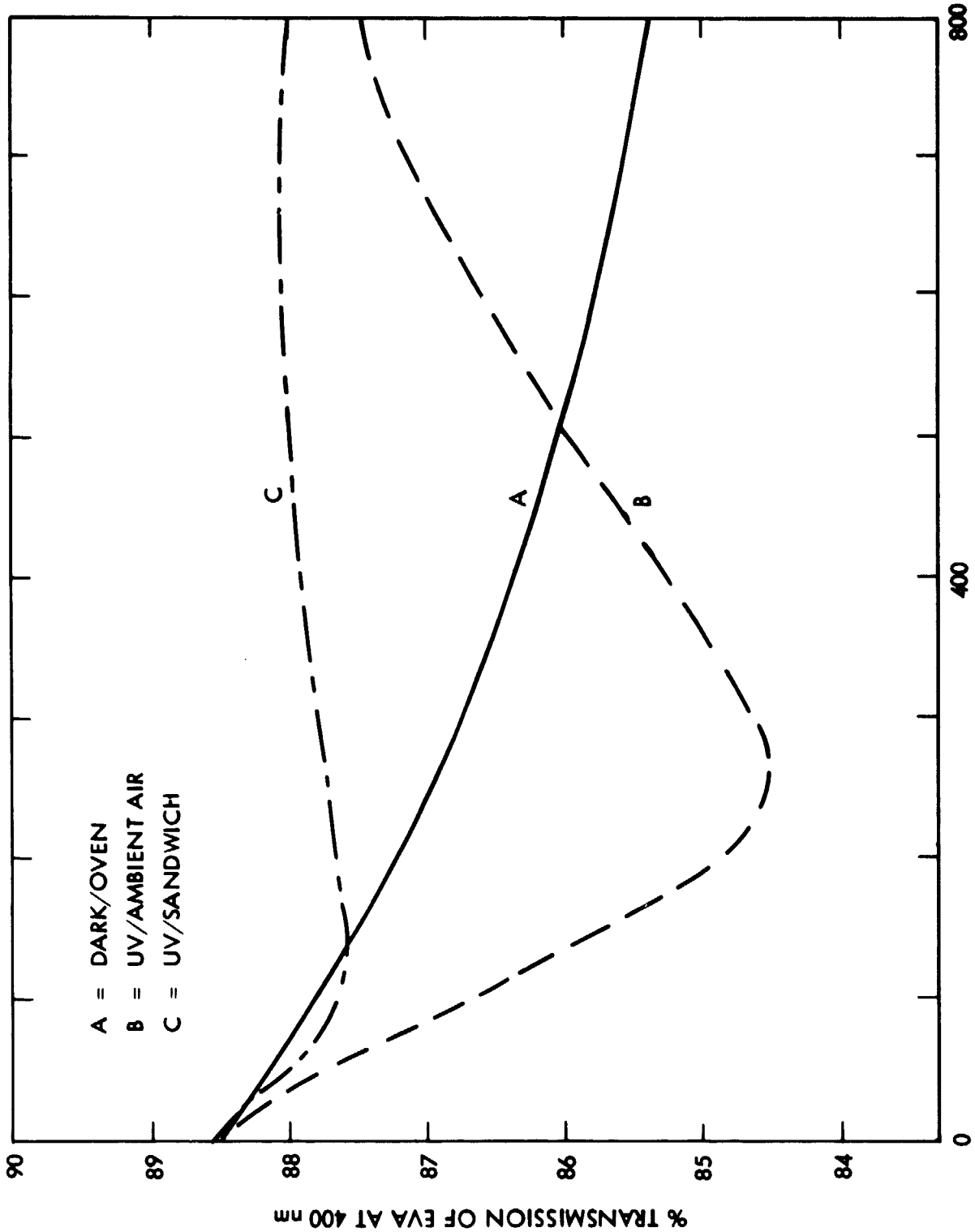

Figure 3-12. Change in Percent Transmission at 400 nm of EVA Films A9918 as a Function of Photothermal Aging at 6 suns and 105°C

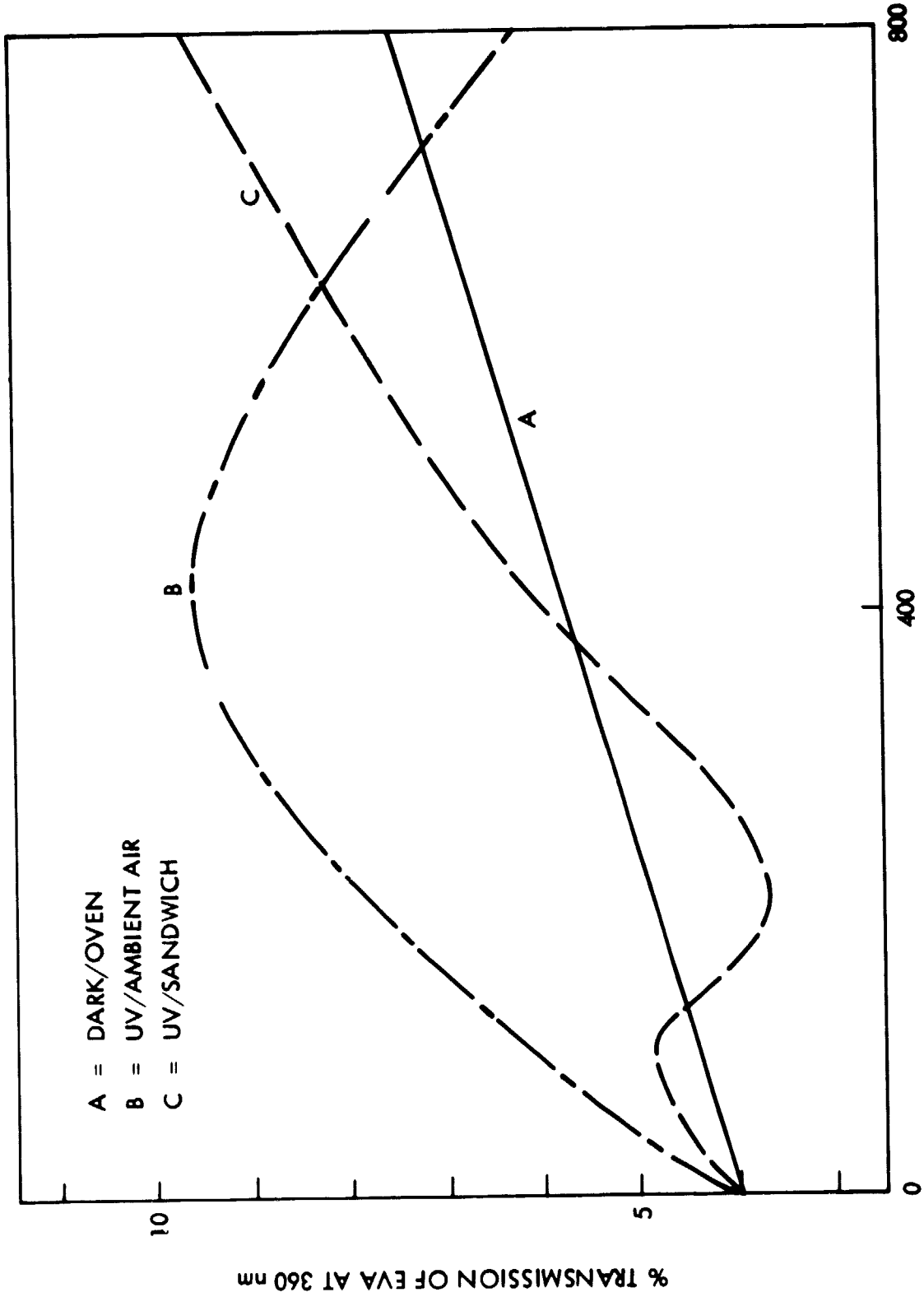

Figure 3-13. Change in Percent Transmission at 360 nm of EVA Film A9918 as a Function of Photothermal Aging at 6 suns and 105°C

absorber can be estimated from Figure 3-12 and Figure 3-13, and the relationship $360 = 8\,\epsilon_{400}$ for the photothermal-degraded products.

It is important to note that the EVA readily turns yellow when heated to 105°C in the absence of UV radiation in a dark oven; nevertheless, loss of optical transmission will not be a failure mode for EVA and photothermal aging.

b. Oxidation. The room temperature studies of EVA (see Section III.C.1) identified rapid destruction of peroxide and a slow formation of hydroxyl group as the principal degradation modes at 30°C. Literature from Du Pont (Ref. 12) describes the process of formation of acetic acid from unformulated EVA at 175°C and higher temperatures. Infrared spectroscopic evidence was found of acetic acid being formed after 800 hours of accelerated aging (at 85°C) and of a faster rate of formation of hydroxyl group at 105°C after 800 hours. The sealed samples (UV/sandwich) had significantly higher concentration of acetic acid than the oven-aged samples, while very little or no acetic acid can be detected in the open (UV/ambient air, Figure 3-14). In a stagnant oven, a certain degree of evaporation of the acetic acid can be achieved, while in a sealed sample (UV/sandwich), most of the acetic acid formed is retained.

Formation of acetic acid and hydroxyl group may cause corrosion of metallic components, resulting in failure at or around hot spots, particularly in superstrate modules containing EVA.

c. Weight Change. Weight loss data have been collected at 70°C, 85°C, and 105°C. They all exhibited similar profiles as a function of aging time. At 70°C, gradual weight loss, up to 0.5% after 500 hours of aging, which is equivalent to 2 years of outdoor UV exposure, was observed. At 85°C, weight loss of up to 1% was observed after 800 hours of aging (3 years outdoors). Figure 3-15 illustrates the weight loss profiles of EVA samples aged at 105°C.

Together with the FT-IR results (Section III.C.1.b), these weight loss data can be interpreted in terms of the following three sequential processes: (1) loss of additives, (2) oxygen uptake through photothermal oxidation leading to formation of volatile products (i.e., hydroxyls), and (3) evaporation of the volatile products. Weight loss is a result of processes (1) and (3), while process (2) leads to weight gain.

Initially, all three samples of EVA experienced a linear weight loss region due to physical loss of additives. Subsequently, they all leveled off to a different percentage of weight loss. Figure 3-16 is used to interpret the data. In the UV/sandwich sample (Figure 3-16a), where process (3) is not important, the difference between the actual weight loss and the extrapolated weight loss due to the loss of additives is the result of total oxygen uptake through oxidation. In the dark oven sample (Figure 3-16b), the additional weight loss (BC) must be due to partial evaporation of the acetic acid in a stagnant oven. In the open (UV/ambient air) sample, BD represented the total amount of acetic acid (or volatile products) formed and evaporated, and AD represented the amount of oxygen uptake through oxidation to form the nonvolatile products. Additional information can be obtained from these

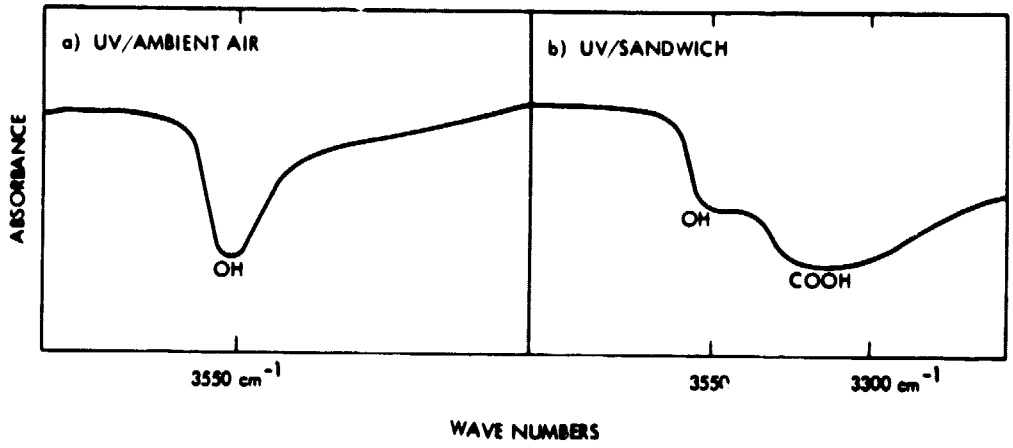

Figure 3-14. Difference in FT-IR Spectra of EVA Film A9918 Photothermally Aged at 105°C and 6 suns for 800 hours in (a) UV/Ambient Air; (b) UV/Sandwich

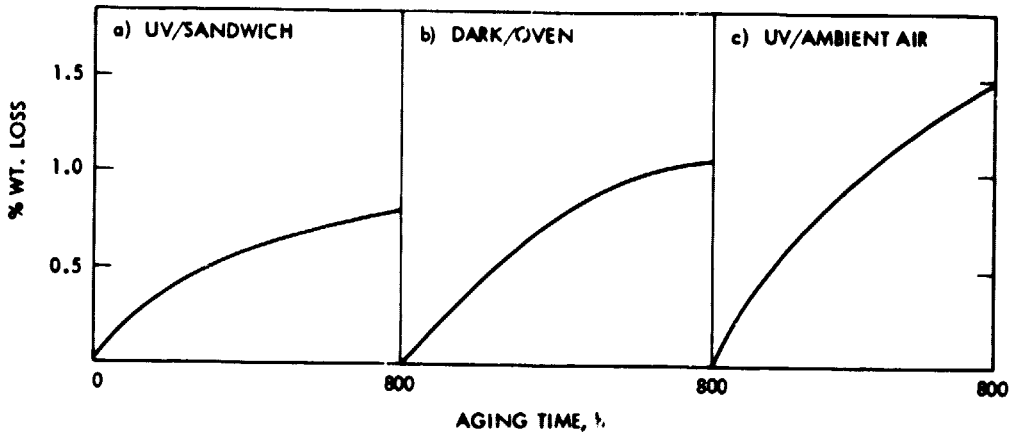

Figure 3-15. Weight Losses of EVA Film A9918 as a Function of Photothermal Aging at 6 suns and 105°C

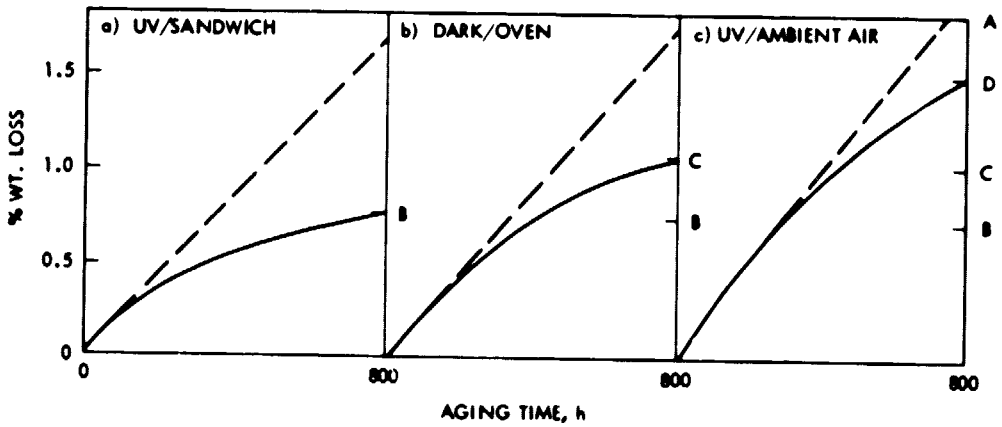

Figure 3-16. Possible Interpretation of the Weight Loss Profiles of EVA Film A9918 as a Function of Photothermal Aging at 6 suns and 105°C

weight loss data measured at different temperatures. Rate of loss of additives at 105°C can be estimated from the initial slope of weight loss in Figure 3-16. When this rate is compared with that obtained at 85°C, energy of activation of the weight loss process is calculated to be 7 kcal/mole, a typical value for physical processes.

d. Chain Scission and Mechanical Properties. Stress-strain measurements were carried out before and after aging in order to determine the change in tensile modulus due to photothermal aging; these measurements are shown in Figure 3-17. The apparent tensile modulus decreases on photothermal aging. A portion of the aged samples was exhaustively extracted in a Soxhlet apparatus for 165 hours in 200 ml of spectrograde CH_2Cl_2. The gel fraction was dried in a vacuum oven (20 Torr, 40°C) to constant weight. Weight percent of extractables was thus determined. The sol fraction was evaporated to dryness under nitrogen and the residues were dissolved in enough chloroform to make a 0.1% W/V solution. This solution was used for HPLC analysis to determine the molecular weight of the extractables. Table 3-5 summarizes the results of the molecular weight analysis. The decrease in percent weight of extractable, the increase in crosslinking density, and the decrease in apparent modulus demonstrate that EVA undergoes crosslinking as a result of photothermal aging. The decrease in apparent tensile modulus is puzzling and needs additional clarification. It is well recognized that equilibrium tensile modulus increase as the material crosslinks. Data obtained from a routine stress-strain experiment, however, give apparent tensile modulus. For material with low crosslinking density such as EVA, it can be shown that its apparent tensile modulus is expected to decrease due to crosslinking.

Table 3-5. Percent of Extractable, Molecular Weight Distribution ($\bar{M}_w$) of the Extract and Crosslinking Density of EVA as a Function of Photothermal Aging at 6 suns

TEMPERATURE, °C	TIME OF TEST, h	TEST CONDITIONS	% EXTRACTABLE	$\bar{M}_w$	CROSSLINKING DENSITY, mole/cm³
CONTROL		AS RECEIVED	48	206,000	1.12×10^{-6}
85	800	DARK/OVEN	35	168,000	2.29×10^{-6}
		UV/AMBIENT AIR	33	118,000	4.32×10^{-6}
		UV/SANDWICH	29	75,000	7.80×10^{-6}
105	800	DARK/OVEN	37	174,000	1.33×10^{-6}
		UV/AMBIENT AIR	33	91,000	5.86×10^{-6}
		UV/SANDWICH	34	44,000	10.10×10^{-6}

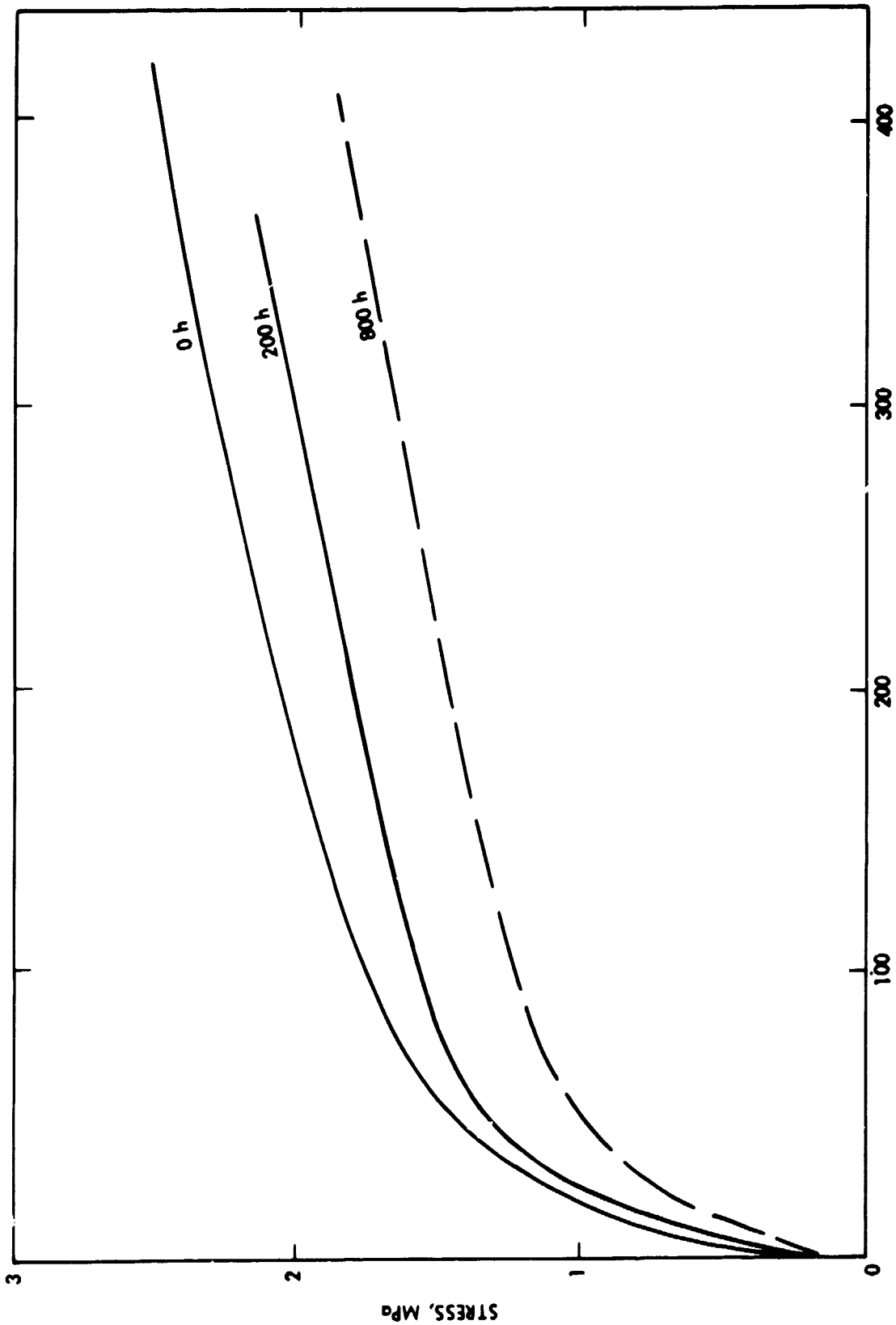

Figure 3-17. Stress-Strain Curves of EVA Film A9918 as a Function of Photothermal Aging in Air at 6 suns and 105°C

B. PHOTOTHERMAL TESTING OF SILICONES

Crosslinked silicone rubbers (polydimethylsiloxane, RTV 615® from GE) undergo very little change in bulk properties under photothermal testing conditions. Tested for 800 hours in the presence of air, or behind Pyrex glass under 6 suns of UV at 105°C, RTV 615 was found to be stable in terms of its optical transmission (<0.5% change) as well as mechanical integrity as measured by tensile modulus (1 to 10% strain). Chemically, Si-H bonds were cleaved and hydroxyl and carbonyl functionalities were formed due to thermal oxidation and photo-oxidation, but with little effect on physical properties.

Temperature coefficients of the rate of change of optical and mechanical properties (activation energies) were found to be 20 kcal/mole for both properties in the temperature range of 70 to 105°C. This value can be used to calculate rate of change of optical and mechanical properties, as illustrated in Section II.C.

Room temperature photodegradation of RTV has previously been reported (Ref. 13). Bond strength to change in chemical structure of the silicone has been linked. Surface chemical changes were also observed. Formation of hydroxyl groups would tend to make the polymer and its surface more hydrophilic; this may cause delamination and decrease optical transmission due to soil retention.

Films of silicone rubber were prepared by casting RTV 615 (GE) and catalyst mixture (10 to 1 weight ratio) over a clean surface of glass and curing at 75°C for 3 hours. Ten-mil-thick sample films were used for all of the photothermal aging.

Samples were aged at 70°C, 85°C, and 105°C under UV suns and dark/oven with three levels of oxygen: open (full access; UV/ambient oxygen), no edge seal (limited access: UV/sandwich, and dark stagnant air oven (dark/oven). Properties measured were changed in optical transmission, weight loss, IR analysis, tensile modulus and swelling/extraction.

1. Optical Properties

Thermal as well as photothermal aging results in little or no change in the spectral region longer than 350 nm. Thermal aging of RTV at 70°C and 85°C resulted in no change in transmission at 300 nm. The open sample (UV/ambient air), however, experienced an initial drop in transmission as a function of photothermal aging at 85°C. This phenomenon was amplified when RTV was photothermally aged at 105°C, as illustrated in Figure 3-18. Apparently, at 85 to 105°C, some photothermal process or processes were initiated and products were formed that caused the increase in absorption at 300 nm. Subsequent bleaching of these products led to a subsequent gain in transmission.

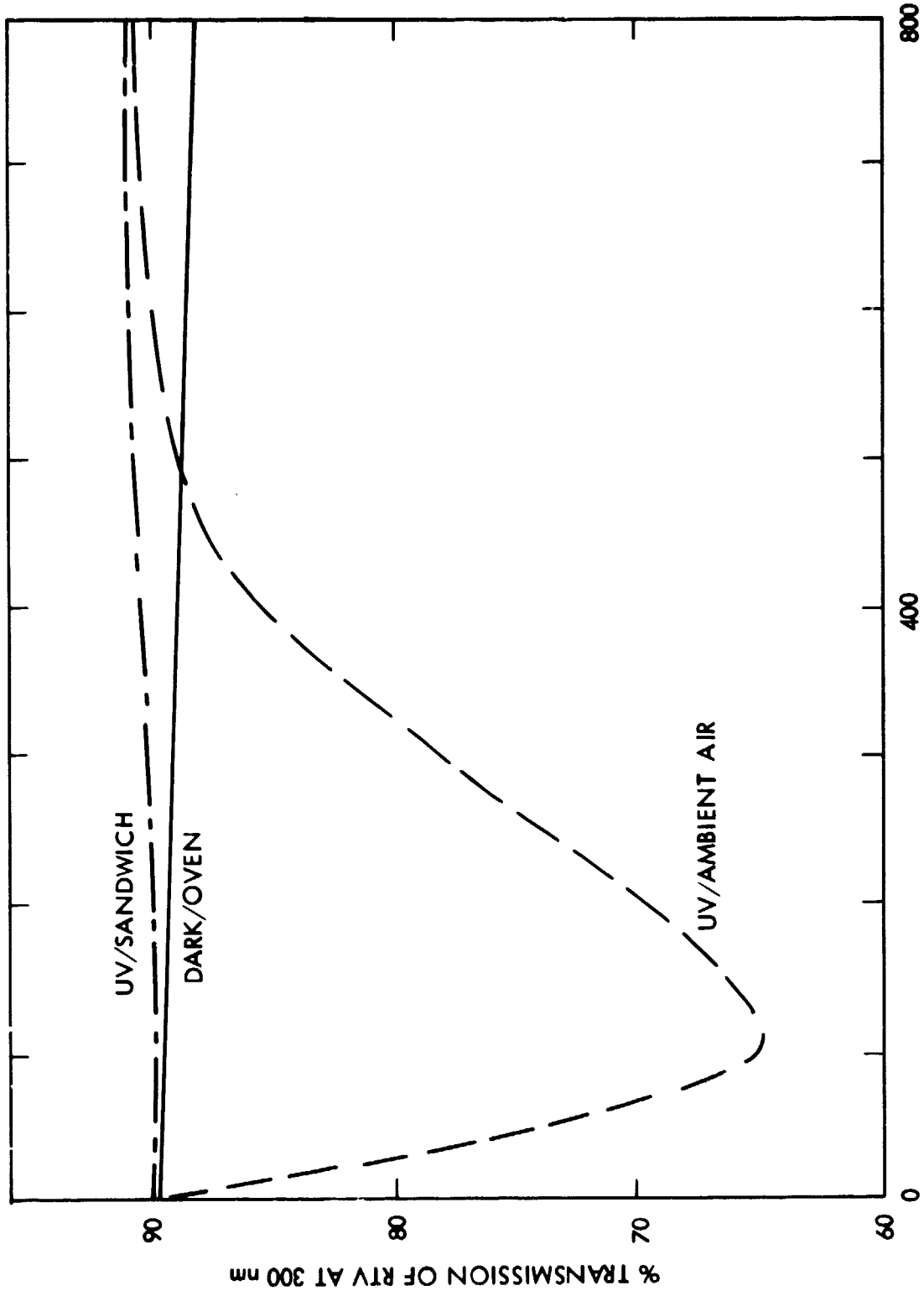

Figure 3-18. Percent Transmission of RTV at 300 nm as a Function of Aging at 6 suns and 105°C

2. Oxidation

Figures 3-19 and 3-20 illustrate the FT-IR difference spectra of RTV before and after aging. Thermal aging at 105°C (Figure 3-19) results in: (1) Si-H bond cleavage (intensity loss at 2150 cm^{-1}), (2) trace hydroxyl formation (3400 cm^{-1}), and (3) no carbonyl formation. Photothermal aging at 105°C (Figure 3-20) leads to:

(1) More rapid Si-H bond cleavage.

(2) Large hydroxyl formation.

(3) Formation of carbonyl chromophore (1750 cm^{-1}). (Formation of hydroxyl and carbonyl are probably due to photo-oxidation.)

3. Weight Change

No appreciable weight change (<1%) has been detected when RTV is exposed to thermal as well as photothermal aging at 105°C for up to 800 hours (equivalent to 3 years outdoors).

4. Chain Scission and Mechanical Properties

One set of photothermally aged RTV was Soxhlet extracted in a Soxhlet apparatus with dichloromethane for 168 hours. The solution was then concentrated and sent through HPLC for molecular weight analysis. Swelling tests were carried out on gel to determine the crosslink density. Stress-strain measurements were carried out on another set of RTV samples and the results are illustrated in Figure 3-21 and Table 3-6. Whereas the percent of extractables remains unchanged and there was no change in molecular weight of the extractables, the polymer network does go through thermal crosslinking, leading to an increase in tensile modulus.

E. PHOTOTHERMAL TESTING OF POLYVINYL BUTYRAL (PVB-SAFLEX)

PVB Saflex has long been used in automobile safety glass, where it is hermetically sandwiched between two sheets of glass. In this application it has lasted for over 20 years without serious degradation. However, little was known about the photodegradation of PVB in a non-hermetic design. Recent reports (Refs. 14 and 15) indicated PVB films without additives degrade readily when exposed to UV light of a Xenon arc. Degradation studies of PVB films were performed at 55°C and 70°C using three different oxygen environments as previously described (see Section II.B, Test Design). Results of tests conducted by the project on free-standing PVB films in the presence of air indicated loss of stabilizers at 55°C, corresponding to a 15% loss within 2 to 4 years of exposure. At 70°C, stabilized PVB undergoes chemical (thermal and photothermal) oxidation, leading to loss of transmission. A 10% loss of transmission at 400 nm was observed as a result of photothermal aging at 6 suns, 70°C in air for 400 hours. A weight loss of up to 8% was also detected during the same period. Chemical crosslinking took place during

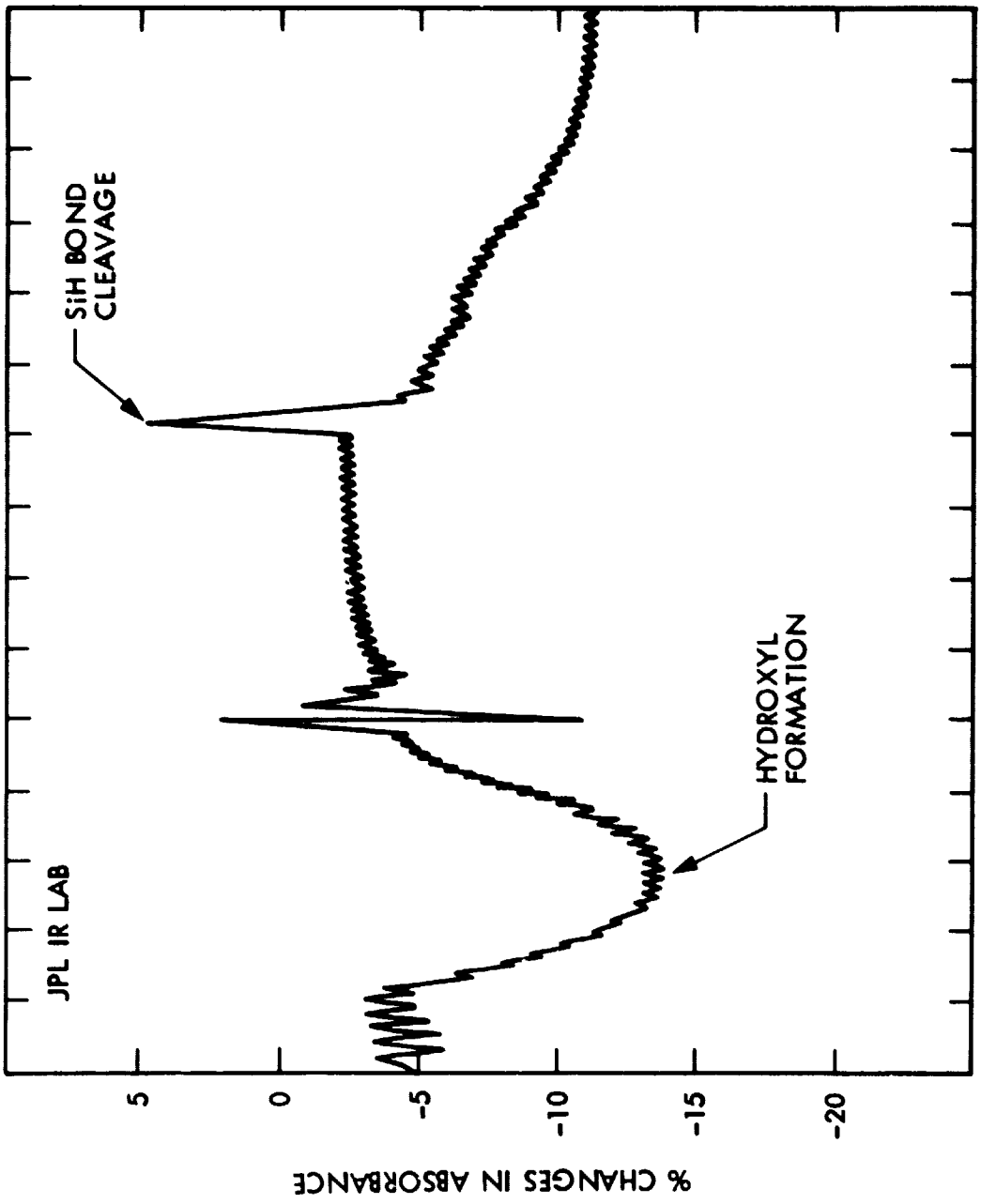

Figure 3-19. FT-IR Difference Spectrum of RTV Before and After 800 hours of Thermal Aging at 105°C in Air

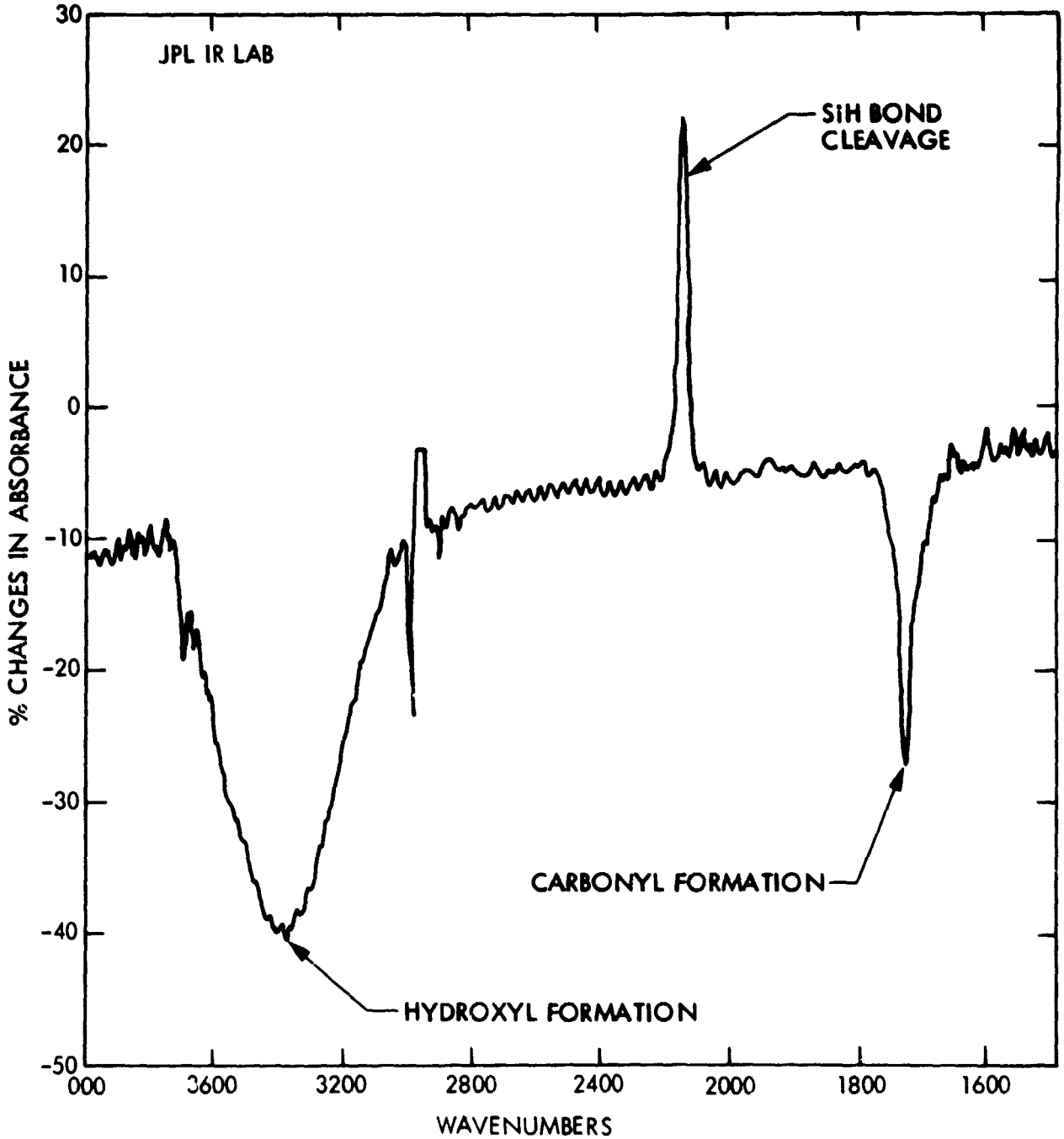

Figure 3-20. FT-IR Difference Spectrum of RTV Before and After 800 hours of Photothermal Aging at 105°C and 6 suns

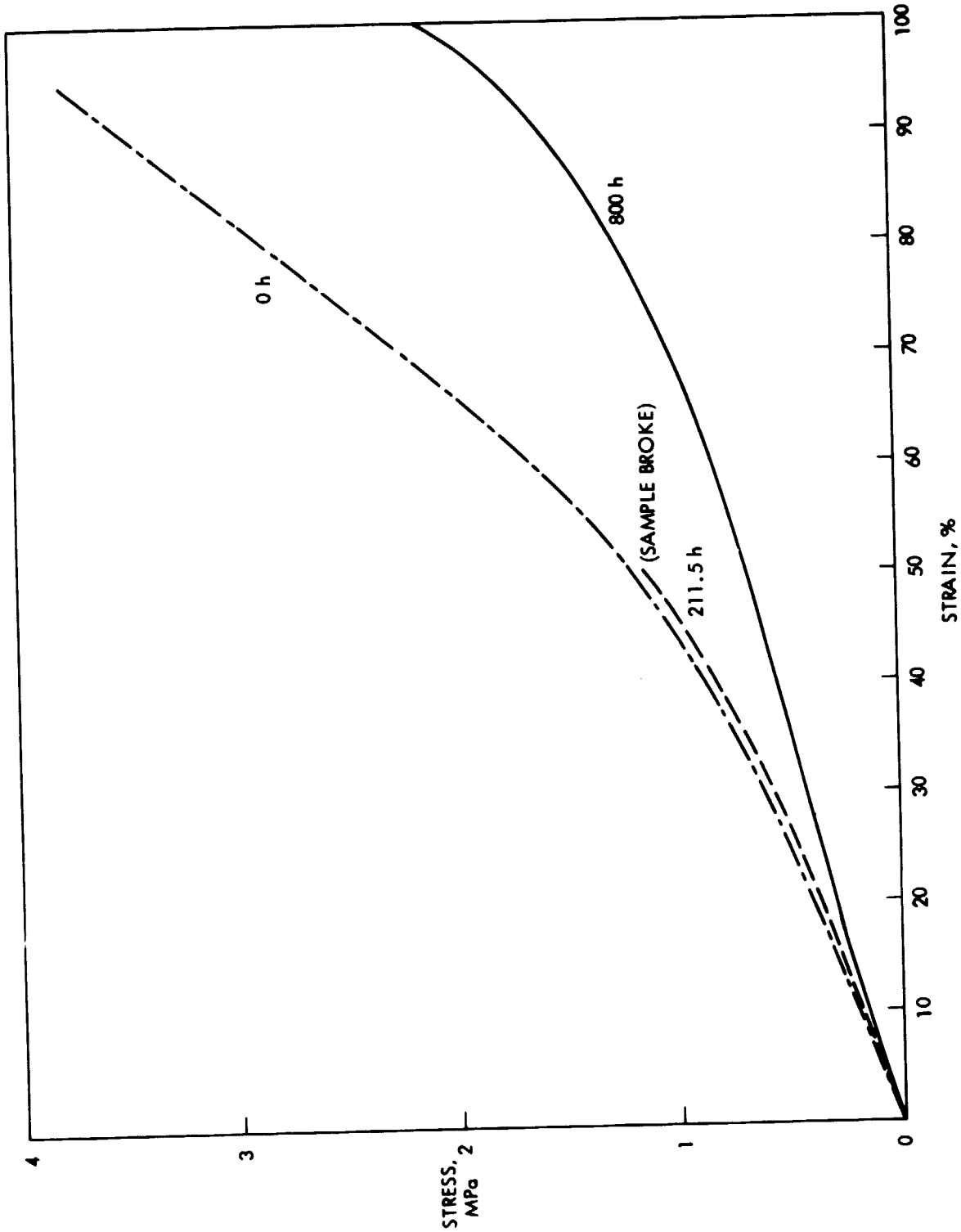

Figure 3-21. Stress-Strain Curves of RTV 615 Films as a Function of Photothermal Aging in Air at 6 suns and 105°C

Table 3-6. Percent Extractable, Molecular Weight Distribution ($\bar{M}_w$) of the Extract and Crosslinking Density of RTV as a Function of Photothermal Aging at 6 suns

TEMPERATURE	TIME OF TEST, h	TEST CONDITION	% EXTRACTABLE	$\bar{M}_w$	CROSSLINKING DENSITY, mole/cm^3
25°C	0.0	AS RECEIVED	4	2,000	7.97×10^{-4}
70°C	525.0	DARK/OVEN	3.5	2,000	NOT MEASURED
		UV/AMBIENT AIR	4.0	2,000	
		UV/SANDWICH	3.0	2,000	
85°C	800.0	DARK/OVEN	4.0	2,000	5.83×10^{-4}
		UV/AMBIENT AIR	4.0	2,000	7.62×10^{-4}
		UV/SANDWICH	4.0	2,000	7.69×10^{-4}
105°C	800.0	DARK/OVEN	3.5	2,000	6.08×10^{-4}
		UV/AMBIENT AIR	4.0	2,000	7.42×10^{-4}
		UV/SANDWICH	4.0	2,000	8.79×10^{-4}

photothermal aging, leading to an increase in equilibrium tensile modulus (following an initial decrease in apparent modulus).

1. Optical Properties

Percent transmission at 400 nm as a function of photothermal aging at 70°C is illustrated in Figure 3-22. Whereas there was no change in percent transmission of the thermally aged sample (Figure 3-22) up to 400 hours, both the photothermally aged samples showed initial transmission gain, which subsequently decreased with longer aging time. The initial gain can be interpreted in terms of loss of UV stabilizer, and the subsequent decrease can be assigned to formation of photo-oxidation products. The activation energy of the rate of loss of UV stabilizer was measured to be 7 kcal/mole (between 55°C and 70°C), a typical value for physical processes. The activation energy of the oxidation was measured to be 40 kcal/mole (between 55°C and 77°C).

2. Weight Change

Weight loss data have been collected as a function of aging time. Figure 3-23 illustrates percent of weight loss as a function of photothermal

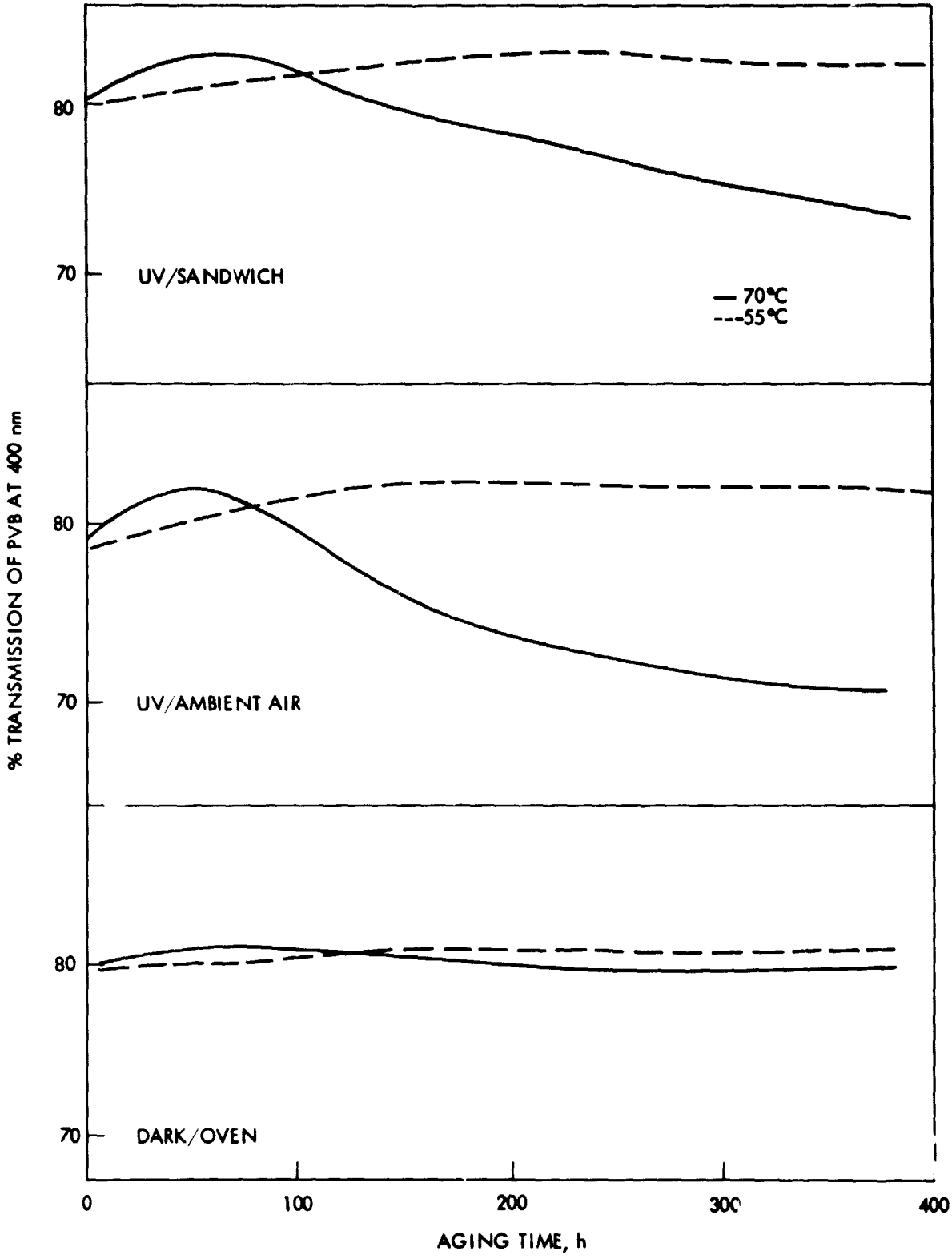

Figure 3-22. Percent Transmission of PVB at 400 nm as a Function of Photothermal Aging at 6 suns and 70°C

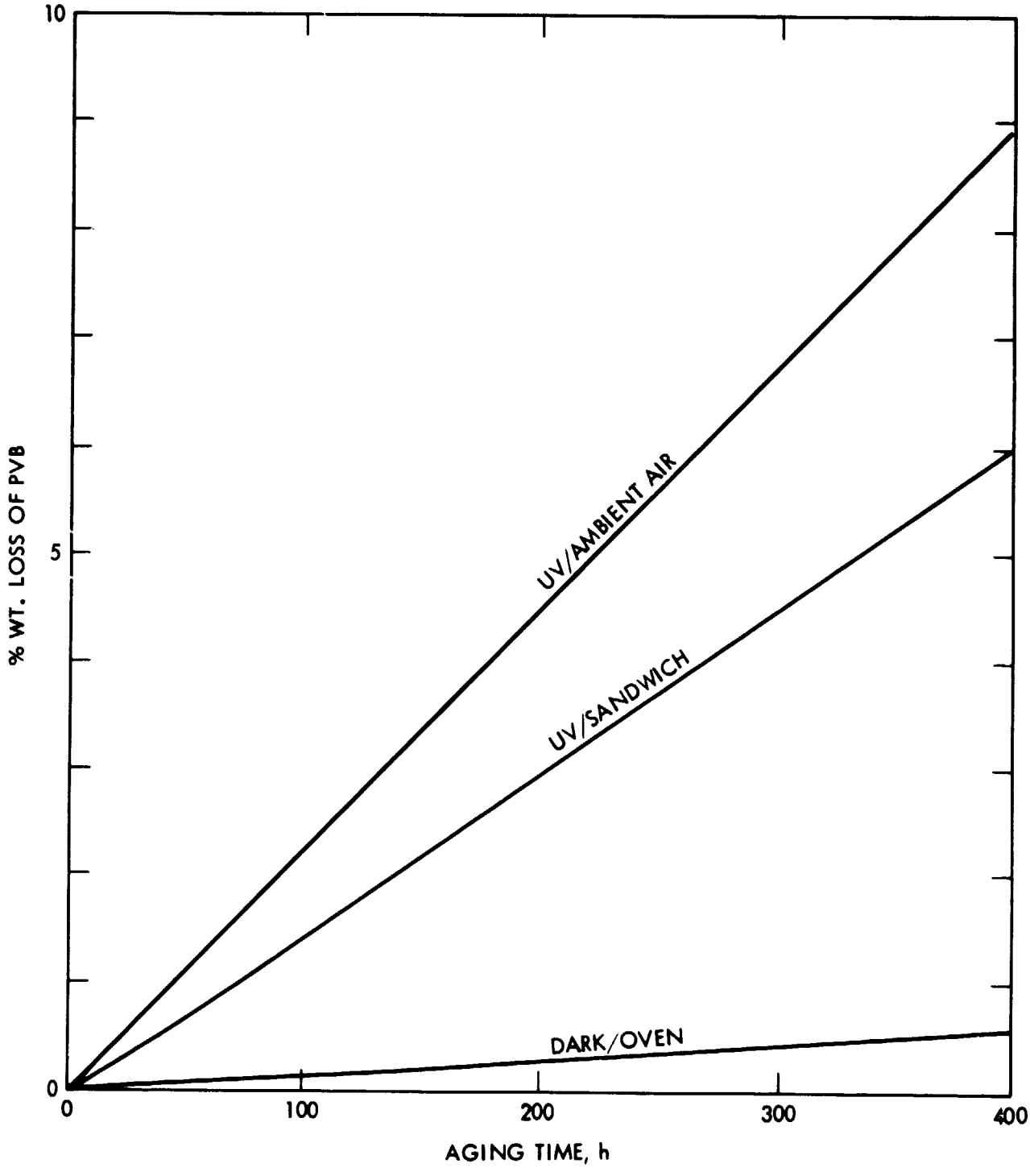

Figure 3-23. Percent Weight Loss of PVB as a Function of Photothermal Aging at 6 suns and 70°C

aging at 70°C. In a dark stagnant oven, a weight loss of less than 0.5% was detected during up to 400 hours of aging time. Rate data were not obtained. During the photothermal aging, however, PVB experienced a weight loss of 9% at 70°C and 400 hours. Activation energy of the weight loss was measured to be 10 kcal/mole, in approximate agreement with that obtained in optical transmission experiment (7 kcal/mole, see Section III.E.1). This led to the conclusion that weight loss is probably due to the loss of additives in PVB.

3. Chain Scission and Mechanical Properties

Sol/gel extraction has been carried out as previously described and tensile modulus of PVB has also been measured and is shown in Figure 3-24. Table 3-7 illustrates the results obtained. The decrease in the percent of extractables clearly indicated that chemical crosslinking took place during photothermal aging. At such a low degree of crosslinking, PVB exhibited a decrease in apparent tensile modulus with photothermal aging, as illustrated in Figure 3-24 and Table 3-7. The equilibrium modulus, however, is expected to increase on chemical crosslinking.

F. PHOTOTHERMAL TESTING OF ALIPHATIC POLYURETHANE

Specimens tested were linear aliphatic polyurethane (PU) by H.S. Quinn directly extracted from a two-cell test module. Three different oxygen environments were tested (see Section II.B). These PU samples readily degraded at 55°C during photothermal aging in air. With 400 hours of aging time at 70°C, PU suffered a weight loss of 16% due to formation of volatile photoproducts and a 50% loss of optical transmission (at 400 nm). Furthermore, chain scission took place leading to a 20% decrease in tensile

Table 3-7. Percent Extractable and Molecular Weight Distribution of the Extract of PVB as a Function of Photothermal Aging at 6 suns

TEMPERATURE	TIME OF TEST, h	TEST CONDITION	% EXTRACTABLE	$\bar{M}_w$
25°C	0.0	AS RECEIVED	100.0	185,000
70°C	400.0	DARK/OVEN	100.0	NOT MEASURED
	400.0	UV/AMBIENT AIR	54.0	21,000
	400.0	UV/SANDWICH	54.0	36,000

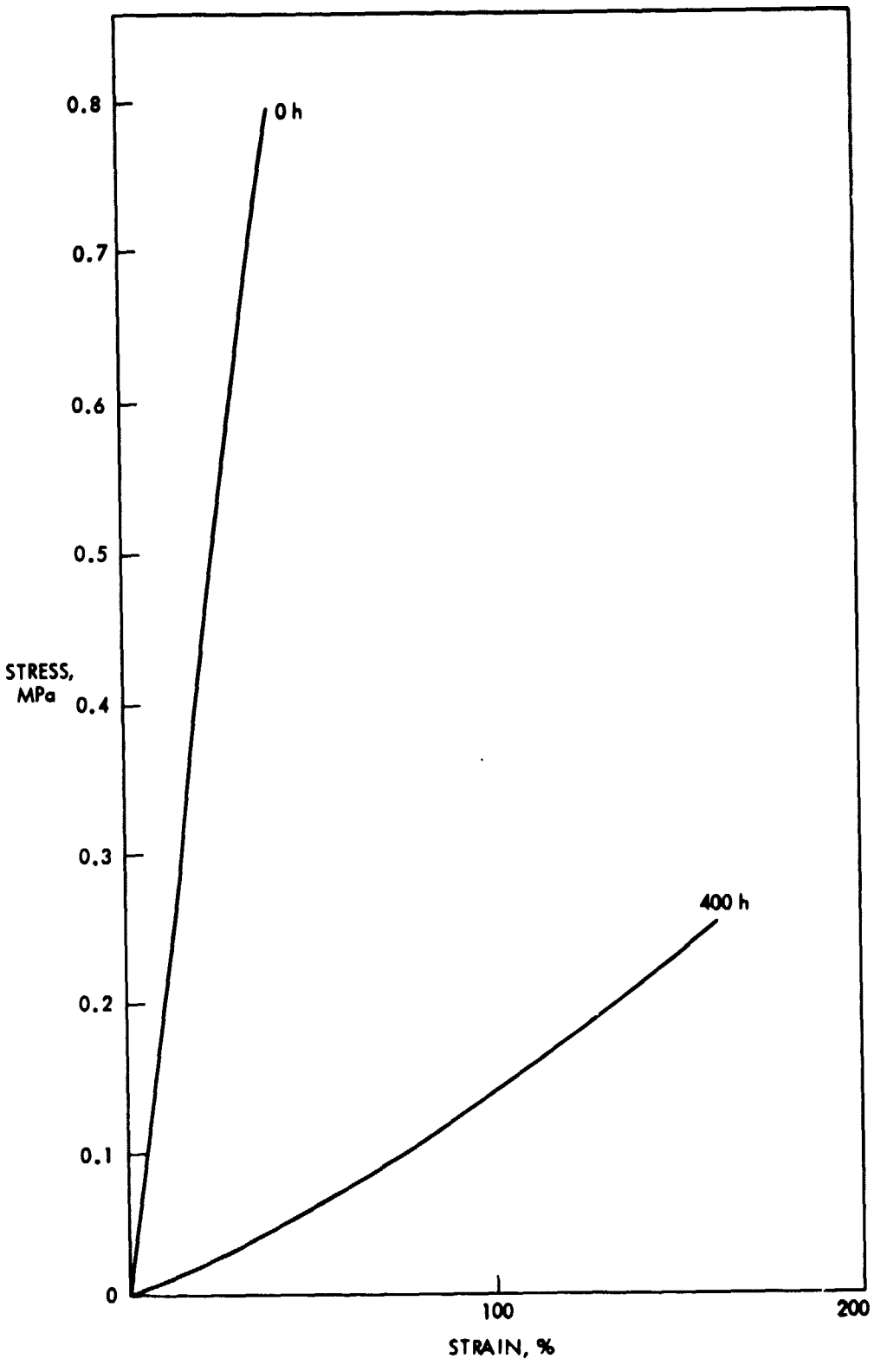

Figure 3-24. Stress-Strain Curves of PVB as a Function of Photothermal Aging in Air at 6 suns and 105°C

modulus measured at 10% strain. Limited data on the sample of PU tested indicate that the pottant will undergo (1) rapid degradation, leading to yellowing, (2) gradual loss of materials, leading to void formation, and (3) decrease of mechanical integrity, leading to creep.

1. Optical Properties

Figure 3-25 demonstrates the decrease in transmission of PU at 400 nm as a function of photothermal aging at 70°C. Apparently, photo irradiation bleaches the thermal products, leading to an increase in transmission as compared with specimens aged in a dark stagnant oven.

2. Weight Change

With 400 hours of photothermal aging of PU at 70°C, a weight loss of 16% was obtained, as illustrated in Figure 3-26. This led to the conclusion that photothermal degradation leads to the formation of volatile products.

3. Chain Scission and Mechanical Properties

Table 3-8 shows the results from sol/gel experiment on PU. The results from stress-strain measurements are illustrated in Figure 3-27. Apparently, chain scission took place during photothermal aging, leading to a decrease in tensile modulus.

Table 3-8. Percent Extractable, Molecular Weight Distribution of the Extract of PU as a Function of Photothermal Aging at 6 suns

TEMPERATURE	TIME OF TEST, h	TEST CONDITION	% EXTRACTABLE	$\bar{M}_w$
25°C	0.0	AS RECEIVED	4	5,000
70°C	400.0	DARK/OVEN	NOT MEASURED	10,000
	400.0	UV/AMBIENT AIR	21	10,000
	400.0	UV/SANDWICH	25	10,000

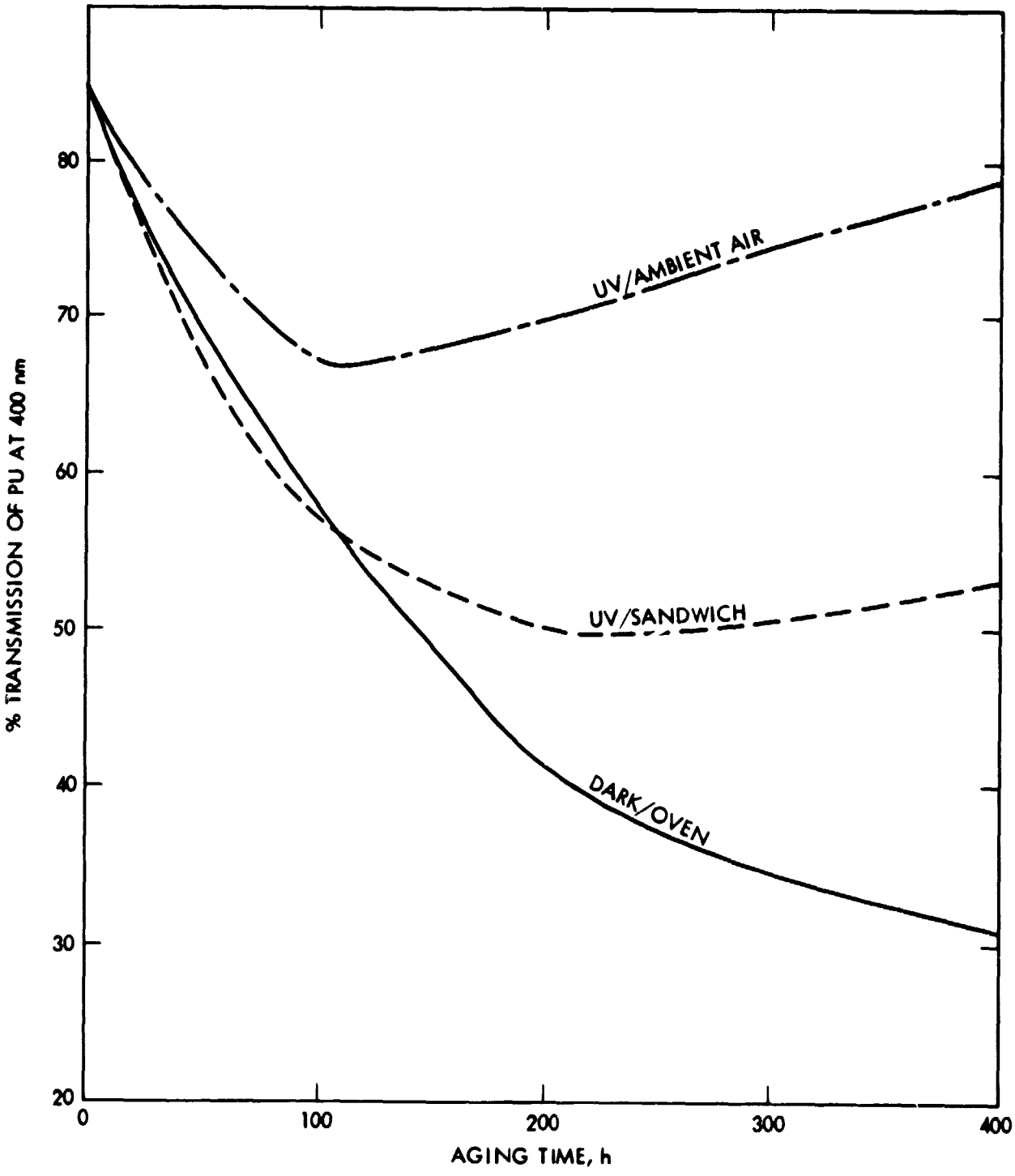

Figure 3-25. Percent Transmission of PU at 400 nm as a Function of Photothermal Aging at 6 suns and 70°C

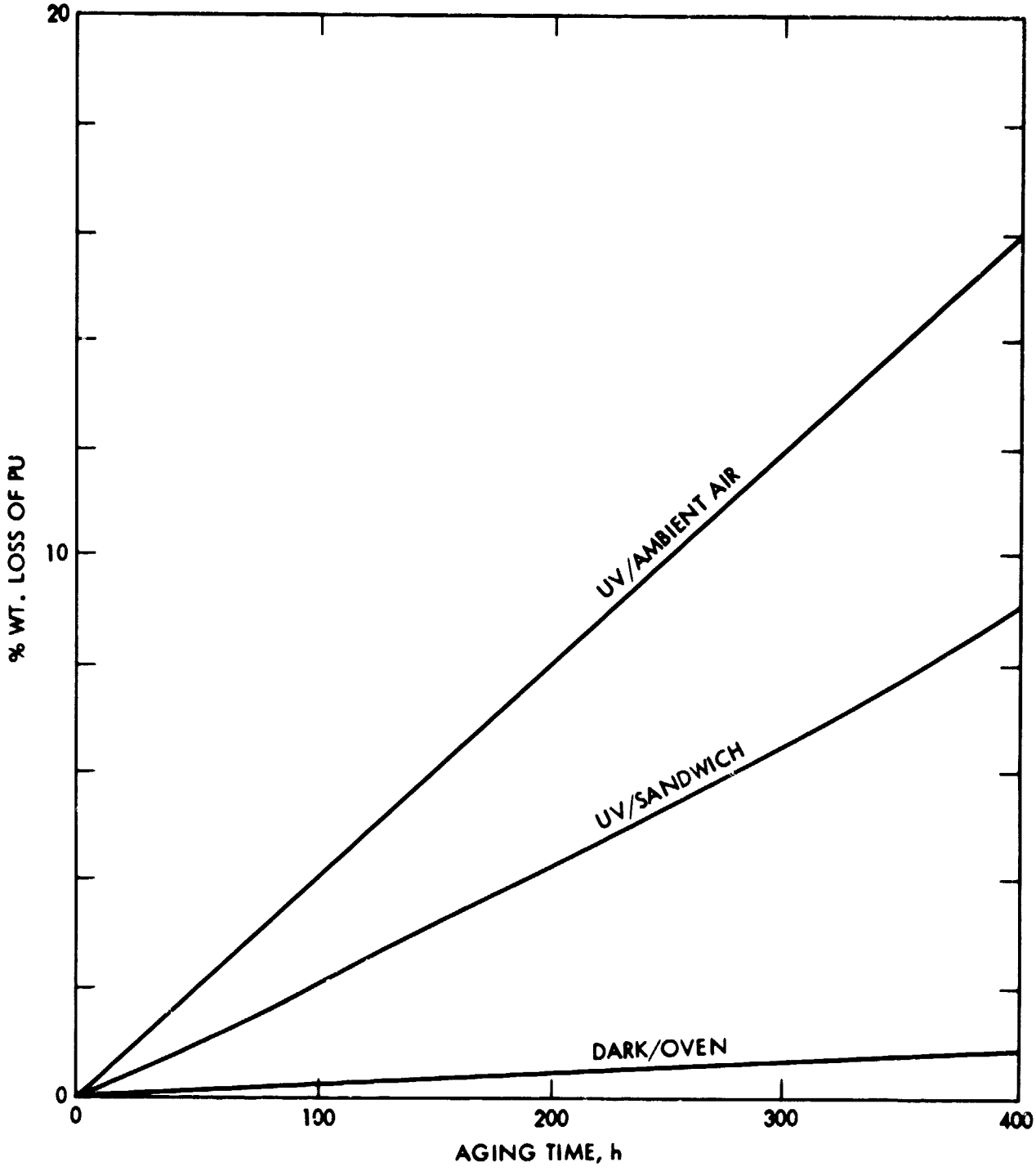

Figure 3-26. Percent Weight Loss of PU as a Function of Photothermal Aging at 6 suns and 70°C

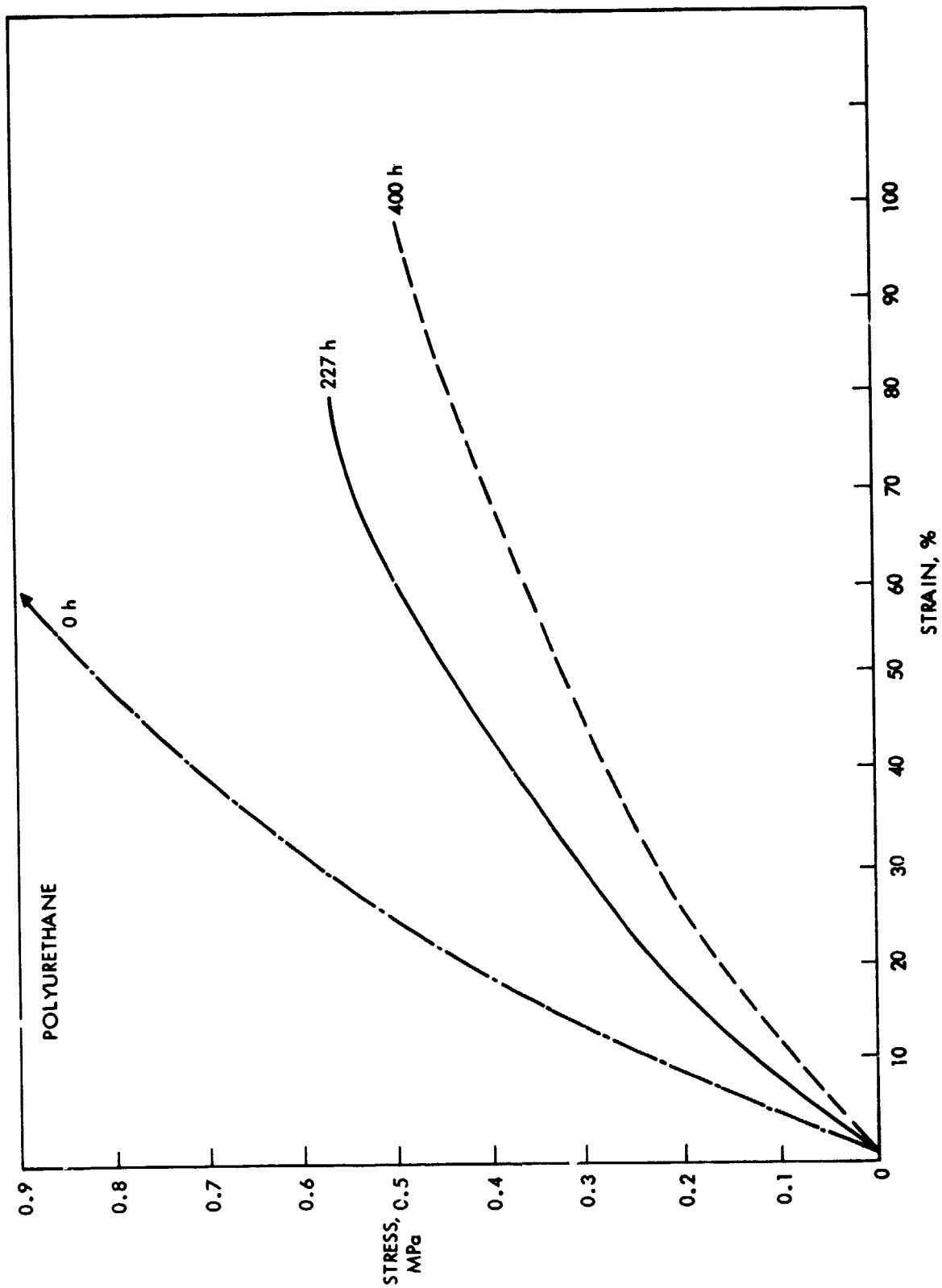

Figure 3-27. Stress-Strain Curves of PU as a Function of Photothermal Aging in Air at 6 suns and 70°C

G. PHOTOTHERMAL TESTING OF POLY-N-BUTYLACRYLATE (PNBA) PREPARED AT JPL

Tests have been initiated on JPL-developed uncrosslinked PnBA. Room temperature photolysis data indicate photo-oxidation takes place, leading to crosslinking (Ref. 16). A stabilized PnBA is being developed and further tests will be carried out.

Work at Case Western Reserve University includes studies to determine the role of photo-oxidation in the giving process. Crosslinking takes place, leading to an increase in tensile modulus as a result of photothermal aging. Photo-oxidative products such as alcohol, aldehyde and ketone have been identified and quantified. Detailed results of Case Western work will be reported in their final report.

H. PHOTOTHERMAL TESTING OF ETHYLENE/METHYLACRYLATE (EMA)

Preliminmary photolysis data indicate surface photo-oxidation when EMA is exposed to UV at 30°C. Photothermal tests have been initiated.

SECTION IV

PHOTOTHERMAL CHARACTERIZATION OF OUTER COVER MATERIALS

A. INTRODUCTION

Three commercially available outer cover film materials were tested: (1) Acrylar, UV screening PMMA films X22416/17 from 3M Corporation, (2) Tedlar films UTB-300 manufactured by Du Pont, and (3) Korad from Hexel Corporation. In addition, three different kinds of acrylic copolymer films prepared at JPL have been evaluated. They were copolymers of methyl methacrylate plus, (1) 5-vinyl, 2-hydroxyphenyl benzotriazole, (2) a JPL developed additive, 4,4'dimethoxy 3-allyl, 2-hydroxybenzophenone, and (3) Permasorb MA (National Starch).

B. PHOTOTHERMAL RANKING OF OUTER COVER MATERIALS

All six materials tested were thin (3 to 5 mil) clear, glassy polymer films. All of them transmit greater than 92% of incoming solar radiation but absorb the ultraviolet portion of solar radiation (295 to 360 nm).

Overall, the copolymer of Permasorb and acrylics was the least effective outer cover material tested. The UV stabilizer rarely attached to the polymeric network, but did oligomerize to form dimers and trimers. The oligomerized Permasorb acrylics remain fugitive and can be extracted by water from the parent polymer. Rate of loss of UV screens is approximately 1.5% per week of water soaking time.

Figure 4-1 illustrates the peak absorption percent of the UV screener remaining in the parent polymer vs. photothermal aging time at 6 suns, 85°C and in air for the other five candidate materials. It clearly demonstrates the superiority of acrylar and acrylic copolymer films of BT and BP as compared to Tedlar and Korad with respect to UV screening capability vs. aging time. Acrylar and acrylic copolymer films of BT and BP retained their UV screening capability during up to 400 hours of aging. Tedlar and Korad, on the other hand, exhibited loss of UV screen as they were exposed to photothermal aging. Tedlar retained 25% of its original screening capability after 400 hours of aging. Chemical analysis such as FT-IR and GPC showed acrylic copolymer of BP underwent slow photo-oxidation as a result of photothermal aging. This leads to the conclusion that acrylar and acrylic copolymer of BT films are the best outer cover candidate materials with respect to photothermal aging of up to 85°C.

C. PHOTOTHERMAL TESTING OF UV SCREENING PMMA FILMS (ACRYLAR X22416/17 FROM 3M CORPORATION)

PMMA films tested were manufactured by 3M Corporation. These films contain a UV absorber whose UV-VIS absorption spectrum is illustrated in Figure 4-2. The samples were biaxially stretched to increase their dimensional stability and surface stiffness. Optical transmission, weight loss, and dimensional stability were monitored as a function of accelerated

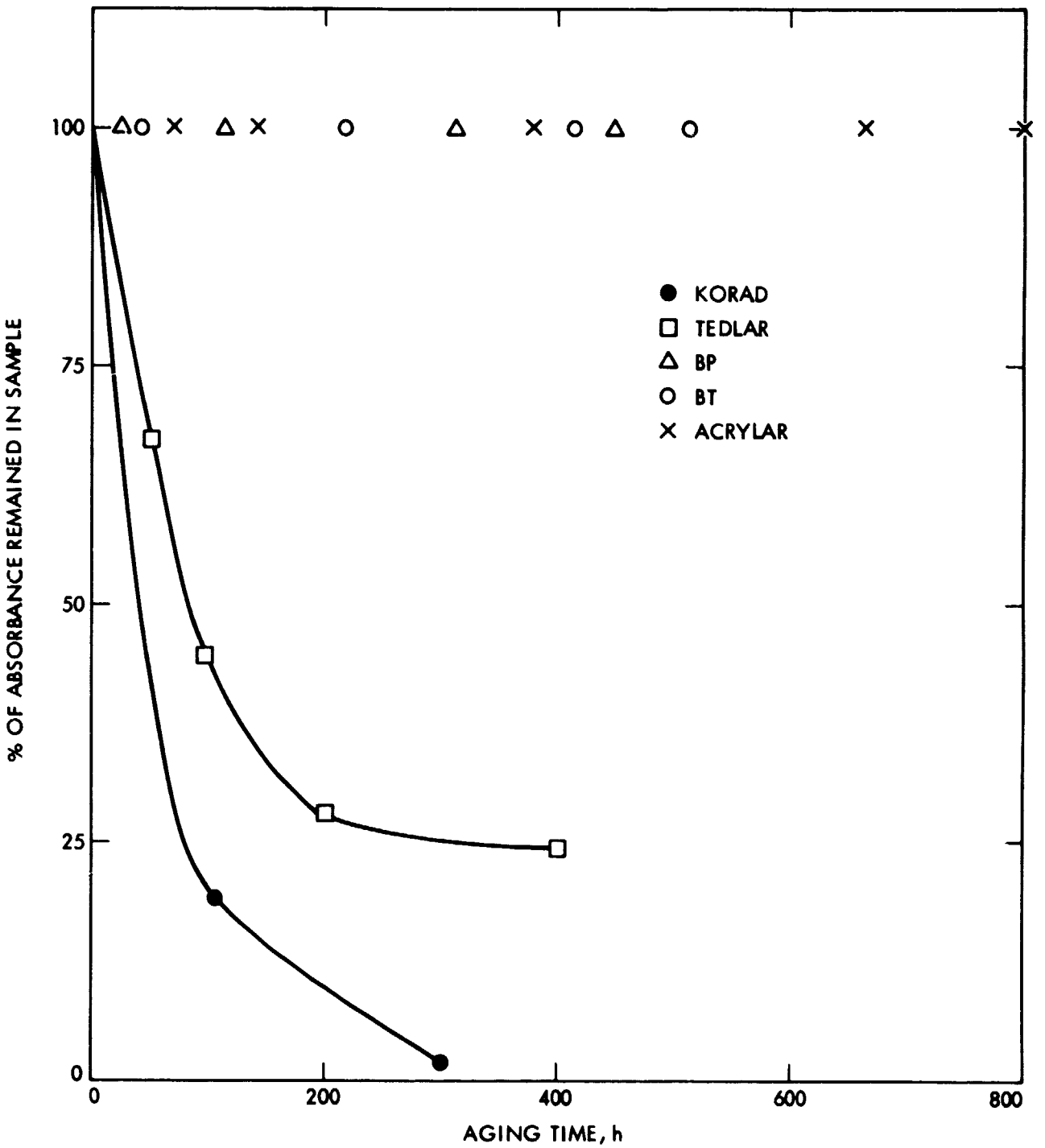

Figure 4-1. UV Screening Capability of Outer Cover Materials as a Function of Photothermal Aging at 6 suns and 105°C in Air

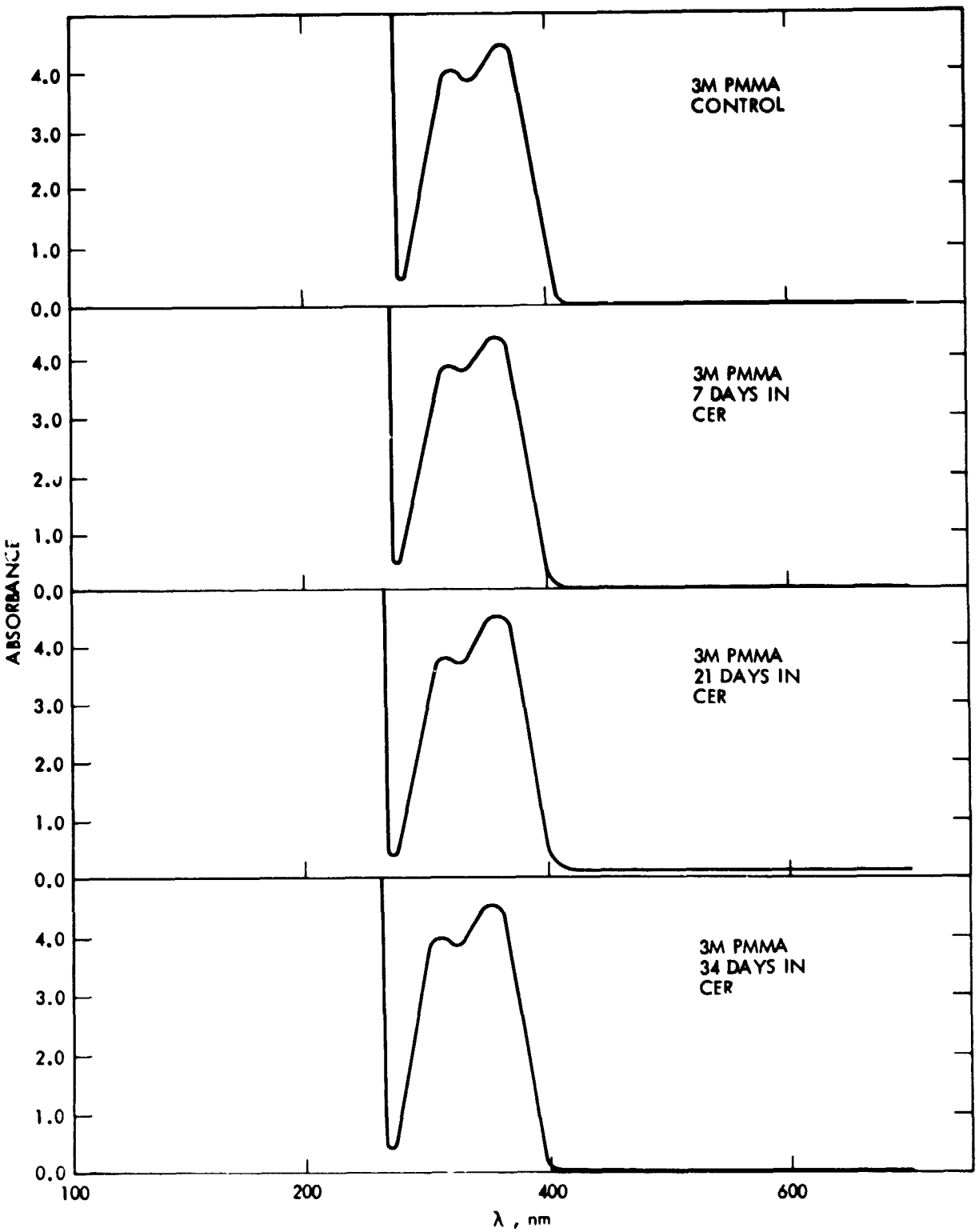

Figure 4-2. UV-VIS Absorption Spectra of PMMA Films (X22416) Before and After 34 days of Aging in CER

photothermal aging in air at 85°C for up to 800 hours (equivalenc to 3 years outdoors) and thermal aging in a dark oven at 85°C for up to 800 hours. No change in direct and hemispherical transmission occurred during this period, nor was there any dimensional change. Less than 0.5% weight change was detected.

With its high absorption coefficient, any leaching of the UV absorber would result in a large decrease in its absorbance in the 300 to 400-nm range. The invariance in absorbance as a function of aging tests, therefore, led to the conclusion that the UV absorbers were "non fugitive" during up to 800 hours of accelerated aging.

Samples of 3M-PMMA films were also aged in a Controlled Environmental Reactor (CER, Ref. 2) for up to 34 days (1 day inside the reactor is equivalent to 16 days outdoors) with simulated rain and fog (2 hours per 24 hours). No change can be detected in either of its UV-VIS or FT-IR absorption spectra (Figures 4-2 and 4-3). In particular, there is no hydroxyl formation in the FT-IR spectrum. Further tests are being conducted on this material.

D. PHOTOTHERMAL TESTING OF 5-VINYL 2-HYDROXYPHENYL BENZOTRIAZOLE/ACRYLIC COPOLYMER (BT) ("VINYL TINUVIN" ACRYLIC COPOLYMER: UNIVERSITY OF MASSACHUSETTS)

The hydroxyphenyl benzotriazole class of UV stabilizers/absorbers are marketed under the general tradename "Tinuvin" (e.g., Tinuvin P) by Ciba Geigy and "Cyasorb" by American Cyanamid. The methacrylate copolymer sample was synthesized at the University of Massachusetts and was solution-cast into 3-mil-thick films. These films have been subjected to accelerated ultraviolet (295 to 370-nm) exposure up to 4000 hours at 35°C, equivalent to more than 18 years of outdoor ultraviolet dosage. Figure 4-4 shows that the chemical structure of the UV absorber group remains unchanged, hence the UV protective properties of the film remain unchanged. Results of molecular weight measurements are shown in Table 4-1. They indicate that the polymeric network undergoes both chain scission and crosslinking processes, but at a rate that will not significantly affect mechanical properties after the 4000-hour test. Surface tension measurements on the film were carried out using the contact angle method as a function of exposure period, as illustrated in Table 4-2. These data indicate that the exposed (sunside) surface gradually becomes more polar and hydrophilic, while the other surface does not change. Chemical changes in surface structure were also detected by FT-IR ATR spectroscopy. The increased hydrophilicity would make the sunside surface more prone to soiling. Water-soaking tests and soaking tests and extraction with boiling solvents were carried out and failed to extract the UV absorber from the polymer. Pico-second spectroscopic studies of 5-vinyl 2-hydroxylphenyl benzotriazole/acrylic copolymer have been reported in Reference 17.

E. PHOTOTHERMAL TESTING OF 4,4'DIMETHOXY, 2-HYDROXY 3-ALLYL BENZOPHENONE/(BP) ("BENZOPHENONE"/ACRYLIC COPOLYMER (A JPL-DEVELOPED OUTER COVER CANDIDATE MATERIAL)

Tests on films of copolymers of this additive with PMMA shows that complete physical stability has been achieved and no chemical change in the UV absorber chromophore can be detected, as evidenced by the invariance of its

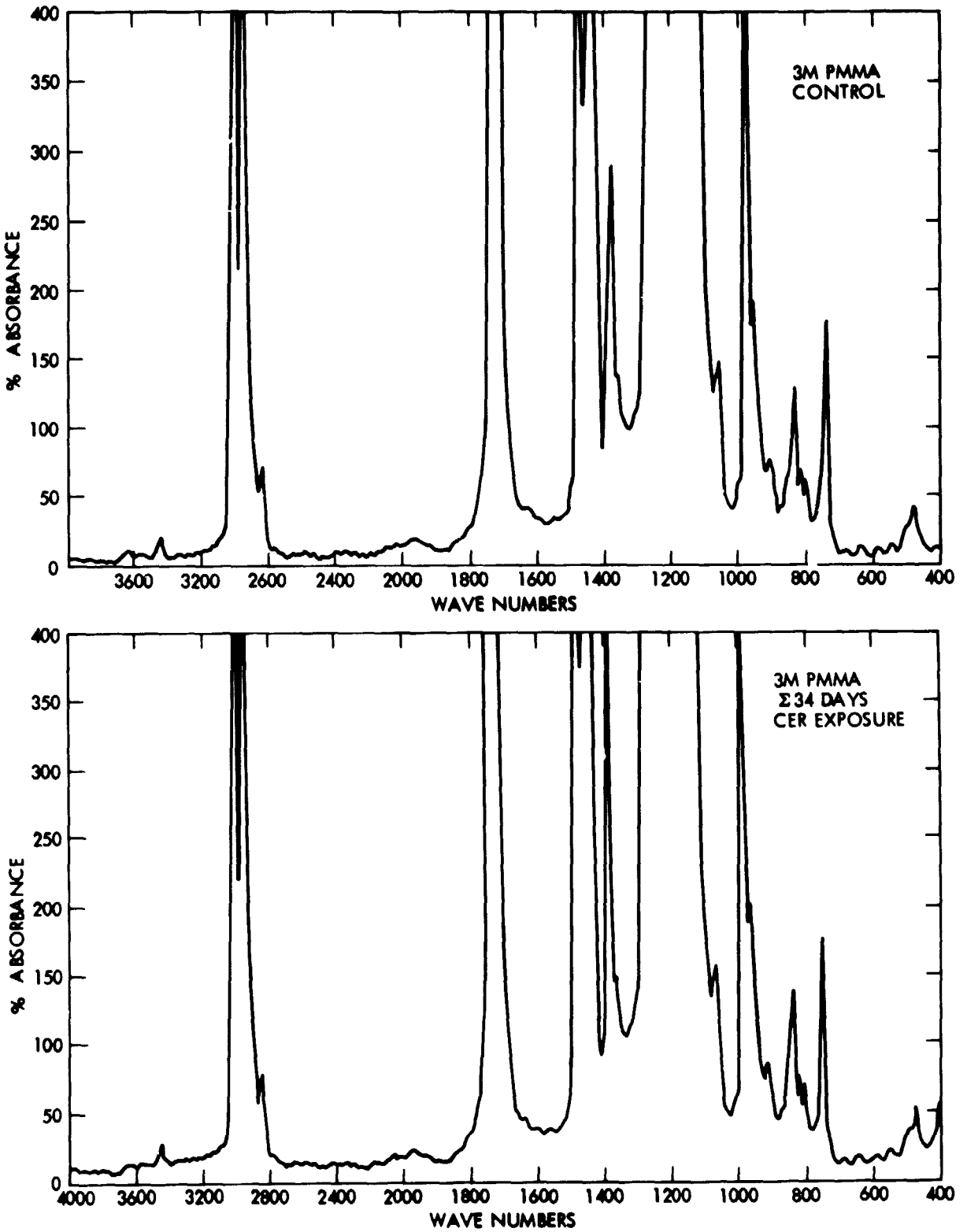

Figure 4-3. FT-IR Absorption Spectra of PMMA Films (X22416) Before and After 34 Days of Aging in CER

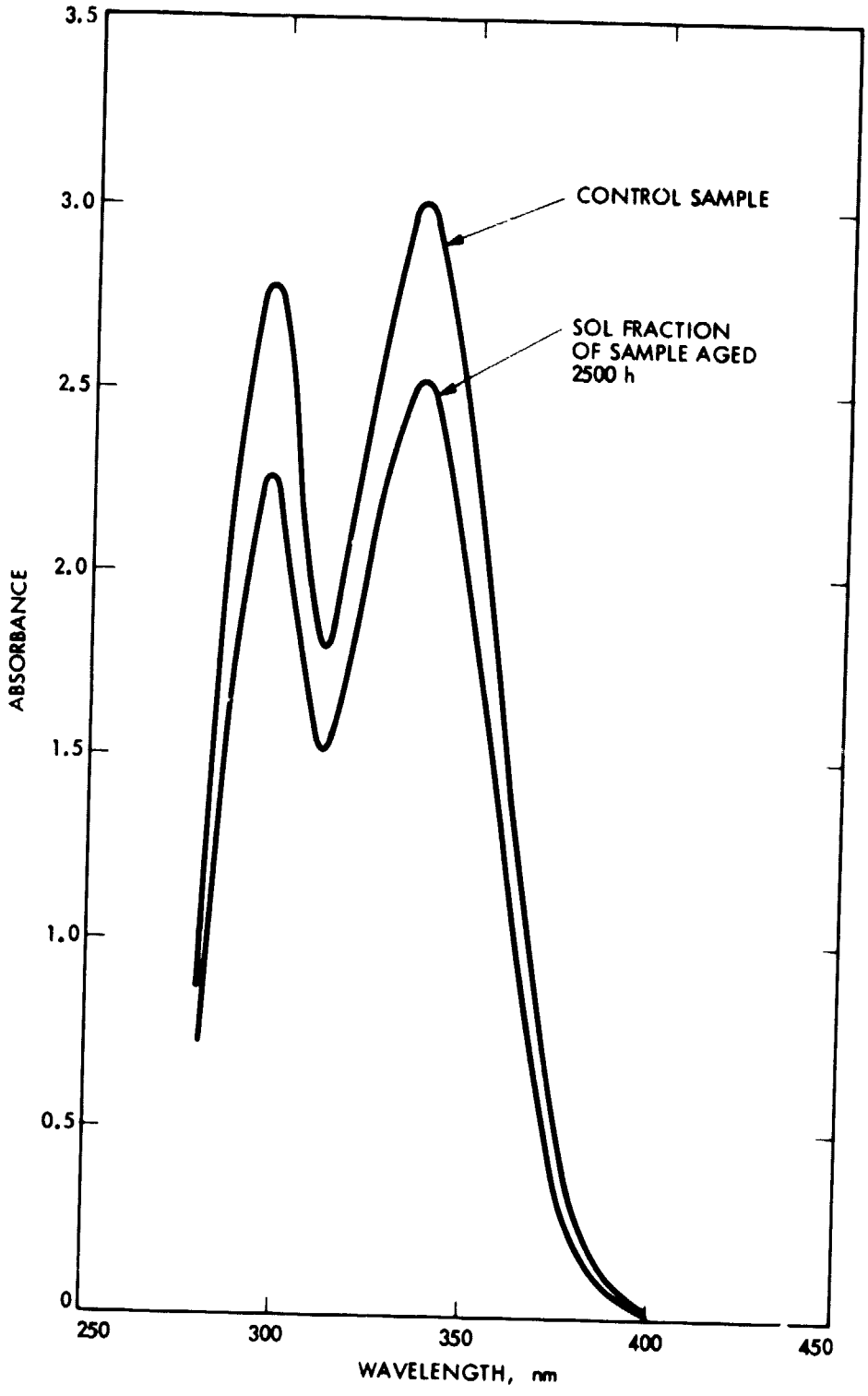

Figure 4-4. UV-VIS Absorption Spectra of 5-Vinyl 2-Hydroxyphenyl Benzotriazole Before and After 2500 hours of Photo-Aging at 6 suns and 35°C

Table 4-1. Molecular Weight Distribution of the Extract of Photo-Irradiated Poly 2,2-Hydroxy 5-Vinylphenyl 2H-Benzotriazole CO(MMA) at 6 suns and 35°C

SAMPLE	$\overline{M}_n$	$\overline{M}_w$	$\overline{M}_n/\overline{M}_w$
CONTROL #1	93,000	188,000	2.03
750 HOURS	98,000	202,000	2.05
1700 HOURS	75,000	273,000	3.62
2170 HOURS	75,000	273,000	3.62
CONTROL #2	64,000	120,000	1.90
3700 HOURS	69,000	171,000	2.49

Table 4-2. Surface Tension (γ_c) Poly 2,2-Hydroxy 5-Vinylphenyl 2H-Benzotriazole CO(MMA) (2-mil-thick Film) Measured as a Function of Aging Time

AGING TIME, h	EXPOSED SURFACE	BACK SURFACE
0	38 - 39	36 - 42
750	40 - 44	20 - 22
1000	45	29 - 30
1770	55	24 - 39
2040	59	27 - 38
2170	60	25 - 32

UV-VIS absorption spectra with photo-aging at 6 suns, 85°C, in air for 400 hours (Fig. 4-5). However, FT-IR spectra of the aged samples show an increase in absorbance at 3580 cm^{-1}, indicating that the PMMA matrix undergoes a slow photo-oxidation that may lead to an onset of chain scission and/or crosslinking (Fig. 4-6). This photo-oxidation is catalyzed by the benzophenone chromophore because (1) all of the light is absorbed by this chromophore, and control films placed in the dark at room temperature for an equivalent period do not show similar increase in absorbance at 3580 cm^{-1}, and (2) control PMMA films exposed to the same radiation flux did not undergo any chemical change. Change in molecular weight of the sample films has also been detected by HPLC equipped with μ-styragel columns, refractive index, and UV absorption detection modes. Table 4-3 shows that the overall average molecular weight decreases while the molecular masses of approximately 67% of all chains (those containing absorber chromophores) increases during the same exposure period.

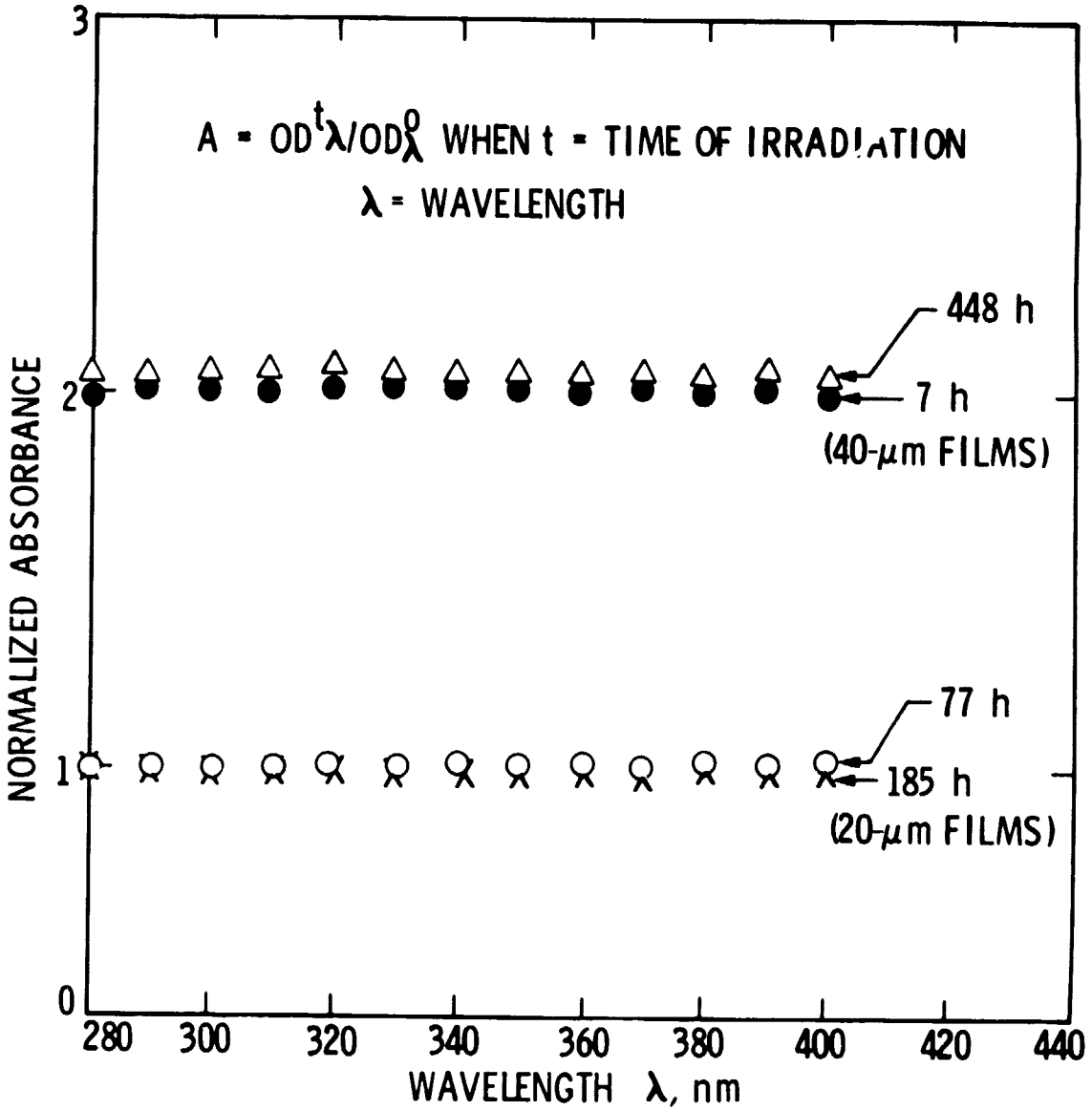

Figure 4-5. Normalized UV-VIS Absorption Spectra of 4,4'Dimethoxy, 2-Hydroxy 3-Allyl Benzophenone as a Functon of Photo-Aging at 85°C

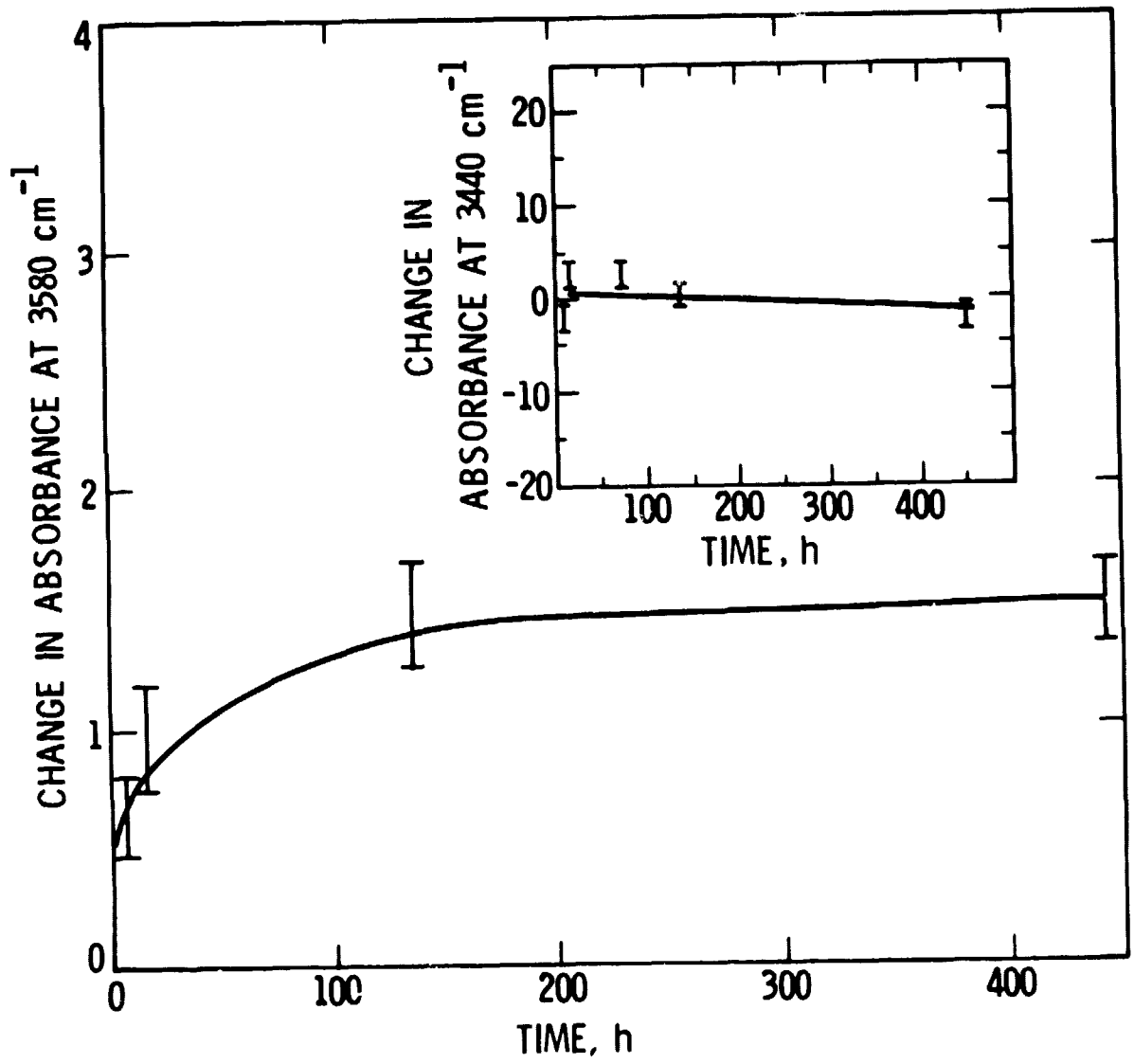

Figure 4-6. Hydroxyl Concentration in 4,4'Dimethoxy, 2-Hydroxy 3-Allyl Benzophenone as a Function of Aging

Table 4-3. Molecular Weight Distribution of Poly 2-Hydroxy, 3-Allyl, 4,4'Dimethoxy Benzophenone CO(MMA) as a Function of Photo-Aging at 6 suns and 35°C

DETECTION MODE	TIME OF EXPOSURE, h	$\overline{M}_n$	$\overline{M}_w$
REFRACTIVE INDEX	0	40,000	87,000
UV ABSORPTION	0	31,000	69,000
REFRACTIVE INDEX	448	32,000	77,000
UV ABSORPTION	448	34,000	79,000

$\overline{M}_n$ = NUMBER AVERAGE MOLECULAR WEIGHT.
$\overline{M}_w$ = WEIGHT AVERAGE MOLECULAR WEIGHT.

A major potential degradation mode in copolymers with high glass transition temperatures (Tg) is the process of sensitized photodegradation, which is caused by transfer of the electronic energy absorbed by the absorber chromophore to the polymeric network. One possible approach to this model-sensitized photodegradation is to correlate the efficiency of this degradative energy transfer process to the rate of deactivation of the excited state of the chromophore molecule, formed on absorption of a UV photon. Such a correlation was indeed possible and pointed to the potential superiority of the 2-hydroxy phenyl benzotriazole class of UV absorbers, because the excited states of these chromophores are known to deactivate at an ultra-rapid rate, and the benzotriazole class of absorbers have higher excitation coefficients within 100 picoseconds. The above rationale led to the selection of 5-vinyl 2-hydroxyl phenyl benxotriaxole as the optimum UV absorber. Excited-state spectroscopic studies of 4,4'dimethoxy, 2-hydroxy 3-allyl benzophenone are reported in Reference 18.

F. PHOTOTHERMAL TESTING OF TEDLAR UTB-300 (DU PONT)

Tedlar UTB-300 is a commercially available ultraviolet screening form of Tedlar film, marketed by Du Pont. Ultraviolet-VIS absorption spectra (Figure 4-7) show that the UV absorber is lost quite rapidly from this material at 85°C, presumably because it is present in a physically blended state. No systematic photodegradation studies have been performed on this material, although there are some indications that in free-standing films, photodegradation does take place at 55°C and causes a change (increase) in absorbance of the film. Similar results have been reported by Boeing Engineering and Construction Co., following their tests on Tedlar (Ref. 19). Test results of Tedlar films in the Controlled Environmental Reactor (CER, Ref. 2) at 3 suns (1 day inside the CER is equivalent to 16 days outdoors) and 50°C with simulated fog and rain are illustrated in Figures 4-8 and 4-9. Again, the UV-VIS absorption spectra (Figure 4-8) demonstrate that the UV absorber is lost from Tedlar films during aging. Hydroxyl functional groups

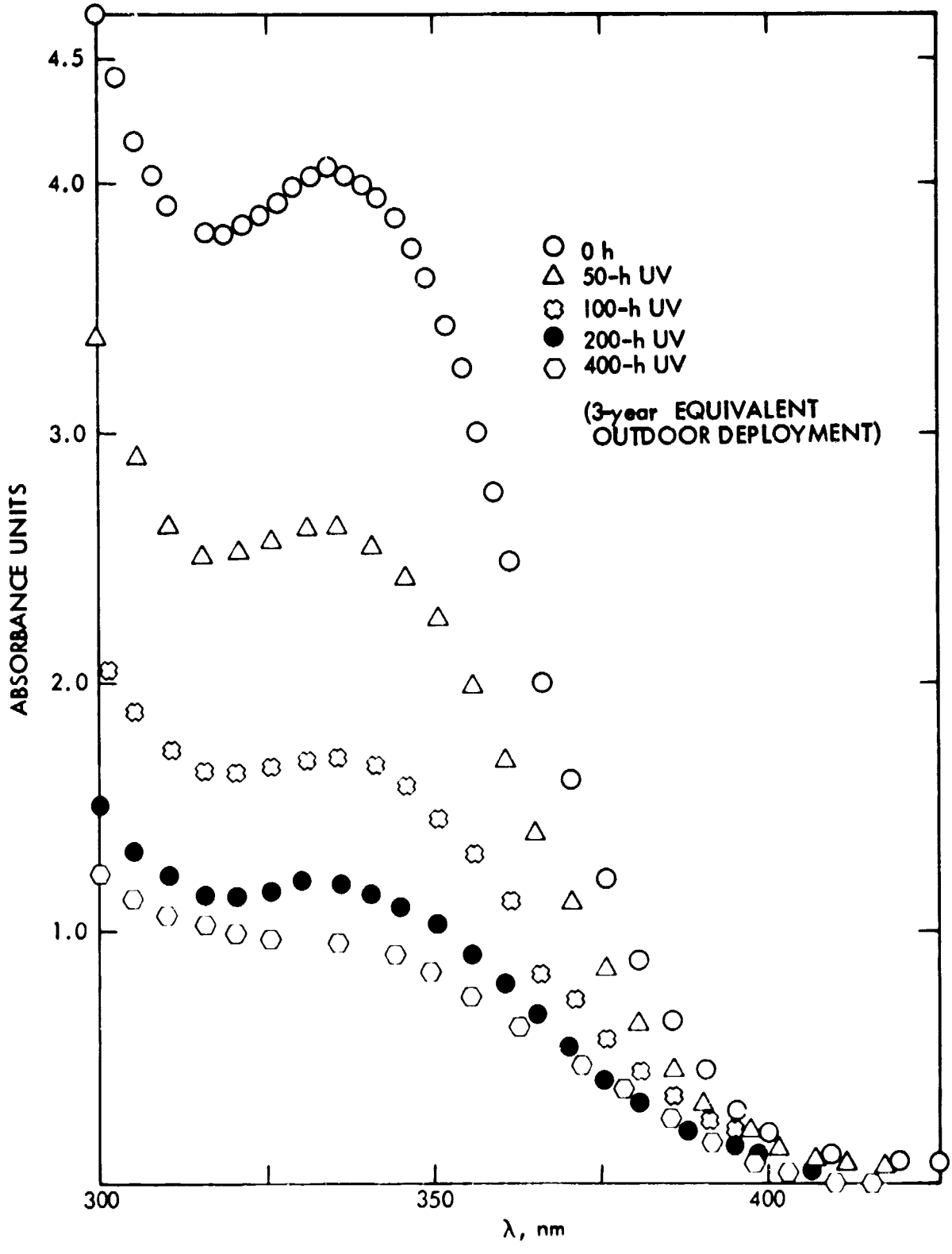

Figure 4-7. UV-VIS Absorption Sepctra of Tedlar UTB-300 as a Function of Photothermal Aging in Air at 6 suns and 85°C

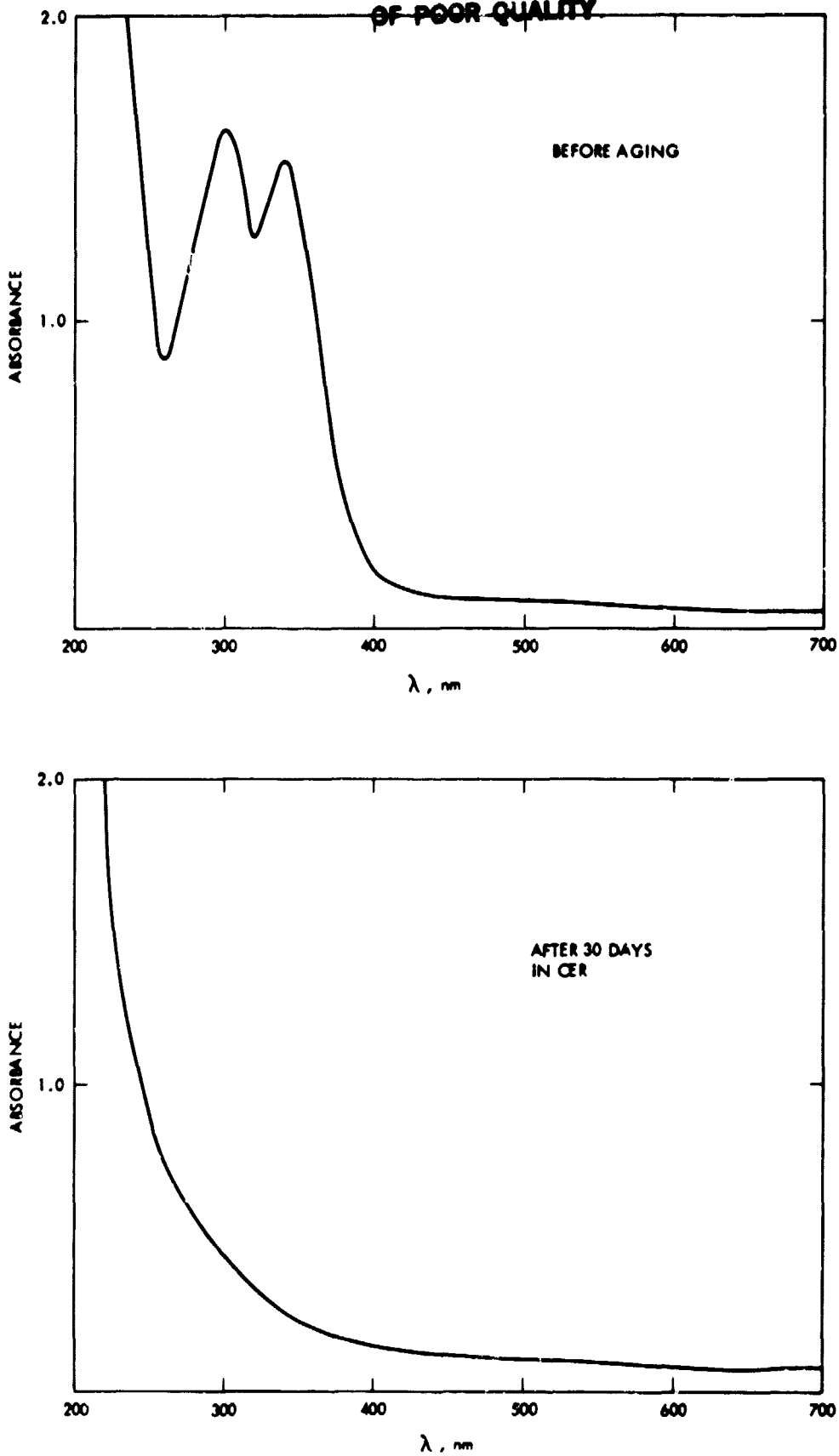

Figure 4-8. UV-VIS Absorption Spectra of Tedlar UTB-300 Before and After 30 days of Aging in CER

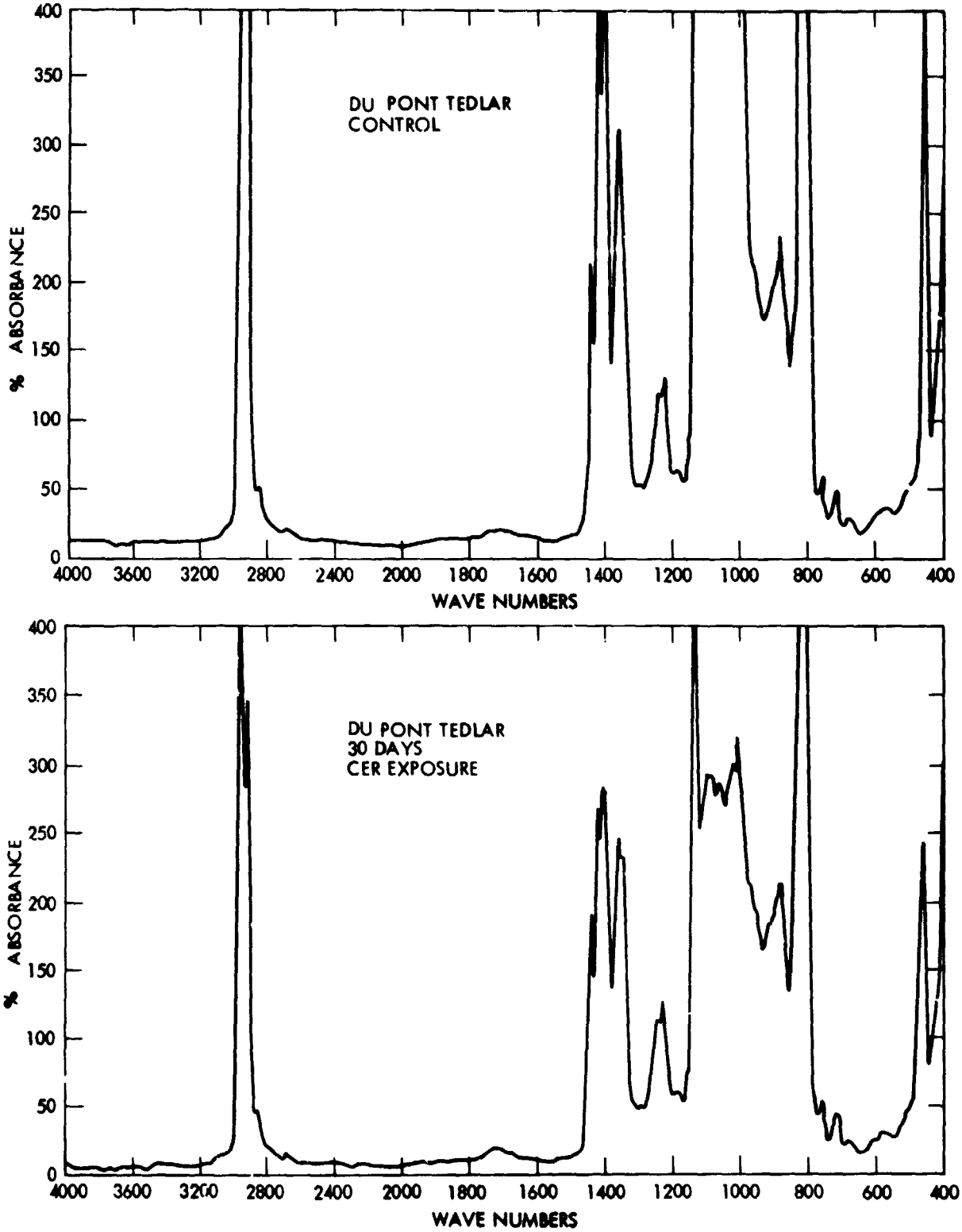

Figure 4-9. FT-IR Absorption Spectra of Tedlar UTB-300 Before and After 30 days of Aging in CER

that are results of oxidation have not been detected in the FT-IR experiment. Significant changes at 1050 cm^{-1}, 1100 cm^{-1}, and 1450 cm^{-1} peaks were also observed in the FT-IR spectra as a function of aging (Figure 4-9). Further testing of Tedlar films is still going on.

G. PHOTOTHERMAL TESTING OF KORAD

"Korad" is a proprietary acrylic film marketed by Hexcel Corporation. It can be purchased unfilled (clear) or filled (white). Preliminary JPL analysis indicated that the acrylic chains in "Korad" contain methyl methacrylate and n-butyl acrylate units. It also contains a ortho-hydroxybenzophenone type UV absorber. The UV absorber is blended in the polymer prior to extrusion, and is not chemically attached to the acrylic chains. Figure 4-10 shows oven test results on Korad, with the increase in UV transmission indicating that the UV absorber is lost from Korad films at an appreciable rate at 85°C. The activation energy of loss of UV screener was determined to be 5 to 7 kcal/mole, a typical value for a physical process.

Photodegradation of Korad was found to result in chain scission mainly, a process that leads to cracking of film. The rate of chain scission was estimated at 55°C in the wavelength range 295 to 350 nm. In accelerated tests on two-cell modules, Korad films cracked after 14 to 28 days (308 to 616 hours of accelerated UV exposure). This period of exposure is equivalent to 1.5 to 3 years of outdoor exposure in the spectral range of 295 to 370 nm. Photodegradation of Korad is thus found to be caused chiefly by UV absorption, with oxygen and water playing a secondary role.

Photothermal aging was performed on this material at 30°C while maintaining full access of air and results were compared with data obtained outdoors. Figure 4-11 is a summary of results. The base polymer in Korad is not weatherable, as it contains butyl acrylate segments. If Korad did not contain the blended in UV absorber, it would undergo chain scission upon exposure to solar radiation and oxygen. The high modulus of the polymer precludes any crosslinking process from occurring. When the average molecular weight ($\bar{M}_w$) is reduced to a certain level, it is expected to crack spontaneously under its own weight or due to daily thermal cycles. Figure 4-11 (A) shows the calculated rate of chain scission of unprotected Korad films. If the UV absorber was permanently bound to the polymer chains, the rate of photo-oxidation would be slower by at least a factor of 20, and the overall bulk rate of photo-oxidation would be represented by the line shown in Figure 4-11 (B). This estimate ignores oxidation occurring at the surface, where no protection is available. Surface oxidation may cause crack initiation at the surface, which could propagate due to thermal cycling. However, sensitization reaction by the UV absorber can lead to rapid degradation of Korad. Figure 4-11 (C) is the projected rate of degradation assuming no leaching/evaporation of the UV stabilizer. Figure 4-11 (D) is the projected rate of degradation, taking into account leaching/evaporation of the UV stabilizers. During outdoor exposure, Korad films were found to crack in 2 to 2.5 years. Points E and F in the figure are the actual datum points obtained, which agree reasonably well with the calculated rate.

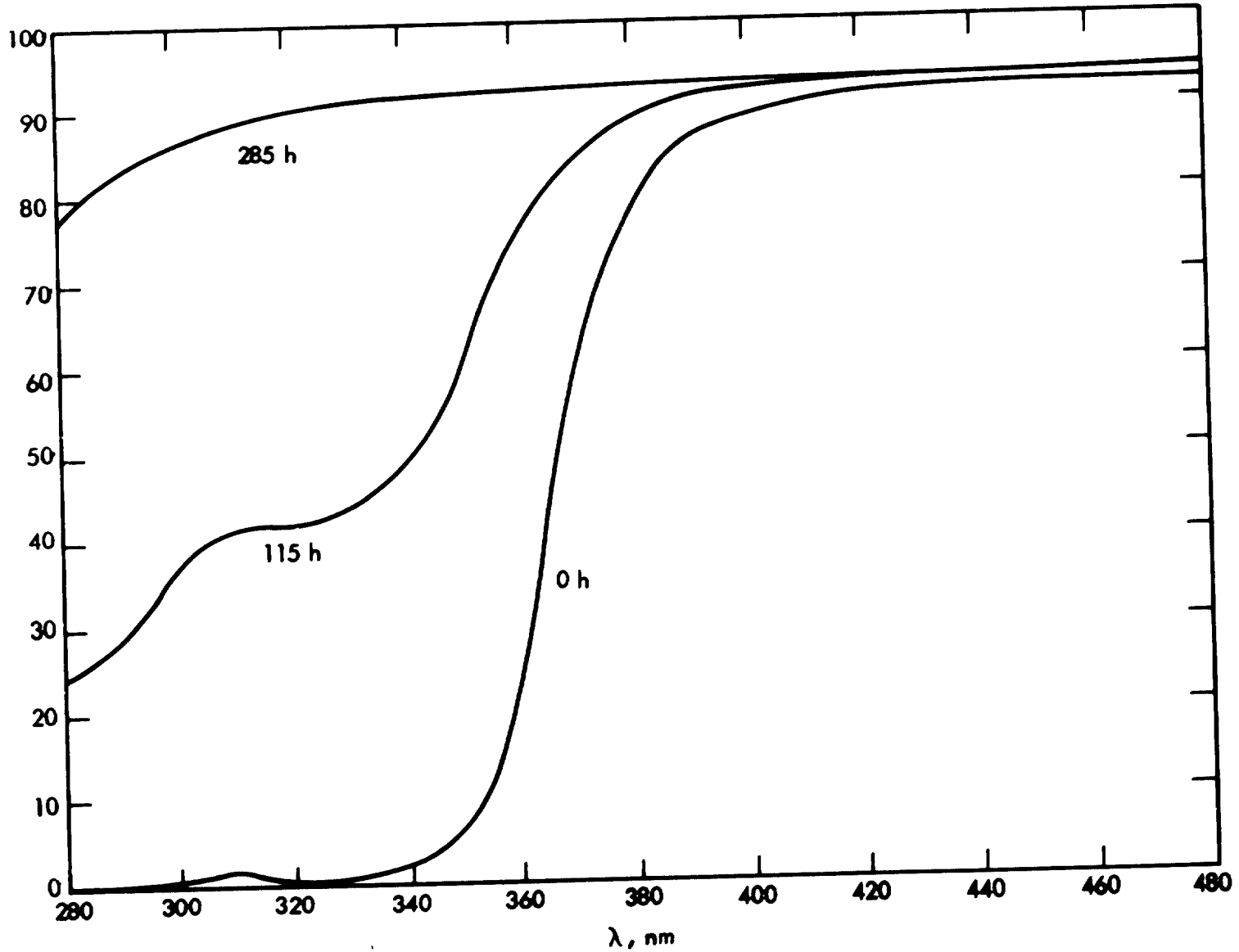

Figure 4-10. UV-VIS Absorption Spectra of Korad as a Function of Photothermal Aging in Air at 6 suns and 85°C

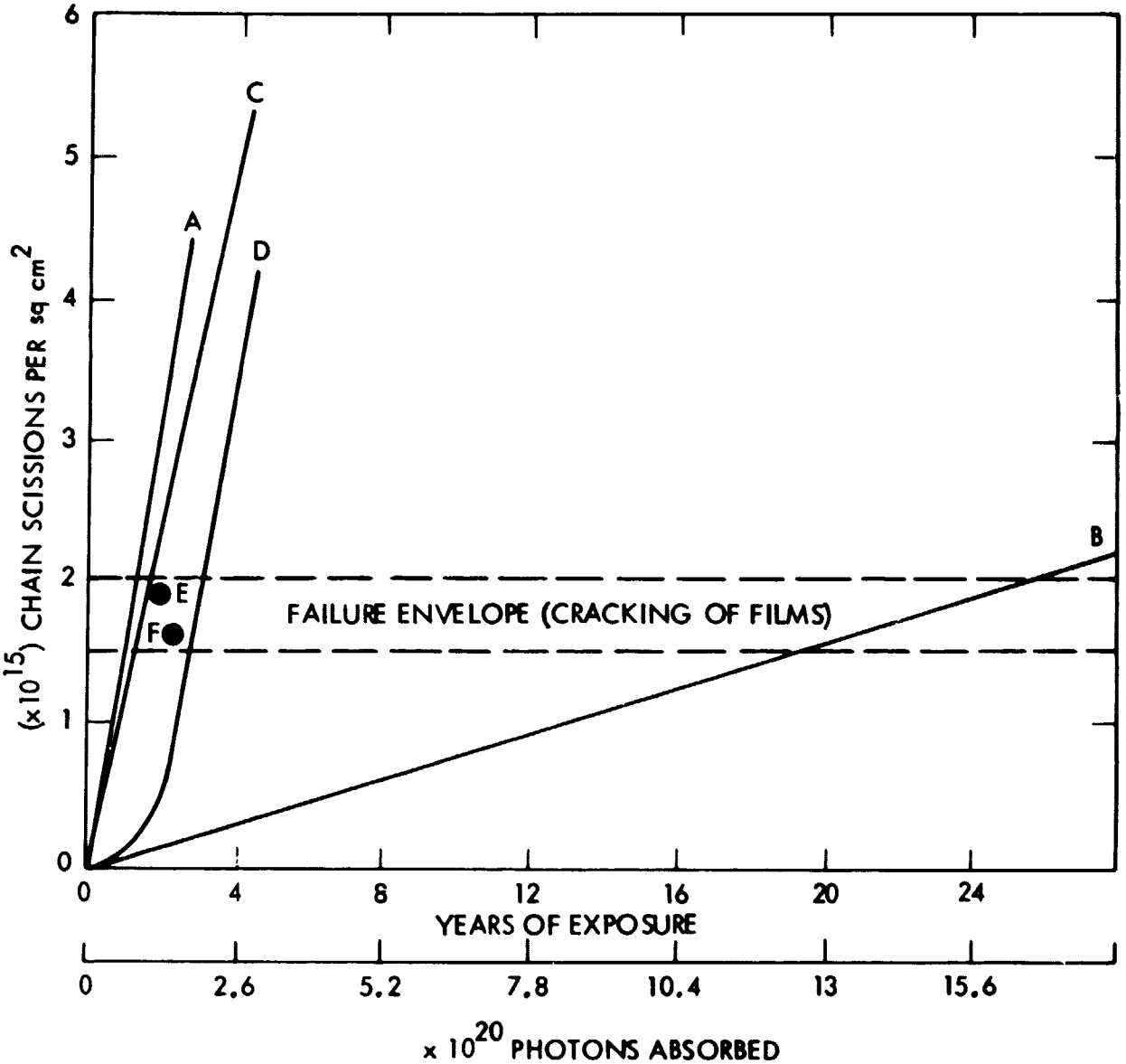

NOTE:
- A. Unprotected Korad (calculated).
- B. Protected Korad (calculated).
- C. Effect of synergism assuming zero loss of UV stabilizer (calculated).
- D. Projected after taking into account leaching of UV stabilizer (calculated).
- E,F. Failure in field observed at two sites (experimental).

Figure 4-11. High UV Service Temperature Test on Korad

H. TESTING OF PERMASORB/MA COPOLYMER

Copolymerization carried out with Permasorb MA indicated that this material has very poor polymerization reactivity. In fact, it was rarely attached to the polymeric network, but did oligomerize to form dimers and trimers which are almost insoluble in solvents such as methanol, which dissolve the monomer. The oligomerized Permasorb MA was found to be quite soluble in water and thus can easily be extracted. Prototype candidate encapsulation materials such as PMMA (polymethyl methacrylate) for outer cover application and PnBA (poly-n-butyl acrylate) for application as pottant were blended with Permasorb MA oligomers, then exposed to distilled water 30°C for periods of up to 14 days. As shown in Figure 4-12, significant leaching rates could be measured in both cases.

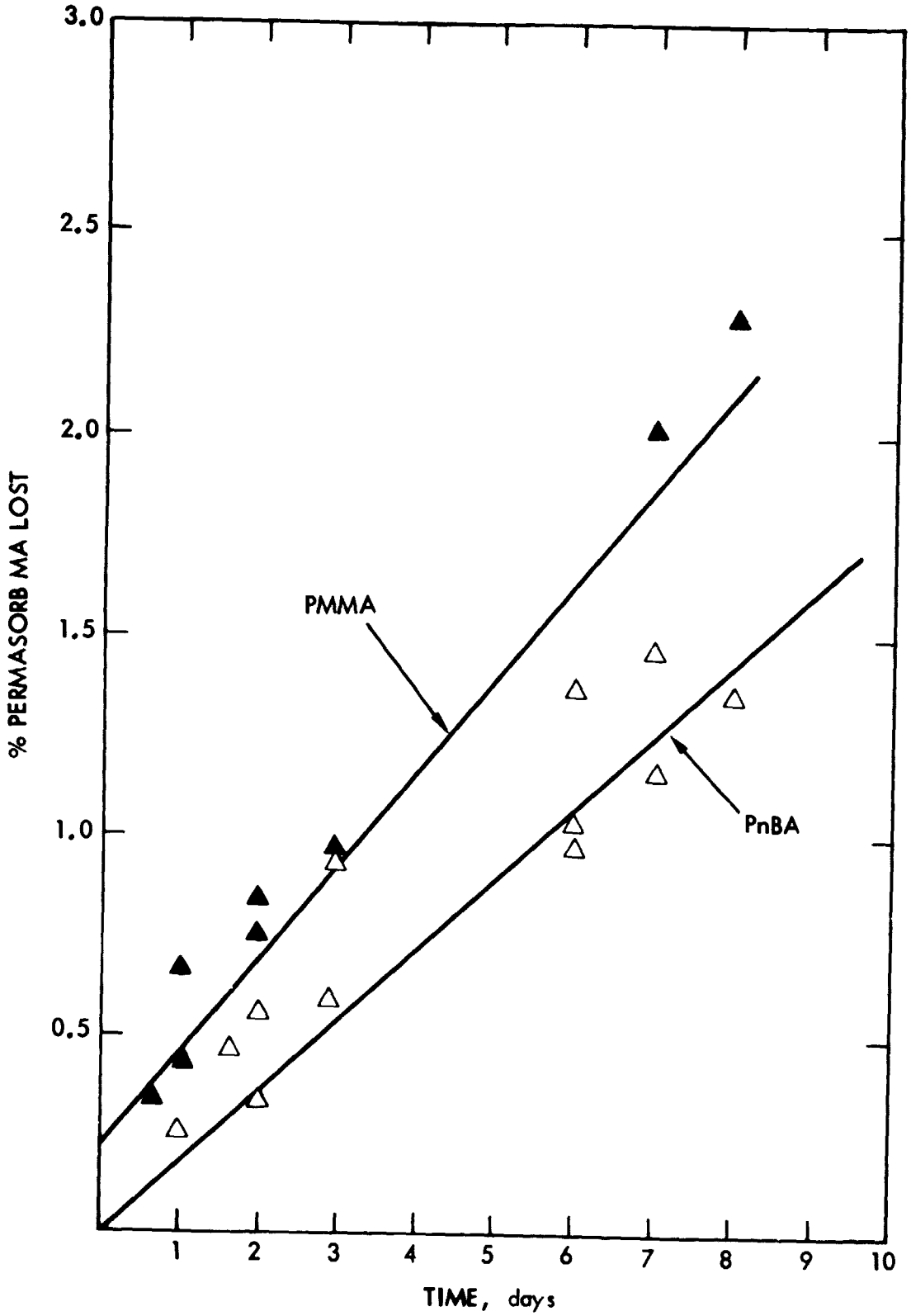

Figure 4-12. Oligomerization of Permasorb-MA Blended with PMMA and PnBA

REFERENCES

1. Griffith, J. S., Environmental Testing of Block II Solar Cell Modules, JPL Internal Document 5101-94, Jet Propulsion Laboratory, Pasadena, California, January 1979.

2. Laue, E., and Gupta, A., Reactor for Simulation and Acceleration of Solar Ultraviolet Damage, JPL Internal Document 5101-135, Jet Propulsion Laboratory, Pasadena, California, September 1979.

3. Design and Analysis of Advanced Encapsulation Systems for Terrestrial Photovoltaic Modules, Interim Report Covering Work Performed from December 1979 to October 1980, Spectrolab, Inc., Sylmar, California.

4. Kaelble, D. H., and Kendig, M., Interfacial Study Program for Encapsulation Materials for Low Cost Silicon Solar Arrays. Interim Report 1980, Rockwell Science Center, Thousand Oaks, California.

5. Moore and Wilson, Photovoltaic Solar Panel Resistance to Simulated Hail, JPL Internal Document 5101-62, DOE/JPL-1012-7816, Jet Propulsion Laboratory, Pasadena, California, October 1978.

6. Guillet, J., Modelling of Photooxidation of Pottants for Flat-Plate Solar Array Applications and Predicting Useful Lifetimes of Such Polymeric Materials, Interim Report, University of Toronto, Toronto, Canada, 1981.

7. Eppley Laboratory, Newport, Rhode Island.

8. Geuskens, G., Borsu, M., and David, C., European Polymer Journal, 8, 883, 1972.

9. Buchanan, K. J., and McGill, W. J., European Polymer Journal, 16, 313-324, 1980.

10. Gupta, A., Photodegradation of Polymeric Encapsulants of Solar Cell Modules, JPL Internal Document 5101-77, Jet Propulsion Laboratory, Pasadena, California, August 1978.

11. Gupta, A., and Di Stefano, S., "Photocatalytic Degradation of a Crosslinked Ethylene/Vinyl Acetate (EVA) Elastomers," Polymer Preprints, 21, 178, 1980.

12. Private Communication.

13. Gupta A., Effect of Photodegradation on Chemical Structure and Surface Characteristics of Silicon Pottants Used in Solar Cell Modules, JPL Internal Document 5101-79, Jet Propulsion Laboratory, Pasadena, California, August 1978.

14. Kaiser, W. D., and Wagner, H., Korrosion, 7, 3, 1976.

15. Reinohl, V., Sedlar, J., and Nararatil, M., Polymer Photochemistry, 1, 165, 1981.

16. Liang, R., Yavrouian, A., and Gupta, A., "Development of a Weatherable Acrylic Elastomer for Solar Cell Encapsulation," Proceedings of 158th Meeting of the Electrochemical Society, Hollywood, Florida, October 1980.

17. Gupta, A., Saraboluoki, M. N., Houston, A. L., Scott, G. W., Pradellok, W., and Vogl, O., "Photochemical Inertness of Poly [2(2-Hydroxy-5-Vinylphenyl) 2H-Benzotriazole] CO(MMA)," Macromolecules, in press.

18. Gupta, A., Yavrouian, A., Di Stefano, S., Merritt, C. D., and Scott, G. W., "Photophysical and Photochemical Properties of Poly 2-Hydroxy-3-Allyl-4,4'Dimethoxy Benzophenone-CO-Methyl," Macromolecules, 13, 821, 1980.

19. Mavis, C. L., The Status and Recommended Future of Plastic-Enclosed Heliostat Developments, Sandia 80-80320, Boeing Engineering and Construction Co., Seattle, Washington, October 1980.